The Thesis Committee for Pedro Antonio Serigos
Certifies that this is the approved version of the following thesis:

Field Evaluation and Analysis of Automated Rut Measurement Systems Data for Texas Conditions

APPROVED BY
SUPERVISING COMMITTEE:

Supervisor:

Jorge A. Prozzi (Supervisor)

Michael R. Murphy

Field Evaluation and Analysis of Automated Rut Measurement Systems Data for Texas Conditions

by

Pedro Antonio Serigos, B.S.C.E.

Thesis

Presented to the Faculty of the Graduate School of

The University of Texas at Austin

in Partial Fulfillment

of the Requirements

for the Degree of

Master of Science in Engineering

The University of Texas at Austin

May 2012

Dedication

I would like to dedicate this work to my parents, wife and brothers, whose love and support helped me to achieve my goals.

Acknowledgements

I would first like to acknowledge my advisor, Dr. Jorge Prozzi, for his constant help and guidance throughout this work. His valuable advice was vital for my completing this thesis and my formation as an engineer.

I would like to acknowledge Dr. Mike Murphy, whose generous sharing of knowledge and great support had a great impact on my thesis. His passion and drive inspired me.

I also would like to acknowledge the following people for their great support during the field testing: Dr. Jose Pablo Aguiar Moya, Ambarish Banerjee, Doug Chalman, Jeawon Hwang, Prasad Buddhavarapu, Boo H. Nam and Dr. Andre de Fortier Smit. Finally, I would like to acknowledge TxDOT for the funding.

Abstract

Field Evaluation and Analysis of Automated Rut Measurement Systems Data for Texas Conditions

Pedro Antonio Serigos, B.S.C.E.

The University of Texas at Austin, 2012

Supervisor: Jorge A. Prozzi

This study evaluated the performance of state-of-the-practice automated rut measurement systems (ARMS) for measuring rutting in the field at highway speeds under Texas conditions. A total of twenty-four 550-ft survey sections were selected with the objective of establishing representative conditions encountered on Texas highways as well as cases considered potentially problematic for automated rutting surveys. Five different ARMS measured the twenty-four sections at highways speeds and reported their best estimates of the transverse profiles coordinates at 552 stations and the Maximum Rut Depth (MRD) values for each wheel-path at 2,664 stations. These measurements were compared with the manual measurements taken statically at the same locations. The reference transverse profiles were manually measured using a laser distance meter and a leveled beam and the reference MRD values were manually measured using a 6ft straight-edge and a gage graduated to 16ths of an inch. In addition, the effect of different experimental variables on each system's measurement errors was analyzed aiming to detect which pavement characteristics are more challenging for the ARMS.

Table of Contents

List of Tables

List of Figures

Chapter 1: Introduction

This thesis is divided into five chapters: Introduction; Literature Review; Rutting Data Collection; Analysis of Rutting Measurements; and, Summary, Conclusions and Recommendations.

This chapter presents the main objectives and motivation for this thesis and includes a background section which provides an introduction to the problem investigated. The last part of this chapter contains a section which describes the scope and methodologies of the analysis performed for achieving the proposed objectives.

BACKGROUND

Rutting is a major distress in flexible pavements which indicates a structural deficiency in the surface, base and/or subgrade layers and can also lead to safety concerns and reduced riding quality. Rutting data collection is necessary to monitor the state of the pavements and detect unacceptable levels of rutting. Rutting data are an essential input into pavement management systems (PMS), which categorize the rutting present at the network providing useful information for decision-making. Collecting accurate rutting data is, therefore, important in order to assess network level pavement conditions, determine treatment funding needs and funding level thus optimizing the use of the available economic resources. In addition, rutting data is used to evaluate pavement conditions, identify the failure mode and to select the most effective strategies for the project-level maintenance and rehabilitation of the pavement.

Rutting is manifested by the distortion of the transverse and longitudinal profile of the pavement surface. The distorted profile is usually characterized by the progressive formation of a depression in each wheel-path of the roadway. These depressions, or ruts,

result from the accumulation of permanent deformations occurring in the pavement structure caused by the repeated loading of traffic. Additional factors such as environmental conditions (high temperatures), and other distress types such as fatigue or longitudinal cracking may accelerate rut development under traffic loads. The increase of rutting with time is indicative of the progressive consumption of the pavement service life.

Figure 1.1 shows a pavement section with severe level of rutting. This picture was taken during manual rutting data collection for this study, while the lane being measured was closed to traffic. The white lines across the pavement section were marked to locate the sections at which transverse profile coordinates were measured. By observing the shape of the white lines in the picture it is possible to clearly see the rut formed at each wheel-path.

Figure 1.1: Picture of a distorted pavement section.

Once the ruts are formed, water may pond, reducing the transverse drainage capacity of the pavement section and increasing the potential for hydroplaning. Therefore, under the same geometric condition of the pavement section (such as its cross slope), greater levels of rutting may be a factor in the occurrence of wet weather accidents. Also, an excessive distortion of the pavement surface may cause handling difficulty for small vehicles at highway speeds.

One of the goals of pavement structural design is to limit the final level of distortion of the pavement surface for a particular period of time and a specific accumulated traffic load level. The presence of a premature excessive level of rutting indicates either a deficiency in the pavement structure, which may be associated with the design of the structure, poorly designed asphalt mixture or the construction of the pavement, or due to excessive traffic loadings (relative to original design criteria).

Therefore, the progressive development of rutting needs to be monitored to detect excessive levels in order to avoid hazardous conditions for the roadway users and to apply preventive maintenance strategies on time to extend the service life of the pavement structure.

There are several methods used for the measurement of rutting, which can be categorized into manual and automated methods. The former have been used for the rutting data collection for many years by many different transportations agencies around the world. Some of the manual methods are standardized and still considered an effective, reliable and low budget option, although they are not efficient for network level data collection. The latter have become available more recently and, when compared to the traditional manual methods, offer advantages such as faster and denser data surveys using

non-contact sensors, lower staffing requirements and no need for traffic control, which makes them more efficient and safer at network-level.

Although there are many possible ways to characterize rutting, the Maximum Rut Depth (MRD) value is the rutting index most widely used. The MRD index is defined for each wheel-path as the maximum distance between a reference straight line, which connects the two maximum points on either side of the rut, and the pavement surface (Figure 2.4). Therefore, the MRD value provides information regarding only one dimension of the rut: its depth. Some manual methods for rutting data collection measure a rutting index statically directly from the pavement, such as the MRD value, whereas other methods categorize the rutting severity level dynamically. Both types of manual methods require the subjective judgment of the rater, which affects both the repeatability and reproducibility of the results. The dynamic methods are preferred over the static ones when collecting rutting data over long distances.

The most popular static manual methods directly measure the MRD value within each wheel-path using a straight-edge or a wire, and a gage. The processes involved in this type of static methods are tedious, time consuming and labor intensive. In addition, the lane being surveyed needs to be closed during data collection which increases the cost and the number of people involved. However, the standardized methods for manual data collection are widely accepted by highway and transportation agencies and therefore are used to establish the reference or baseline values for the calibration and validation of automated methods.

Dynamic manual evaluation of rutting typically consists of a trained rater that categorizes the severity of the rutting present in the section by visual inspection, while travelling along the surveyed roadway in a vehicle. For example, the 2010 rater's manual

[TxDOT, 2009] for data collection of the Texas Department of Transportation (TxDOT) Pavement Management Information System (PMIS), indicates that the rater *"should travel along the side of the road (with traffic, on the roadbed being rated) at no more than 15 miles per hour (24 kilometers per hour)"*. Also, as an example the TxDOT PMIS Rater's Manual defines the following categories for rut severity level:

1. No Rut: MRD < 4/16 of an inch.
2. Shallow Rutting: 4/16 of an inch ≤ MRD < 8/16 of an inch.
3. Deep Rutting: 8/16 of an inch ≤ MRD < 16/16 of an inch.
4. Severe Rutting: 16/16 of an inch ≤ MRD < 32/16 of an inch.
5. Failure Rutting: MRD ≥ 32/16 of an inch.

Regardless of which method is adopted for determining the MRD values of the section, transportation agencies usually use severity of rutting categories (such as the ones presented above) as one method to describe the condition of the pavement and one of the factors used to rationally decide when and where to apply maintenance and rehabilitation treatments. For example, a threshold adopted by some state transportation agencies to trigger the need for treatment is an MRD value equal to, or greater than, 0.5 inches.

The implementation of a system for automated high-speed rutting data collection aims at increasing the accuracy and efficiency of the measurements and eliminating the subjective elements present in visual or manual rating at both network and project levels. These systems incorporate non-contact sensors that are usually mounted on the rear of a vehicle, and the rutting data are automatically collected while the survey vehicle travels the pavement section.

Automated systems for rutting data collection have become available in the last few years, and their capabilities have been continuously evolving as more advanced technologies are developed. An important improvement in their capabilities has been the increase in the number of coordinates measured per profile. The first automated systems were capable of measuring three to five coordinates per transverse profile whereas current systems can measure more than a thousand points, which is essentially a continuous profile. Therefore, automated systems for the measurement of rutting can be divided into two major categories: punctual (or discrete) systems and continuous systems.

Automated punctual systems use point-based ultrasonic or laser sensors that measure the distance to the pavement at pre-determined points along a rut bar mounted to the vehicle. The number of sensors determines the number of points measured per transverse profile and which can vary between seven to thirty sensors. However, automated punctual systems using three and five sensors are still being used by many state transportation agencies in the United States and internationally.

The measured transverse profile coordinates are used to calculate rutting indexes by applying vendor-specific algorithms. The algorithms used for the calculation of the MRD values, for example, simulate the placement of a virtual straight-edge at different locations within the boundaries of the measured profile until the maximum rut depth value is found. This process is repeated for each wheel-path. A general observation is that the greater the number of measured coordinates per transverse profile, and lane width coverage, the better the representation of the actual shape of the transverse profiles. A well-defined, full lane-width transverse profile can result in more accurate MRD measurements assuming that the rut depth algorithm is properly coded. Thus, punctual systems typically underestimate the MRD values since they provide fewer data points and

usually cover less than the full lane width. Punctual point systems may miss measuring the deepest point of the rut, whereas continuous systems provide full lane width coverage which provides greater opportunity to determine the MRD with a properly coded MRD location algorithm.

Figure 1.2, illustrates the situation described above, MRD is missed due to the limited number of coordinates per profile and the fact that the rut bar does not cover the full lane width which is typical of a punctual automated system. The system shown in Figure 1.2 [Huang, 2009] is a five-point ultrasonic sensor rut measurement system that TxDOT has developed in-house and has been using for the last 15 years. TxDOT has recently developed in-house a new automated system capable of measuring the continuous transverse profile using a 3-D camera and a laser.

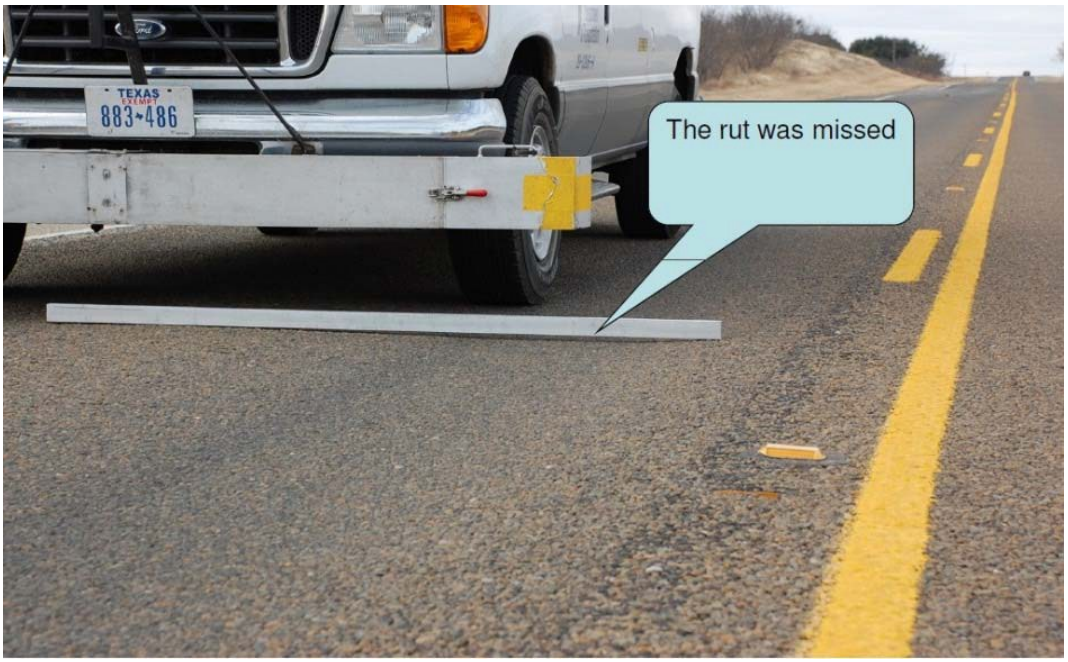

Figure 1.2: Rut missed by automated punctual system [Huang, 2009].

The results produced by automated punctual systems can also be affected by the lateral wandering of the survey vehicle and environmental conditions. Since it is practically impossible to ensure that the driver of the vehicle will travel the section at the same lateral location in successive runs, the measured points at each run will be different. As an example, if the punctual system in Figure 1.2 were located closer to the inner stripe of the lane, the rut would not have been totally missed. Therefore, if the same punctual system were used for collecting rutting data in two consecutive years, it would not be possible to determine if the difference between the two produced values is due to the increase in rutting over the year, or just because of the effect of the lateral wandering of the survey vehicle. In addition, environmental factors such as wind speed and direction and humidity can affect the accuracy and ability of ultrasonic punctual systems.

Continuous automated systems are designed to obtain a complete representation of the entire lane width of the section, and therefore, ideally the measurements produced by these systems are not affected by the lateral placement of the survey vehicle.

Continuous automated systems currently available on the market can measure more than a thousand points per transverse profile, with a profile spacing of 5mm (0.2inches) at 100km/h (62mph), and a vertical (depth) resolution of ±1mm. These systems can be categorized in two major groups according to the technology applied: Optical systems and Scanning Lasers systems. The description of the basic working principles of these two technologies is covered in Chapter 2: Literature Review.

MAIN OBJECTIVES

A key factor for the success of a PMS is that it is provided with accurate and reliable pavement distress data. Rutting is a major form of distress in flexible pavements. In Texas, flexible pavements constitute approximately 94% of the state maintained

roadway network which comprises over 195,000 lane miles. Thus, accurate and reliable rut measurements are required for thousands of lane miles of pavement with different surface types and under different environmental testing conditions to correctly characterize pavement conditions.

Continuous automated systems represent the state-of-the-art for collecting rutting data. Current automated rut measurement systems are not only capable of collecting multiple coordinates for each transverse profile, but are also capable of collecting hundreds of transverse profiles for each PMS rating section while operating at highway speeds. These combined features provide an effective solution for network level surveys. However, continuous automated systems have been recently developed, and the claimed superior quality of their measurements needs to be validated by independent studies.

The study presented in this thesis evaluated the quality of the rutting measurements produced by different continuous automated rut measuring systems under real-world conditions.

The three main objectives of this thesis were:

- To evaluate the quality of the rut measurements taken in the field at highway speeds by different continuous automated systems at roadway sections in Texas with different pavement characteristics.
- To determine if the source of error of the rut measurements produced by the different systems was either related to the measurement of the pavement surface coordinates (hardware) or to the calculation of the rutting indexes (software), or both.
- Evaluate the influence of different pavement characteristics (e.g.: lane width or surface texture) on the errors of the reported measurements.

SCOPE AND METHODOLOGY

The rutting data measurements analyzed in this thesis were obtained during Phase One of TxDOT research project: "0-6663 Evaluation of Pavement Rutting and Distress Measurements" [Serigos et al, in press] performed by the Center for Transportation Research (CTR) of the University of Texas at Austin (UT-Austin). The author of this thesis participated as a member of the research team in the mentioned project.

One of the objectives of the 0-6663 research study was to evaluate the recently developed TxDOT 3-D laser rut measurement system by comparing it in the field to other commercially available system. Four different vendors participated in this study: Pathway Services Inc., Dynatest Consulting Inc., Fugro-Roadware Inc. and Applus RTD. Therefore, a total of five different continuous automated systems participated in the experiment. Each participant operated their equipment, and applied proprietary algorithms for the processing and calculation of the requested rutting data. All of the automated systems operated by the five participants were optical systems.

The sections at which the rutting data was collected by the automated systems were selected in order to be representative of the pavement characteristics encountered in Texas. Additionally, some sections were selected which included features considered to be challenging for the measurements of the automated systems.

The analysis and findings of this thesis are therefore limited to the five automated rut measurement systems that participated in the study and to the highways characteristics included in the twenty-four sections selected for the study. The description of each participant's system and the characteristics of the twenty four selected highway section, are presented in Chapter 3: Rutting Data Collection.

Each participant was requested to report their best estimate of the MRD value of both the inner wheel-path (IWP) and the outer wheel-path (OWP) at 111 stations per section and their best estimate of the transverse profile coordinates at 23 stations per section, for each of the twenty-four total sections in this study.

In order to achieve the first listed objective, the rutting measurements reported by the participants were compared to the reference values collected by the research team at corresponding stations. The reference values were established by manually measuring both the MRD values and the transverse profile coordinates at the corresponding stations of the experiment. Additional experiments were carried out to estimate the overall precision of the manual measurements.

From the comparative analysis of the reported rutting data, the bias and precision of the measurements errors for each automated system were estimated for the overall experiment. Additional statistical parameters were computed for each set of data to evaluate the quality of the measurements and compare the performance of the different systems.

Lastly, the effect of different characteristics of the pavement sections on the errors of the MRD values reported by each participant was study by evaluating the estimated coefficients of multiple linear regression models developed for the observed values of the experimental variables of the study.

Chapter 2: Literature Review

This chapter covers the literature review conducted for this thesis regarding the definition and characterization of rutting, and the different practices and methods used for rutting data collection.

The first section of the chapter contains different definitions of rutting and presents a selection of indices to characterize rutting as found in the literature. The second section of the chapter describes the most commonly used manual and automated methods for the measurement of rutting. The advantages and limitations of each of the methods are discussed, and a description of the technologies applied by the different automated systems, along with the technical specifications provided by their manufacturers, are included in the chapter.

DEFINITION AND CHARACTERIZATION OF RUTTING

Rutting is defined as the progressive consolidation or displacement of materials under repeated loads either in the asphalt pavement layers or the underlying base [Roberts et al., 1996]. The distorted surface shape of a rutted pavement is a consequence of the permanent deformations present at each layer and at the subgrade. While there is some consensus on the definition and mechanisms behind rutting, there is not a unified way to characterize and quantify it.

Other definitions of rutting do not include the association to wheel loads. For instance, the American Society for Testing and Materials (ASTM) defines a rut as *"a contiguous longitudinal depression deviating from a surface plane defined by transverse cross slope and longitudinal profile"* [ASTM E867-06]. The most used index to characterize rutting is rut-depth, which is defined by ASTM as *"the maximum measured perpendicular distance between the bottom surface of the straightedge and the contact*

area of the gage with the pavement surface at a specific location". This definition is used in ASTM Standard E1703 for measuring rut-depth using a straight edge. The rut-depth index may also be obtained using a wire instead of a straight edge. These methods are described with more detail in the next section.

Simpson [Simpson, 2001a] listed several rutting indices considered for use in the Long-Term Pavement Performance (LTPP) studies which may be grouped into: area, depth, width indices and radius of curvature. The area indices were: "Negative Area"; "Positive Area"; and "Fill Area". For the case of the rut depth and width, different indices were considered whether measured using a 1.2 or a 1.8m straight-edge, or a wire line. Thus, the postulated indices were named, for example, *"1.2-m rut depth"* and *"1.2-m rut width"*. That is, the indices were associated with the particular instrument.

Another depth index considered was the "water depth". The radius of curvature of the rut was also considered by Simpson, although the author did not recommend the use of it due to *"the difficulties in defining and calculating the index"*.

Figures 2.1 to 2.4 show illustrations of some of the indices considered for use in the LTPP. The thick line in all the schemes of the figure is the transverse profile of a rutted pavement and the thin line is a straight line that connects the first and the last coordinate of the lane. Figure 2.1 illustrates the negative and positive area indices. Having the coordinates of the profile, it is possible to calculate the areas formed between the profile coordinates and the straight line connecting the end points. The areas below the straight line are defined as negative areas and the ones above the straight line are defined as positive areas. The Negative Area index is calculated as the sum of the negative areas and the Positive Area index is calculated as the sum of the positive ones. The Fill Area index is obtained by calculating the total area between the profile

coordinates and the straight lines connecting the peaks of the profile. Figure 2.2 shows the Fill Area of the rutted surface in gray. All these area indices provide a two dimensional characterization of rutting. The negative and positive areas provide information about the severity of rutting, and according to Simpson, they may potentially indicate the cause of the rutting. The Fill Area index may be used as an estimate of the amount of material necessary to repair the pavement.

Figure 2.1: Negative and positive areas.

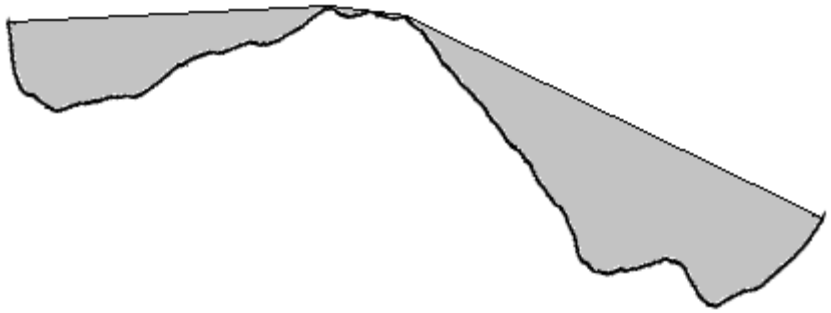

Figure 2.2: Fill area.

Figure 2.3: Water depth.

Figure 2.4: Rut depth and rut width.

The water depth index is illustrated in Figure 2.3. Water may pool in the formed rut reducing the pavement drainage capacity and increasing the likelihood of wet-weather accidents due to hydroplaning. As shown in the picture, this index is obtained for each wheel-path as the maximum vertical distance (indicated in the figure as WD) between the profile coordinates and a horizontal line positioned at the maximum point at which water would pond. This index is not commonly calculated during rutting data collection. A possible reason for this may be that not all the systems currently measure the cross-slope of the pavement, which is required to calculate the index.

The rut depth index is the most frequently used to characterize rutting. Figure 2.4 shows the rut depth (RD) and the rut width (RW) obtained for each wheel-path of the rutted pavement. The rut depth is the maximum distance perpendicular to the straight edge or wire line, and the profile coordinates, whereas the rut width is defined as the distance between the points at which the straight edge of wire is supported. The straight edge and wire will provide the same information as long as the straight edge length is long enough to cover the same support points at the ends of the wheel-path. Simpson disregarded the 1.2 m straight edge rut depth and width indexes and indicated that 1.8 m (6 ft.) straight edge and wire line provide essentially the same information. In other studies, the rut depth was estimated perpendicular to the elevation datum instead of to the straight edge or wire line as shown in Figure 2.4. Bennett [Bennett et al, 2002] estimated the difference in magnitude for both cases concluding that the difference is not significant for the range of rut depth commonly found.

MEASUREMENT OF RUTTING

All the indexes to characterize rutting presented in the previous section require the transverse profiles coordinates of the pavement while some of them can be directly measured in the field. Rutting data collection methods can be grouped into two main categories: manual and automated methods. This section is divided in two parts: the first part presents the most used manual methods and the second part covers the different technologies developed for the automated measurements.

Manual Methods

Manual methods have been traditionally used for rut data collection until automated methods became an option. They are currently used to establish the

benchmark reference or "true" rutting for automated instrument evaluation or as the preferred option for agencies where rutting is not a major distress or agencies that have a low budget. Manual rutting measurements are also preferred for project level evaluations because the values are more trusted.

The most common method to directly measure the rut depth of each wheel path uses either a straight edge or a wire and a gage. The "wire string" method consists of stretching a wire from the ends of the lane perpendicularly to the direction of traffic, and measuring the maximum distance between the wire and the pavement surface using a gage. For this reason, two persons are required to stretch the wire at the extremes while a third operator measures the rut depth for each wheel path [Wang, 2005]. The Straight Edge method uses a straight edge instead or a wire, and requires one operator to place the straight edge in the correct position of each wheel-path and take readings from the gage. Although one operator is the minimum required, usually two operators (one per wheel-path) are involved in the process. Measurements obtained by manual methods contain human error which is expected to be affected by factors such as fatigue caused by extreme weather or extended physical activity. These methods are slow and tedious and require traffic control, making them impractical when collecting data at network level. A more efficient approach for collecting rutting data over long distances consists of an experienced manual data collector visually determining the rutting level of every section. The manual visual data collector travels the sections in a vehicle, which may eliminate the need for traffic control and speeds up the process. The results from the visual inspection contain a high degree of human judgment which affects the accuracy, repeatability and reproducibility of the measurements. Also, the accuracy of the

measurements can be affected by climatic conditions such as bright sunlight or shadows which can obscure or reveal some types of distresses.

The methods described above allow for the direct measurement or estimation of the rut depth and in some cases the rut width indices. In order to obtain other rutting indices, the collection of the pavement surface coordinates is necessary. Nowadays, the collection of transverse profile coordinates is being made with automated equipment at highway speeds; in the U.S., manual equipment is mainly used for calibrating automated systems. A traditional way of collecting the coordinates of the pavement surface is by using a rod and a level although many contact and non-contact manual transverse profile measurement devices have been developed for use at Accelerated Pavement Testing facilities, forensic investigations and other detailed applications.

The FACE® Dipstick Road Profiler is a manual instrument used for the transverse profile measurement of the LTPP as well as in different project-level projects [Simpson, 2001a]. This instrument is operated by one person that pivots the dipstick from one leg to the other following the line of the profile being measured. The instrument uses an inclinometer to calculate the elevation difference between the two legs, obtaining the coordinates of the transverse profile once the operator pivoted the dipstick along the entire width of the lane.

Different agencies also use more advanced manual equipment for the measurement of transverse profiles. Texas Department of Transportation (TxDOT) owns a slow speed manual profiler referred to as the MLS profiler. This equipment requires an operator to roll a wheel along the transverse profile. The wheel is guided by a leveled beam and contains an LVDT that measures the changes in elevation respect to the

reference plane for each horizontal coordinate. The system is connected to a computer which stores the measured coordinates of the transverse profile.

Several others manual profilers can also be found in the literature such as the "Transverse Profile Beam (TFB) reference profiler" (Figure 2.5) [Bennett et al., 2002] commercialized by Road Measurement Data Acquisition System (ROMDAS). These systems are generally similar in concept and usually they are capable of collecting multiple points of the profile using sensors with high accuracy and resolution, although their operation is slow and they cannot be used for network level data collection in Texas.

Figure 2.5: ROMDAS "TPB Reference profiler" [Bennett et al., 2002].

Straightedge Method

Manual straightedge rut measurement is a widely accepted standard rut measurement method. Its procedure is described by ASTM E1703, and consists of directly measuring the depth of the rut at a chosen location in a pavement surface using a straightedge and a gage (Figure 2.6).

Figure 2.6: Straightedge method field measurement.

Straightedge lengths are usually 1.8 meters (6 ft.) and 2.0 meters (6.6 ft.), although any length can be used as long as it ensures that it spans the two highest points on either side of the rut. The straightedge is placed on the pavement surface in a plane perpendicular to the direction of traffic movement, and the measurement is taken as the perpendicular distance between the bottom surface of the straightedge and the contact area of the gage with the pavement surface (Figure 2.7).

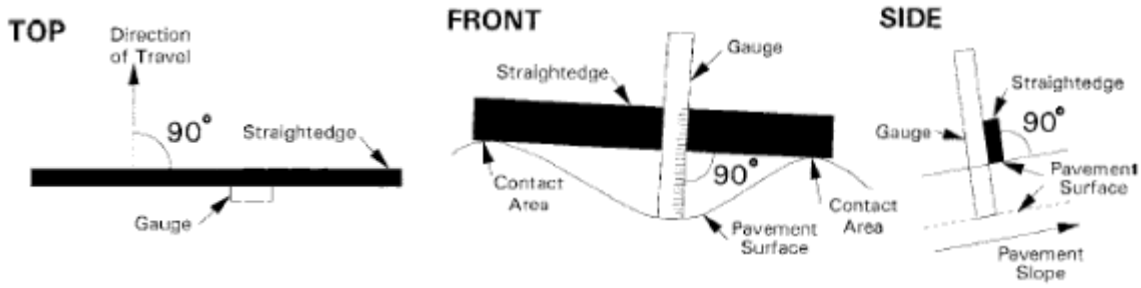

Figure 2.7: Straightedge method [ASTM E1703].

Automated Methods

Automated methods were developed with the objective of performing faster, more accurate and higher data density collection of transverse profiles. They measure the distance to points on the pavement surface using sensors which are mounted on a vehicle. Thus, by running the survey vehicle at highway speeds and without interrupting the traffic, it is possible to obtain multiple points of the transverse profile of the pavement (from 3 to around 1,300 profile coordinates) at high frequencies (intervals as short as one profile per inch of travel at 60 mph).

Automated systems for rutting measurement are usually categorized into four groups according to the technology applied: Ultrasonic, Point Laser, Optic and Scanning Lasers. The first two systems generally collect 3 to around 30 points whereas the last two collect up to approximately 1,300 points, which is in essence a continuous profile. Therefore, the four groups might also be divided into two groups according to the amount of points collected per transverse profile, point-based (or discrete) methods, which includes the first two, and continuous methods, which includes the last two.

Ultrasonic and Laser Punctual Systems

Automated data collection systems use either ultrasonic or laser sensors, or a combination of these to measure the distance to the pavement surface. The sensors are fixed to a bar which is usually mounted on the front of the survey vehicle. The number of sensors varies from the most basic configurations of 3 points, such as the Kansas Department of Transportation (KDOT) South Dakota Profilometer [Vedula et al, 2002] or the TxDOT acoustic rut bar, to more dense configurations of 28 points or more, such as the ROMDAS Transverse Profile Logger Ultrasonic Rut Bar [ROMDAS TPL-URB Spec Sheet] or the Automatic Road Analyzer (ARAN) Smart Rutbar [ARAN Smart Rutbar

Spec Sheet], shown in Figure 2.8. Corrections due to temperature, humidity and wind speed for distances measured by these systems are usually applied automatically while reporting the transverse profile of the road. Some of these systems are fitted with additional wings to extend the coverage of the transverse profile of the road.

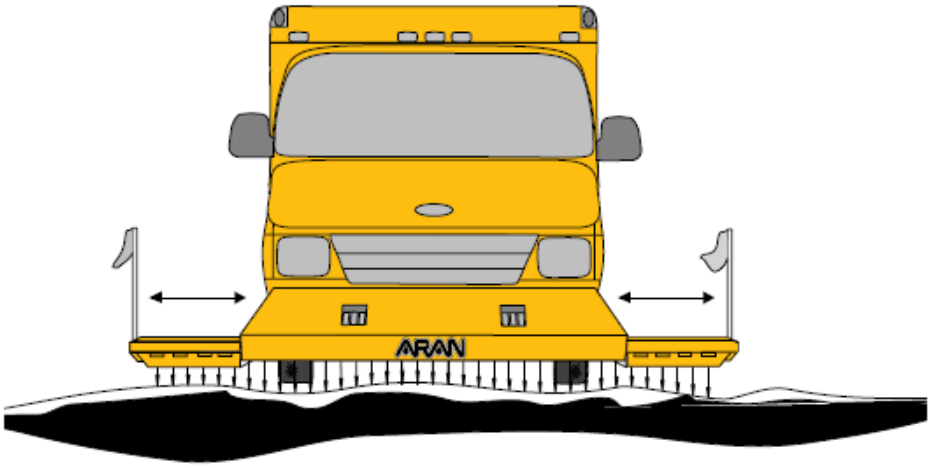

Figure 2.8: ARAN Smart Rutbar punctual system [ARAN Smart Rutbar Spec Sheet].

When measuring transverse profiles using equipment with three or five sensors, the only index estimated is the rut depth of each wheel-path. For the case of three coordinates, the rut depth is estimated by an index defined as pseudo-ruts (Figure 2.9), which is calculated as the difference between the highest and lowest points on the transverse profile of the road. The high point coordinate is estimated as the reading from the center sensor whereas the low-point coordinates are estimated as the reading taken from the sensors at the sides.

For the case of five coordinates, the rut depth may be calculated using the formula from AASHTO R48: outer_wheelpath = $D_2 - \frac{D_1+M}{2}$ and inner_wheelpath = $D_4 - \frac{M+D_5}{2}$, where $M = \min(D_3, \frac{D_1+D_5}{2})$. The values of D_1 to D_5 are the measurements taken from the

sensors, as indicated in Figure 2.10, obtained from AASHTO R48 [AASHTO R48-10]. The main problem of using three or five-sensor systems, which are used by several agencies, is that they tend to underestimate the actual rut depth. For this type of equipment to produce good results, the position of the sensors should be close to the position of the maximum and minimum points of the each rut, as in the hypothetical case illustrated in Figure 2.10. Huang [Huang et al, 2009] estimated that the five-point system underestimates the rut depth value obtained manually by up to 40%.

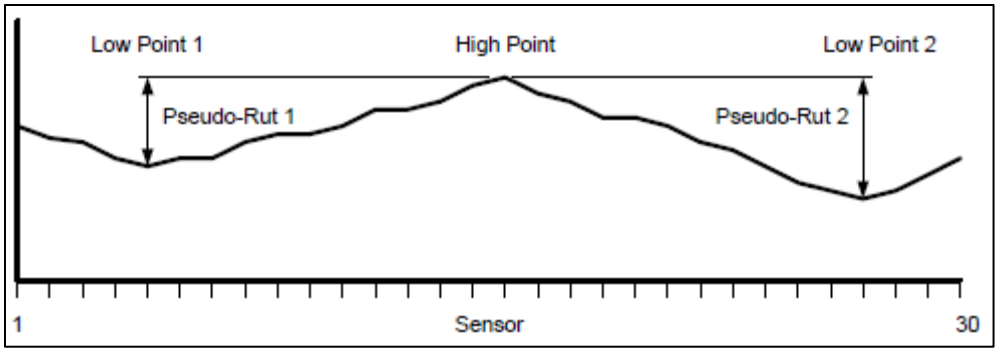

Figure 2.9: Definition of Pseudo-Ruts [Bennett et al., 2002].

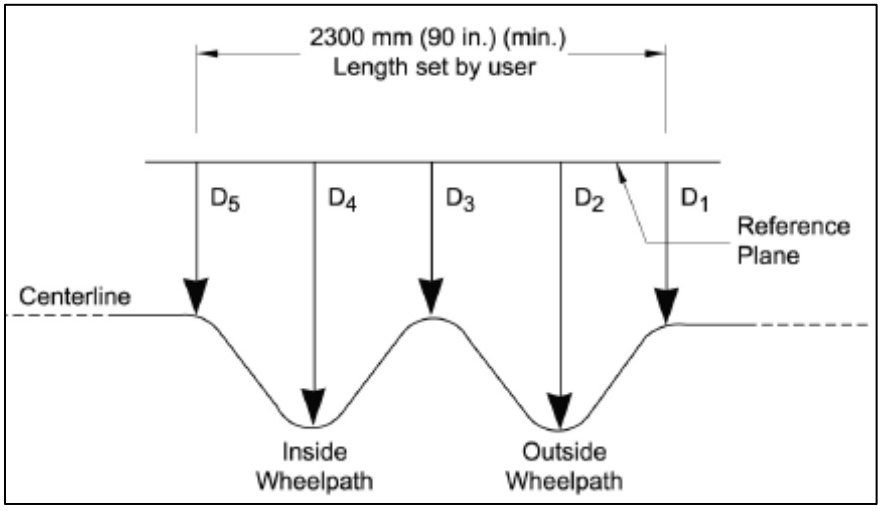

Figure 2.10: Determination of rut depths using five coordinates [AASHTO R48-10].

A greater number of sensors can result in a more accurate estimation of the actual rut depth, which motivated the development of several rut bars available in the market today that use multiple sensors. The more sensors are placed in the bar, the closer they are to each other which, in the case of ultrasonic sensors, may cause interference. To avoid this problem, sometimes the measurements are made progressively along the road, as illustrated in Figure 2.11 [Bennett et al, 2002]. Thus, the coordinates of the measured profile using multiple ultrasonic sensors are not from the same transverse profile but from combining the readings taken at the consecutive firings. The error introduced by this approach increases as the longitudinal profile variations increase.

Laser sensors, on the other hand, are much faster than ultrasonic sensors and are not affected by adjacent sensors which allows for simultaneous firing. However, ultrasonic sensors are less expensive than the lasers and, therefore, ultrasonic systems usually contain a larger number of sensors than laser systems.

Regarding the sampling effect on the accuracy of the measurements, Simpson [Simpson, 2001b] concluded that when cubic splines are used to interpolate between the points, nine sensors can be used to represent the profile with sufficient accuracy for pavement management. These points should be located such that they take measurements at 0, 305, 914, 1524, 1829, 2134, 2734, 3353 and 3658 mm from the edge of the lane.

Another significant source of error that discrete point automated systems measurements have originates from the lateral wander of the survey vehicle during testing. If the survey vehicle runs the same section twice, the lateral placement of the vehicle during both runs will likely not be the same resulting in variations in the measurements of the pavement surface. Thus, lateral placement clearly affects the variability of the results reported by point-based systems. Continuous systems, on the

other hand, are designed to avoid this issue and therefore they are ideally not affected by lateral placement of the survey vehicle.

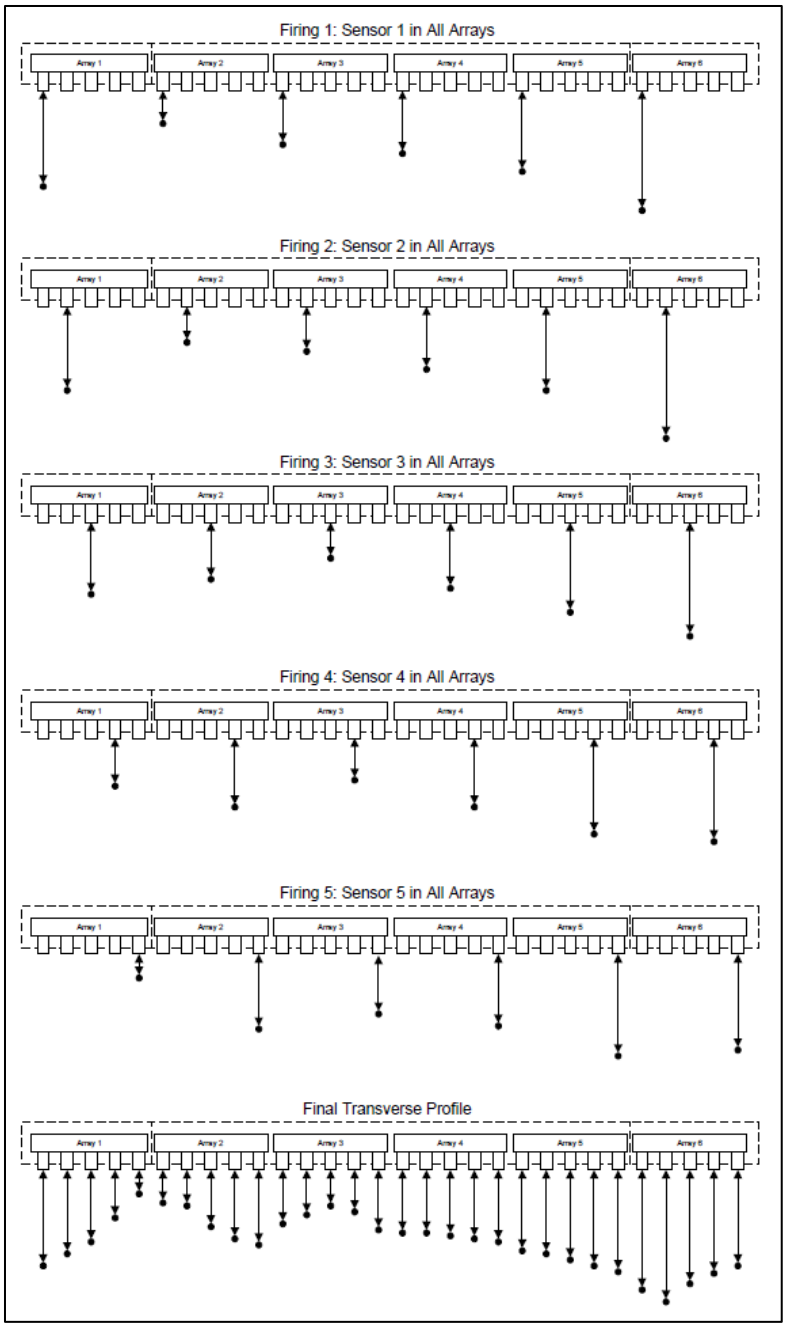

Figure 2.11: Sequential firing of ultrasonic sensors [Bennett, et al., 2002].

As an example of an ultrasonic system, the specifications given by ROMDAS [ROMDAS TPB-Reference Profiler Spec] are:

6. Sensor type: Ultrasonic;
7. Scan rate: 100 Hz;
8. Number of sensors: 28;
9. Sensor spacing: 125 mm;
10. Sensor resolution: +/- 0.2 mm;
11. Standoff: 300 mm;
12. Range: 250 mm;
13. Dimensions: 2.2 m main housing with 2 x 0.6 m fold out extensions.

As an example of a point laser system, the main characteristics of the RoadSTAR transverse evenness measuring device, obtained from Wang, 2005 are presented. The RoadSTAR system contains a fan-shaped measuring beam with 23 laser sensors (Figure 2.12). The laser sensors have an accuracy of 0.1mm and the separation between sensors is 150mm. The fan shape of the beam allows for a measuring width of 3.3 m, even though the rut bar is 2.5 m wide as indicated in Figure 2.12 [Wang, 2005]. According to Bennett [Bennett, 2002], laser systems are capable of measuring transverse profiles every 10 mm in the travelled direction, presenting an advantage when compared to the 1.0 or 2.0 meters sampling intervals of the ultrasonic systems.

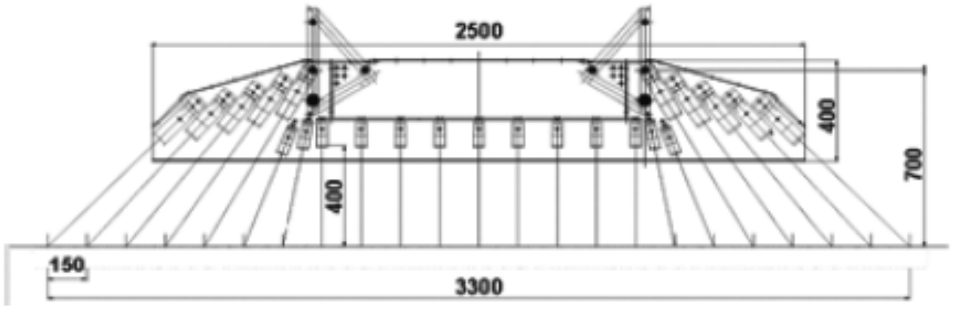

Figure 2.12: RoadSTAR Fan-shaped measuring beam [Wang, 2005].

Optical Systems

Optical systems for rutting measurement digitalize the transverse profile of the pavement by using a laser and a camera. The methodology uses the same techniques that are often used to develop 3-dimensional images in industrial applications. A thin laser line is projected on the pavement surface while a camera captures the laser line image at an angle (Figure 2.13). The captured image is digitalized and then processed to obtain a continuous transverse profile of the road.

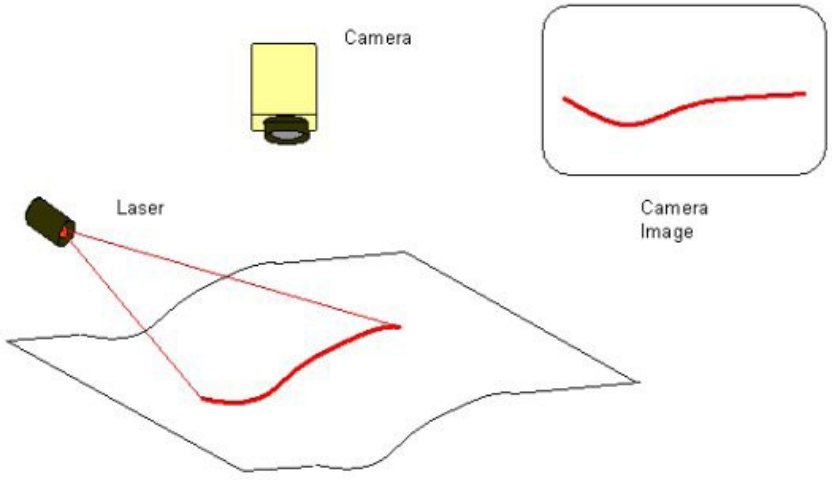

Figure 2.13: Optical system diagram [Wang, 2005].

Triangulation principles are used to calculate the shape of the pavement surface. Figure 2.14 shows the diagram of the system for the case where the laser plane is projected vertically, where: h is the elevation or depression of the pavement surface at a specific point; f is the focal length of the camera; C is the center of the camera; H and L are the respective vertical and horizontal distances of C from the intersection between the laser plane and the camera plane; and y is the distance h captured by the camera image. The values of H, L and f are obtained during calibration. The angles θ and α are calculated as $\theta = \tan^{-1}(H/L)$ and $\alpha = \tan^{-1}(y/f)$. Lastly, $h = L\tan(\theta + \alpha) - H$. Thus, the transverse profile of the section of the pavement is obtained by calculating the value of h for each point of the digitalized laser line.

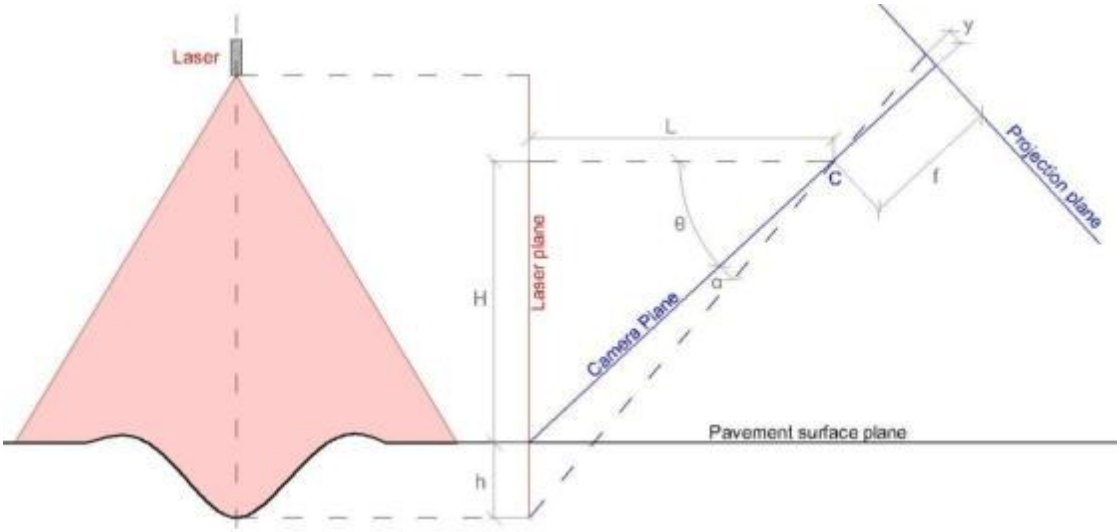

Figure 2.14: Triangulation principle used by optical systems.

It should be noted that the accuracy of the measurements can be affected by environmental factors like spray of water from a wet pavement. The accuracy of the systems depends on the precision, power, and quality of the laser line, as sun light still

can influence the line image quality as sun energy may not be completely blocked in the filter system. The general design of the optic system, camera resolution and performance can also impact the rutting data quality.

Once the pavement profile is obtained, algorithms are applied to calculate the desired rutting indexes. As the survey vehicle moves forward, the camera captures consecutive images of laser lines, which might be used to compute a 3-D representation of the pavement surface, as shown in Figure 2.15 [Li et al, 2009].

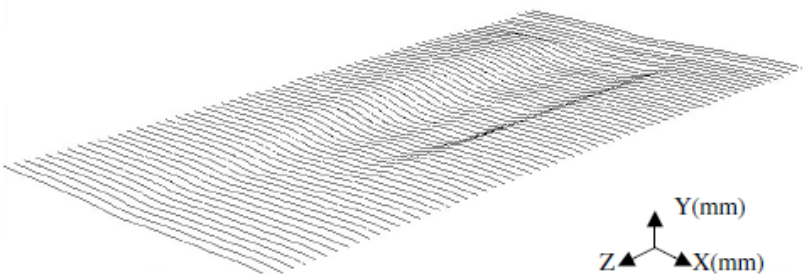

Figure 2.15: 3-D Representation of the pavement surface [Li et al, 2009].

The *Institut National d'Optique* (INO) Laser Rut Measurement System (LRMS) is widely used in the U.S. for collecting network-level rut depth data. Following are brief descriptions of the INO LRMS, the INO Laser Crack Measuring System (LCMS) and the TxDOT 3-D VRUT systems.

INO LRMS and INO LCMS

In 2001, the National Optics Institute of Canada, also known as INO (Institut National d'Optique), working with the Ministry of Transportation of Quebec (Ministère des Transports du Québec) developed a laser system to characterize and measure pavement rutting, called LRMS. In 2009 INO created Pavemetrics Systems Inc., which commercializes the INO LRMS as well as other INO products. INO LRMS hardware is

used and marketed by other companies, such as Mandli Communications Inc., in their rut data collection systems, but using their proprietary algorithms to process the raw data. Thus, different systems with the same hardware could produce different rutting values for the same pavement section due to differences in software and algorithms.

INO LRMS consist of two profilometers that digitize the transverse section of the pavement with 1,280 points (Figure 2.16). These profilometers are mounted on the rear of the vehicle, and each one measures half of the width of the transverse section of the pavement.

Figure 2.16: Pavemetrics INO LRMS mounted on vehicle.

Each profilometer contains a laser and a camera that form the optical system. Custom optics and high-power pulsed laser line projectors allow the system to operate in full daylight or in night-time conditions. The LRMS can acquire full 4-meter width profiles of a highway lane at normal traffic speeds, with two options of maximum sampling rate: 30 or 150 Hz.

The specifications given by the provider are [Pavemetrics INO LRMS Sprec] are:

1. Number of laser profiles: 2
2. Number of 3D points per profile (max): 1,280 points
3. Sampling rate: Standard (30 profiles/s) and High-Speed (150profiles/s)
4. Vehicle speed: 0 to 100 km/h
5. Profile spacing: adjustable
6. Transversal field-of-view (nominal): 4 m (13 ft)
7. Transversal resolution: ±2 mm (0.08 inches)
8. Depth range of operation: 500 mm (@30 profiles/s) or 450 mm (@150 profiles/s)
9. Depth accuracy (nominal): ±1 mm (0.04 inches)
10. Laser profiler dimensions (approx.): 108 mm(W) x 692 mm(H) x 220mm(D)
11. Laser profiler weight (approx.): 12 kg.

INO has also developed the LCMS which according to their specifications, it is capable of collecting up to 4,160 points of the road transverse profile at highways speeds. As shown in Figure 2.17, INO LCMS projects the laser plane vertically onto the pavement surface, as opposed to the INO LRMS, which does it at an angle of 20° with respect to the horizontal.

Figure 2.17: INO LCMS mounted on vehicle [Pavemetrics INO LCMS Spec].

The specifications given by the provider are [Pavemetrics INO LCMS Spec]:

1. Number of laser profiles: 2
2. Number of 3D points per profile (max): 4,160
3. Sampling rate: 5,600 profiles/s
4. Vehicle speed: up to 100 km/h (62 mph)
5. Profile spacing: 5mm (0.2 inches) (adjustable)
6. Transversal field-of-view: 4 m (13 ft)
7. Transversal resolution: 1 mm (0.039 inches)
8. Depth range of operation: 250mm (adjustable)
9. Depth resolution: .5 mm;
10. Laser profiler dimensions (approx.): 428mm(h) x 265mm (l) x 139mm (w)
11. Laser profiler weight (approx.): 10 kg.

TxDOT VRUT 3-D System

In 2009, TxDOT developed an optic system for rutting measurement called VRUT 3-D system. This system, which is currently under evaluation, will replace the five-point acoustic system that TxDOT has been using for the last fifteen years.

The VRUT 3-D system is mounted on the rear of the survey vehicle (Figure 2.18). It consists of a metallic box housing a high-power infrared laser line projector and the high-speed 3-D camera that form the optical system The laser is projected vertically onto the pavement surface. Since the laser projector has a 90° fan angle, the measured width on the pavement will be equal to twice the height at which the laser projector is mounted.

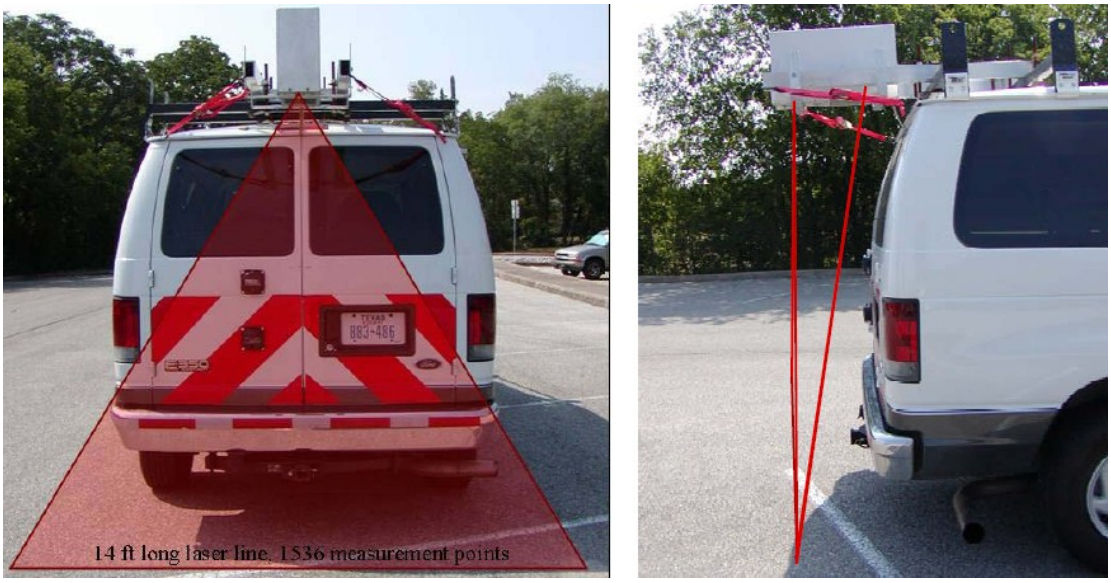

Figure 2.18: TxDOT VRUT 3-D System mounted on survey vehicle [Huang et al, 2009].

According to TxDOT, [Huang et al., 2009] the Center of Gravity Algorithm (CGA) used in the 3-D camera *"gives a final system height resolution sixteen times higher than traditional pixel level laser line detection methods"*. Another interesting characteristic of the system is that the camera used can perform the majority of the image

processing and locate the laser line before sending the data to the host computer, achieving a higher sampling rate compared to traditional optical systems.

The software of the system has also been developed in-house by TxDOT personnel. Figure 2.19 and 2.20 show the intensity and the range image respectively, which are produced concurrently by the 3-D camera. The intensity image is useful for surface feature detection and it is currently only processed for lane stripe and sealed crack detection. The range image (depth image) represents the elevation changes on the pavement surface and is also used to detect the pavement edge, roadside vegetation, curbs, and other lane width limitation information [Huang et al, 2009].

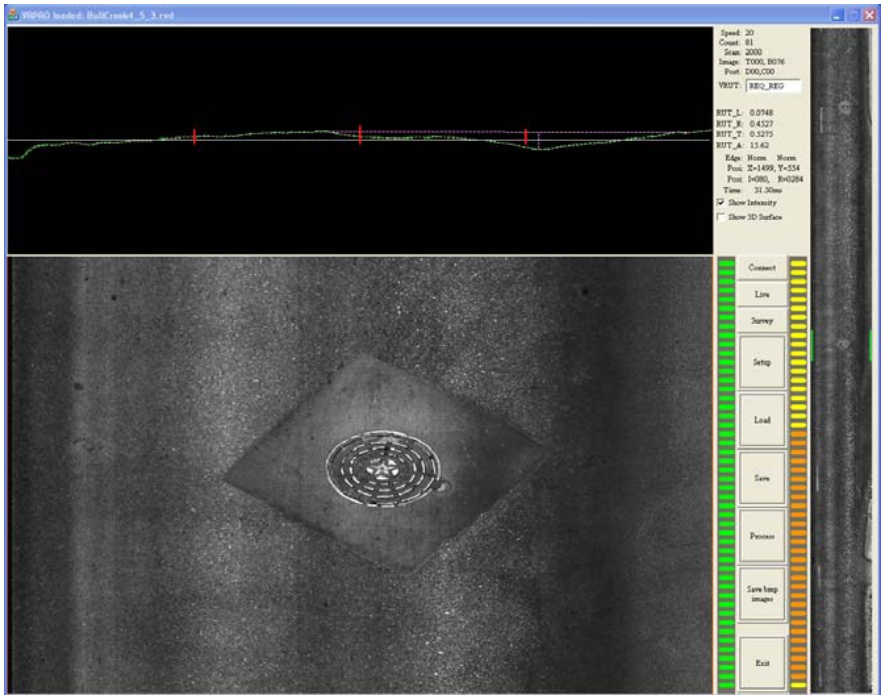

Figure 2.19: TxDOT VRUT 3-D system intensity image display [Huang et al, 2009].

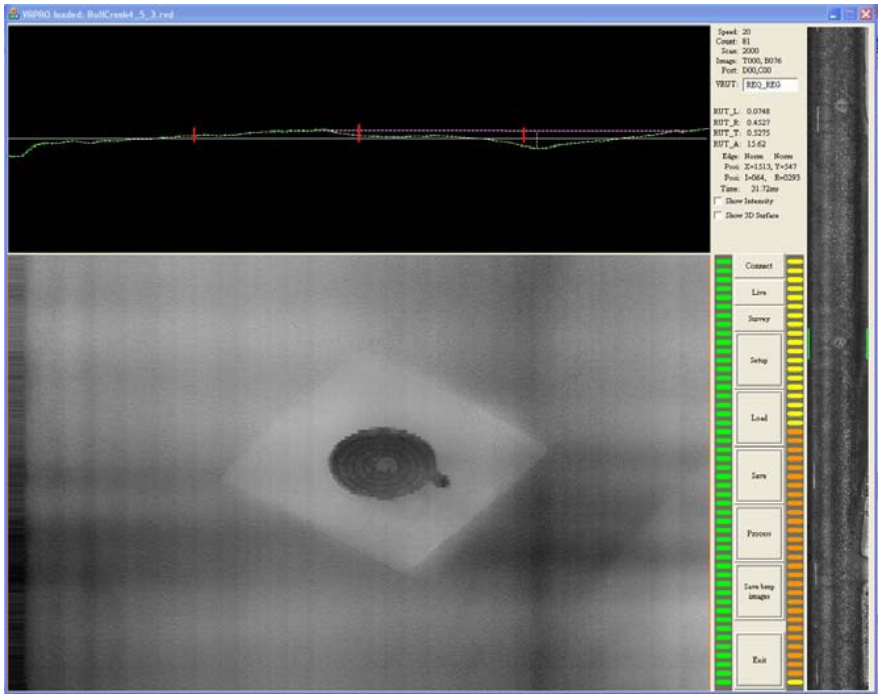

Figure 2.20: TxDOT VRUT 3-D system range image display [Huang et al, 2009].

Figure 2.21 shows a screen capture of a transverse profile measured by the VRUT 3-D system, with an illustration of the rut depth calculation for each wheel-path. The green data points are the measured coordinates of the profile, the white lines are virtual straight edges and the red lines are the maximum rut depth at each profile.

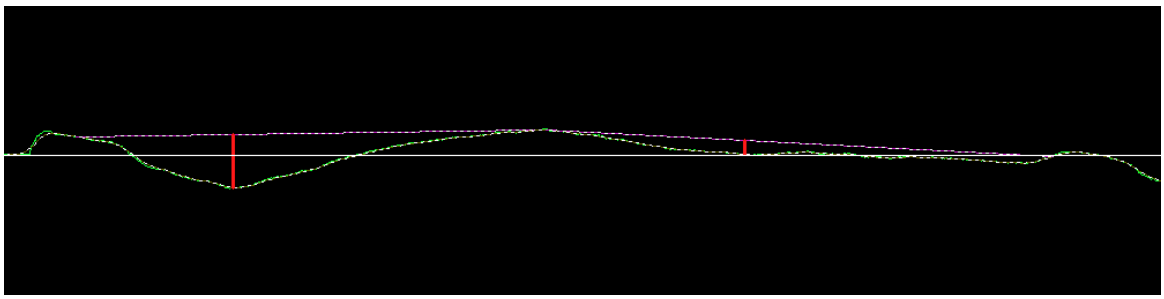

Figure 2.21: Transverse profile measured by VRUT 3-D system [Huang et al, 2009].

The accuracy of the system is not affected by aggregate size due to the filtering effect of averaging twelve consecutive sample profiles [Huang et al, 2009]. Selected VRUT system specifications include the following:

1. Number of laser profiles: 1
2. Number of 3D points per profile (max): 1,536 points
3. Vehicle speed: 10 to 70 mph (16 to 113km/h)
4. Height resolution: 0.03 inches (0.76 mm)
5. Transverse resolution: 0.11 inches (2.79 mm)
6. Longitudinal resolution: network level (1 inch); project level (adjustable)
7. Transversal field-of-view (nominal): 14 ft (4.27m)

Scanning Lasers Systems

Scanning lasers use Phase Measurement Laser Radar technology to measure the profile of a pavement. This technology consists of a laser sensor and a rotating polygonal mirror (Figure 2.22). The laser sensor consists of a transmitter and a detector to measure the distance to the pavement surface. The polygonal mirror changes the direction of the laser light while it rotates, measuring distances of consecutive points along a line. Thus, the scanner sweeps the profile of the pavement. These measurements are then transmitted to a computer which processes the data. Figure 2.22 shows a typical configuration of the scanner, which has a 90 degree field of view and therefore, a scan line length equal to twice the polygon height.

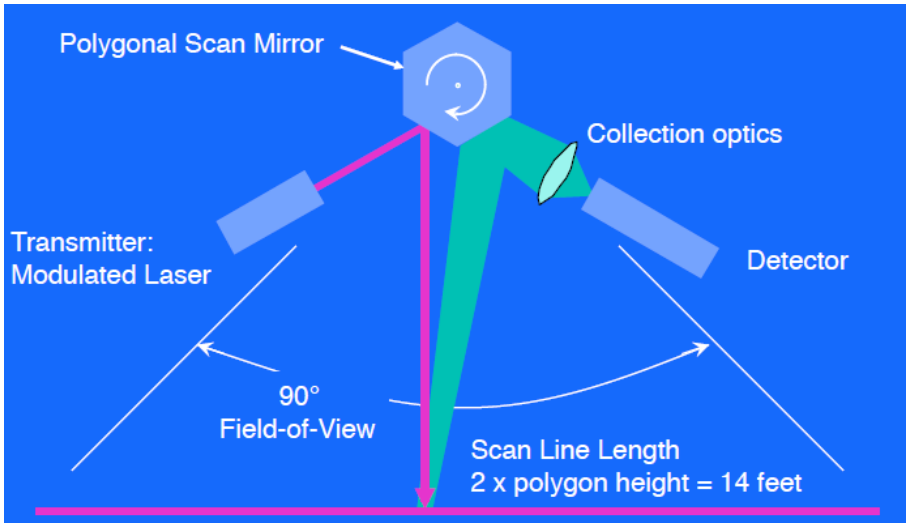

Figure 2.22: Scanning Laser system scheme [Herr, 2001].

The orientation of the scanner plane of measurement depends on the measurement desired (Figure 2.23). A transverse scan obtains the transverse profile of the pavement, which is used to measure rutting. A longitudinal scan might be used to calculate ride quality indexes such as the International Roughness Index (IRI) and Ride Number (RN).

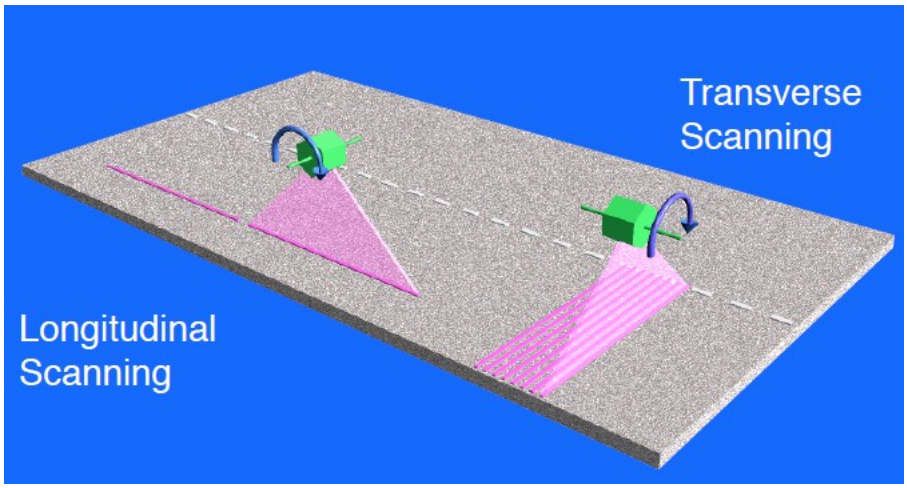

Figure 2.23: Scan orientation [Herr, 2001].

PSI Pavement Profile Scanner

Phoenix Scientific Inc. (PSI) developed a proprietary system, named the Pavement Profile Scanner (PPS), for the Rolling Wheel Deflectometer (RWD). This system was and later adapted by PSI for obtaining pavement condition data such as rut and ride indexes. PSI's PPS scanner is mounted on the rear of the survey vehicle (Figure 2.24) at a height of at least half of the width that is needed to be measured. Mounted at 2.15 meters above the pavement, PPS measures a profile 4.3 meters wide in 0.75 milliseconds. The system takes 943 measurements per transverse profile spaced at a constant angle from the polygonal scan mirror, which are then converted to two-dimensional coordinates. The number and separation of points can be specified by the operator [PSI PPS White Paper, 2004].

Figure 2.24: PSI PPS Scanner mounted on survey vehicle (Herr, 2009)

PPS 2005 specifications given by the provider are [PSI PPS-2005 Spec]:

1. Data Rates and Structure:

- Scan Rate (scan/second): 1000 Hz
- Scan Separation, at 100 km/h: 2.8 cm
- Points per scan: 944 pts.
- Point spacing: center/average/edge 3.8/4.8/7.2 mm.

2. Scan coverage
   - Field of view: ±45°
   - Scan width, polygon centered at 2.15 m: 4.3 m
3. Scan accuracy
   - Spot/line width, cross scan: 22 mm
   - Spot width, along scan, instantaneous 7 mm
   - Precision, center/average/edge of scan (std. dev.) 0.07/0.15/0.25 mm
   - Bias, overall: maximum/nominal average ±0.50/0.00 mm
4. Mechanical
   - Scanner Dimensions: 47 (H) x 51 (D) x 69 (W) cm
   - Scanner Weight: 54Kg

Chapter 3: Rutting Data Collection

This chapter covers the rutting data collection phase, which consisted of the measurement of transverse profiles and Maximum Rut Depth (MRD) values on different pavement sections using manual methods by the researchers to establish reference values and automated data collection systems operated by the study participants. The test sections were selected with the objective of establishing representative conditions encountered on Texas highways as well as cases considered potentially problematic for automated rutting surveys. The manual rutting data collection comprised the measurement of the MRD value, for both the inner wheel-path (IWP) and the outer wheel-path (OWP), using a 6-ft straight-edge and a gage and the measurement of transverse profiles using a laser distance meter and a leveled beam. The automated rutting data collection was performed by five different automated systems that surveyed the sections at highway speeds and reported the transverse profiles and the MRD values.

The chapter is divided into four major sections. The first section explains the experimental variables taken into consideration for the selection of sections. The second section contains a description of the main characteristics of the selected survey sections used in the study along with the main experimental variables encountered in each of them. The third section describes the methods and criteria adopted for the manual measurement of transverse profiles and MRD values. The fourth section of this chapter documents the rutting data collection performed by the automated systems that participated in the survey.

EXPERIMENT DESIGN

The variables considered in the experiment design were included to account for representative characteristics of the Texas flexible pavement highway network and were

selected to evaluate automated data collection methods under a wide variety of conditions. Additional variables were included which were thought to represent a challenge for the automated systems. The error of the measurements produced by the automated systems were expected to be higher than the one reported by the systems manufacturers, which is usually determined under conditions on selected pavements not necessarily representative of the highway network.

A list of experimental variables was identified prior to the selection of sections whereas other variables were added during test section selection as new variables were identified and considered relevant to the study. Rigid pavements were not included in the experiment design since, in Texas, rutting does not affect them. Therefore, only flexible pavements, which constitute approximately 94% of the Texas highway system total mileage, were included in the experiment.

The experimental variables considered for the selection of sections are the following:

14. Pavement surface type, such as dense hot mix asphalt (HMA), Permeable Friction Course (PFC), surface treatment or cold mix patches.
15. Surface texture: coarse or fine.
16. Pavement lane width: narrow to wide lanes (from 8ft to 12ft)
17. Facility type, such as US Highways (US), or Farm-to-Market Roads (FM).
18. Level of rutting (i.e., No Rut, Shallow, Deep, Severe, and Failure)
19. Geometric design: tangent section or presence of horizontal and/or vertical curve; flat or steep grades.
20. Shoulder type: paved or unpaved.
21. Rut width: narrow and wide widths.

22. Type and Presence of center line and/ edge stripping

23. Presence of other distresses, such as sealed and unsealed cracks, shoving or edge drop-off.

24. Presence of constructive joints

25. Presence of grass and vegetation on the edge

26. Presence of patches

27. Variability or localized rutting within a section

28. Other anomalies: such as the effect of channelized traffic in narrow lanes which produces rutting on the centerline, dual rutting in one wheel path from dual wheels, etc.

Variable stripping conditions were included in the test sections since it was known to the researchers that automated data collection vehicle transverse profiles measurements and filtering use the location of stripes as references. The methods used to consider stripping in reporting transverse profiles could potentially affect the accuracy of MRD measurements.

Once the experimental variables were defined, the test sections were selected to ensure that as many of the variables as possible were included in the study.

Some of the survey sections were selected to include two or more possible levels for the same variable, such as change in surface texture from coarse to fine. In addition, sections were selected which exhibited two or more variables that coincided such as a sag curve within a horizontal curve or rutting, cracking and patching within the same rating section.

The length of each survey section was defined as 550-ft, which is approximately the minimum section length used by Texas Department of Transportation (TxDOT) for distresses data collection for their Pavement Management Information System (PMIS). A

total of twenty-six survey sections were finally selected. The next section contains a description of the selected survey sections used in the experiment and the variables accounted by them.

SURVEY SECTIONS

A total of twenty-six 550-ft survey sections were selected for the rutting data collection to cover the experiment design. The first two sections were later discarded after manual data had been collected because they were rehabilitated by the Austin District prior to automated data collection. The remaining twenty-four sections were used for the evaluation of the measurements produced by the automated systems. Figure 3.1 shows a map with the location of these twenty-four sections.

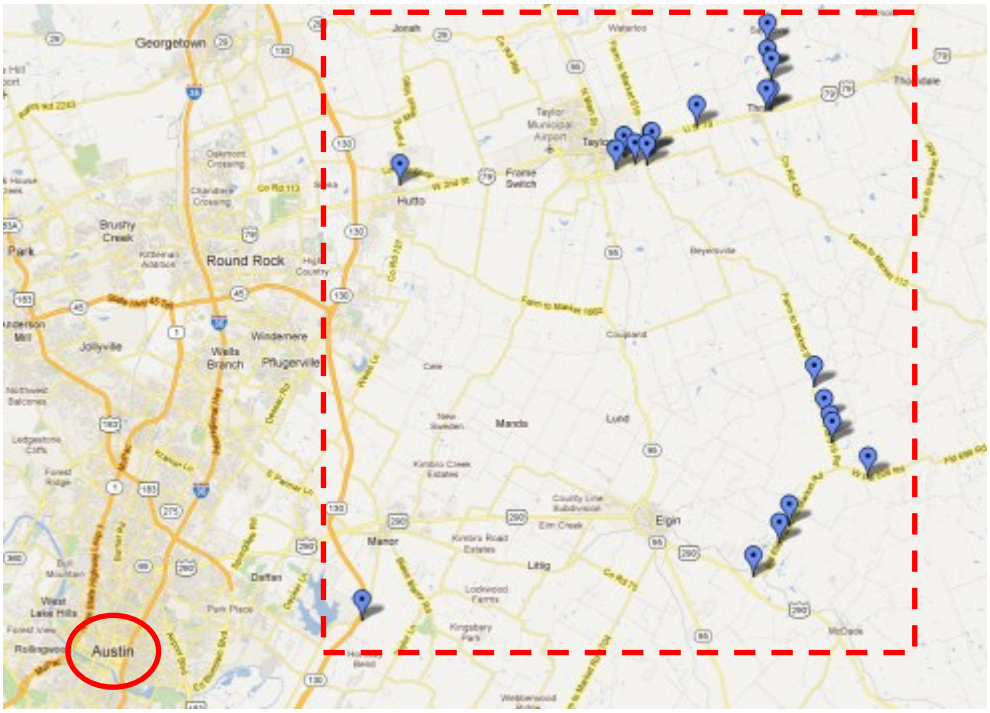

Figure 3.1: Survey section map.

The section locations are indicated by the blue globes and the dashed red rectangle shows the area at which all the sections were contained. As shown in the map all the sections were located north-east from the city of Austin, in the proximity of the cities of Manor, Elgin, Hutto, Taylor and Thrall. The automated systems were able to measure the twenty-four sections departing from Austin and coming back to the same place in approximately six hours.

Section Demarcation

The evaluation of the measurements produced by the automated systems consisted of the comparison between the values reported by each system and the manual measurements (defined as the reference value for the comparison) taken at the same locations. The location of each test section station included in the comparison was marked with paint prior to the rutting data collection so that every participant was aware of the location at which manual measurements were taken. The painted marks were durable and served as a reference marking for all the different automated systems.

Each 550-ft section was divided into stations evenly spaced every 5ft. Therefore, each test section comprised 111 (= 550/5+1) stations, resulting in a total of 2,664 (= 24*111) stations included in the study. The MRD values were measured for both the IWP and the OWP at each station, and therefore 5,328 (=2,664*2) MRD values were reported by each automated system, as well as manually measured. The transverse profiles were measured at the stations located every 25ft, resulting in a total of 23 (= 550/25+1) transverse profiles per section, or a total of 552 (= 23*24) transverse profiles in the study. Each station was numbered according to its progressive distance from the starting point of the section, thus the stations were named: 0, 5, 10, and so on until 550.

Figure 3.2 shows a picture of a section of the study which includes legends indicating the different types of demarcation used. The starting (Station 0) and ending (Station 550) stations of each section were marked painting a double stripe and leaving a 2-in wide area without paint in between to indicate the location of the station (Figure 3.3 shows a close-up picture of this type of marking). Three feet before the first station, and after the last station (travelling in the direction of traffic), a yellow or orange arrow was painted approximately in the center of the lane, big enough to be seen by the driver or data collection operator of the vehicle and indicating the proximity of the starting (or ending) station of the section. The arrow shown in Figure 3.2 is indicating the ending point of the section.

Figure 3.2: Demarcation of survey sections.

The stations spaced every 5ft were marked by painting dots in the inner side of the surveyed lane, as indicated in Figure 3.3. The location of these marks was determined using a surveyor wheel.

Figure 3.3: Mark used to indicate the starting and ending stations of the section.

Figure 3.4 shows a close-up picture of the mark used to indicate the location of the stations at which the transverse profiles were measured (spaced every 25ft). The dimensions of the mark are indicated in the figure.

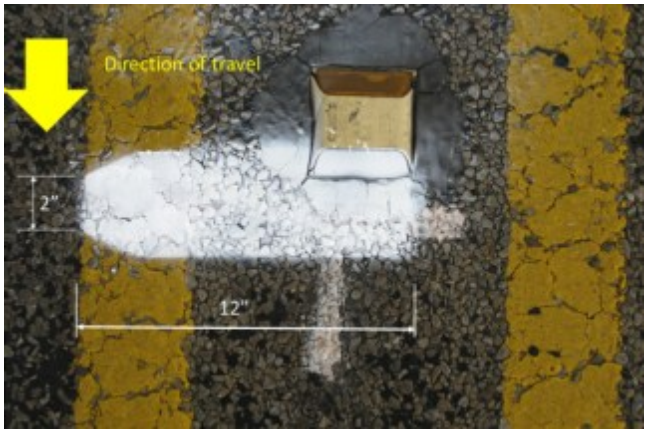

Figure 3.4: Mark used to indicate the stations at which the transverse profiles were measured.

Description of Survey Sections

This section presents the pictures and the main characteristics of the twenty-six selected sites of the study. The number of each section corresponds to the order in which they were selected. The test section name is the highway route designation followed by the numeric order in which they were selected for a particular highway. Thus, "Section 10: FM 619-4" is the 10^{th} section selected for the study, it is located in FM619 and it is the fourth section selected in FM619.

Section 1: FM1660-1

Characteristics of the section:

- Surface texture type: Coarse.
- Lane width: Irregular, between 9.5ft to 11.0ft.
- Shoulder: No paved shoulder.
- Horizontal curve: Straight path.
- Vertical curve: Flat.
- Observed pavement distresses: Extensive sealed and unsealed cracks.
- Additional comments: This section was resurfaced between the reference data collection and the automated measurements. Therefore, it was discarded for the comparison.

Figure 3.5: Section 1: FM 1660-1.

Section 2: FM 1466

Characteristics of the section:

- Surface texture type: Coarse.
- Lane width: Irregular, between 10.0ft to 11.5ft.
- Shoulder: No paved shoulder.
- Horizontal curve: Straight path.
- Vertical curve: Uphill.
- Observed pavement distresses: Several unsealed cracks.
- Additional comments: This section was resurfaced between the reference data collection and the automated measurements and therefore it was discarded for the comparison.

Figure 3.6: Section 2: FM 1466.

Section 3: US 79-1

Characteristics of the section:

- Surface texture type: Fine original pavement surface with coarse patches.
- Lane width: Uniform, 12.0ft.
- Shoulder: Paved shoulder.
- Horizontal curve: Slight curve.
- Vertical curve: Slightly uphill.
- Observed pavement distresses: presence of patches within and between the wheel paths and sealed cracks.
- Additional comments: Possible ponding of water between patches.

Figure 3.7: Section 3: US 79-1.

Section 4: US 79-2

Characteristics of the section:

- Surface texture type: Coarse.
- Lane width: Regular, 12.0ft.
- Shoulder: Paved shoulder.
- Horizontal curve: Straight.
- Vertical curve: Flat.
- Observed pavement distresses: No distresses observed.
- Additional comments: Very open surface texture.

Figure 3.8: Section 4: US 79-2.

Section 5: FM 696-1

Characteristics of the section:

- Surface texture type: Coarse.
- Lane width: Regular, 10.0ft.
- Shoulder: No paved shoulder.
- Horizontal curve: Straight.
- Vertical curve: Flat.
- Observed pavement distresses: Some unsealed cracks and flushing.
- Additional comments:

Figure 3.9: Section 5: FM 696-1.

Section 6: FM 619-1

Characteristics of the section:

- Surface texture type: Coarse.
- Lane width: Regular, 10.0ft.
- Shoulder: paved shoulder.
- Horizontal curve: Straight.
- Vertical curve: Flat.
- Observed pavement distresses: No distresses observed.
- Additional comments:

Figure 3.10: Section 6: FM 619-1.

Section 7: FM 696-2

Characteristics of the section:

- Surface texture type: Coarse.
- Lane width: Irregular, between 10.0ft to 11.0ft.
- Shoulder: No paved shoulder.
- Horizontal curve: Left horizontal curve.
- Vertical curve: Flat.
- Observed pavement distresses: Minor bleeding along wheel-paths.
- Additional comments:

Figure 3.11: Section 7: FM 696-2.

Section 8: FM 619-2

Characteristics of the section:

- Surface texture type: Coarse.
- Lane width: Irregular, between 9.5ft to 11.5ft.
- Shoulder: No paved shoulder.
- Horizontal curve: Straight.
- Vertical curve: Flat.
- Observed pavement distresses: Presence of raveling.
- Additional comments:

Figure 3.12: Section 8: FM 619 -2.

Section 9: FM 619-3

Characteristics of the section:

- Surface texture type: Coarse.
- Lane width: Irregular, between 9.5ft to 10.0ft.
- Shoulder: No paved shoulder.
- Horizontal curve: Straight.
- Vertical curve: Slightly uphill.
- Observed pavement distresses: Minor unsealed cracking.
- Additional comments:

Figure 3.13: Section 9: FM 619-3.

Section 10: FM 619-4

Characteristics of the section:

- Surface texture type: Coarse.
- Lane width: Irregular, between 10.0ft to 10.5ft.
- Shoulder: No paved shoulder.
- Horizontal curve: Straight.
- Vertical curve: Slightly uphill.
- Observed pavement distresses: Presence flushing.
- Additional comments:

Figure 3.14: Section 10: FM 619-4.

Section 11: FM 619-5

Characteristics of the section:

- Surface texture type: Coarse.
- Lane width: Irregular, between 9.0ft to 10.5ft.
- Shoulder: No paved shoulder.
- Horizontal curve: Sharp right curve.
- Vertical curve: Slightly uphill.
- Observed pavement distresses: Presence of patches and several sealed and unsealed cracks, edge drop offs, variable surface coloration
- Additional comments:

Figure 3.15: Section 11: FM 619-5.

Section 12: FM1063-1

Characteristics of the section:

- Surface texture type: Coarse.
- Lane width: Irregular, between 11.0ft to 12.0ft.
- Shoulder: No paved shoulder.
- Horizontal curve: Slight right curve.
- Vertical curve: Flat.
- Observed pavement distresses: Edge drop-off and presence of sealed cracks.
- Additional comments: Section start point just beyond a narrow load zoned bridge. Some stations present centered rut (as shown in picture).

Figure 3.16: Section 12: FM1063-1.

Section 13: FM 1063-2

Characteristics of the section:

- Surface texture type: Coarse.
- Lane width: Irregular, between 10.5ft to 11.0ft.
- Shoulder: No paved shoulder.
- Horizontal curve: Straight.
- Vertical curve: Flat.
- Observed pavement distresses: Some sealed cracks.
- Additional comments:

Figure 3.17: Section 13: FM 1063-2.

Section 14: FM 1660-2

Characteristics of the section:

- Surface texture type: Fine between Station 000 and Station 260 and coarse between Station 260 and Station 550.
- Lane width: Regular, 12.0ft.
- Shoulder: No shoulder (curb and gutter).
- Horizontal curve: Straight.
- Vertical curve: Flat.
- Observed pavement distresses: Several sealed cracks (between 260ft to 550ft).
- Additional comments: This section is located in an urban area, with a posted speed limit of 30mph. Repeatability and reproducibility tests for the manual measurement of MRD were performed in this section.

Figure 3.18: Section 14: FM 1660-2.

Section 15: FM 112-1

Characteristics of the section:

- Surface texture type: Coarse.
- Lane width: Irregular, between 10.5ft to 11.0ft.
- Shoulder: No paved shoulder.
- Horizontal curve: Sharp left curve.
- Vertical curve: Slightly uphill.
- Observed pavement distresses: Severe Bleeding OWP, variable flushing IWP. along wheel-paths and some sealed cracks.
- Additional comments:

Figure 3.19: Section 15: FM 112-1.

Section 16: FM 696-3

Characteristics of the section:

- Surface texture type: Coarse between Station 000 and Station 300 and fine between Station 300 and Station 550.
- Lane width: Regular, 11.0ft.
- Shoulder: Paved shoulder.
- Horizontal curve: Moderate left curve.
- Vertical curve: Slightly uphill.
- Observed pavement distresses: No major distresses observed.
- Additional comments: Variation in surface coloration and texture.

Figure 3.20: Section 16: FM 696-3.

Section 17: FM 696-4

Characteristics of the section:

- Surface texture type: Coarse between Station 165 and Station 390 and fine everywhere else.
- Lane width: Regular, 11.0ft.
- Shoulder: Paved shoulder.
- Horizontal curve: Straight.
- Vertical curve: Flat.
- Observed pavement distresses: Presence of patches.
- Additional comments:

Figure 3.21: Section 17: FM 696-4.

Section 18: FM 973

Characteristics of the section:

- Surface texture type: Fine.
- Lane width: Regular, 12.0ft.
- Shoulder: Paved shoulder.
- Horizontal curve: Sharp left curve.
- Vertical curve: Slightly down-hill.
- Observed pavement distresses: Few sealed cracks.
- Additional comments: Presence of construction joint.

Figure 3.22: Section 18: FM 973.

Section 19: FM 619-6

Characteristics of the section:

- Surface texture type: Coarse.
- Lane width: Irregular, between 11.0ft to 12.0ft.
- Shoulder: No paved shoulder.
- Horizontal curve: Straight.
- Vertical curve: Flat.
- Observed pavement distresses: Several wide unsealed cracks and few sealed cracks.
- Additional comments: Adjacent to Section 20 (as shown in Figure 3.23).

Figure 3.23: Section 19: FM 619-6.

Section 20: FM 619-7

Characteristics of the section:

- Surface texture type: Coarse.
- Lane width: Irregular, between 11.0ft to 12.0ft.
- Shoulder: No paved shoulder.
- Horizontal curve: Straight.
- Vertical curve: Flat.
- Observed pavement distresses: Several wide unsealed cracks and few sealed cracks.
- Additional comments: Adjacent to Section 19 (as shown in Figure 3.24).

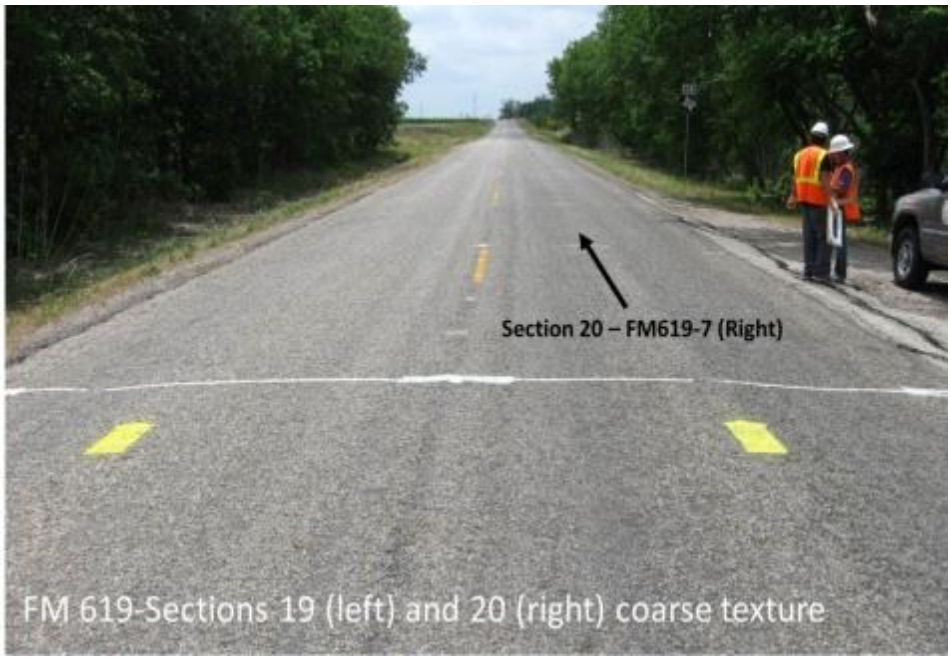

Figure 3.24: Section 20: FM 619-7.

Section 21: US 79-3

Characteristics of the section:

- Surface texture type: Coarse.
- Lane width: Regular, 11.0ft.
- Shoulder: Paved shoulder.
- Horizontal curve: Slight right curve.
- Vertical curve: Flat.
- Observed pavement distresses: No distresses observed.
- Additional comments: Open surface texture. Located immediately preceding Section 22.

Figure 3.25: Section 21: US 79-3.

Section 22: US 79-4

Characteristics of the section:

- Surface texture type: Fine.
- Lane width: Regular, 11.0ft.
- Shoulder: Paved shoulder.
- Horizontal curve: Slight left curve.
- Vertical curve: Flat.
- Observed pavement distresses: No distresses observed.
- Additional comments: Immediately follows Section 21.

Figure 3.26: Section 22: US 79-4.

Section 23: FM 1063-3

Characteristics of the section:

- Surface texture type: Coarse.
- Lane width: Irregular, between 10.0ft to 11.0ft.
- Shoulder: No paved shoulder.
- Horizontal curve: Straight.
- Vertical curve: Uphill.
- Observed pavement distresses: Presence of both sealed and unsealed cracks.
- Additional comments: Adjacent to Section 24 (as shown in Figure 3.27). Repeatability and reproducibility tests for the manual measurement of MRD were performed in this section.

Figure 3.27: Section 23: FM 1063-3.

Section 24: FM 1063-4

Characteristics of the section:

- Surface texture type: Coarse.
- Lane width: Irregular, between 9.5ft to 11.0ft.
- Shoulder: No paved shoulder.
- Horizontal curve: Straight.
- Vertical curve: Downhill.
- Observed pavement distresses: Presence of both sealed and unsealed cracks.
- Additional comments: Adjacent to Section 23(as shown in Figure 3.28). Repeatability and reproducibility tests for the manual measurement of MRD and transverse profiles were performed in this section.

Figure 3.28: Section 24: FM 1063-4.

Section 25: FM 112-2

Characteristics of the section:

- Surface texture type: Coarse.
- Lane width: Irregular, between 10.0ft to 12.0ft.
- Shoulder: No paved shoulder.
- Horizontal curve: Sharp right curve.
- Vertical curve: Uphill.
- Observed pavement distresses: Presence of several sealed cracks.
- Additional comments: Adjacent to Section 26 (as shown in Figure 3.29). Presence of crest vertical curve.

Figure 3.29: Section 25: FM 112-2.

Section 26: FM 112-3

Characteristics of the section:

- Surface texture type: Coarse.
- Lane width: Irregular, between 10.5ft to 11.5ft.
- Shoulder: No paved shoulder.
- Horizontal curve: Sharp left curve.
- Vertical curve: Downhill.
- Observed pavement distresses: Presence of several sealed cracks.
- Additional comments: Adjacent to Section 26 (as shown in Figure 3.30). Presence of crest vertical curve.

Figure 3.30: Section 26: FM 112-3.

Summary of Survey Section Characteristics

Table 3.1 presents a summary table with the main characteristics of the sections at which rutting data was collected.

Section number	Facility type	Surface texture	Lane Width	Horizontal curve	Vertical curve	Shoulder Presence	Observed distresses
1	FM	*Discarded for comparison due to later maintenance treatments.*					
2	FM	*Discarded for comparison due to later maintenance treatments.*					
3	US	Both	12.0’	slight right	uphill	Yes	Several patches
4	US	Coarse	12.0’	No	No	Yes	No
5	FM	Coarse	10.0’	No	No	No	No
6	FM	Coarse	10.0’	No	No	Yes	No
7	FM	Coarse	10.5’	slight left	No	Yes	Some flushing
8	FM	Coarse	10.5’	No	No	No	No
9	FM	Coarse	10.0’	No	uphill	No	Some flushing
10	FM	Coarse	10.5’	No	uphill	No	Flushing
11	FM	Coarse	10.0’	sharp right	uphill	No	Sealed cracks
12	FM	Coarse	11.5’	slight right	No	No	Sealed cracks
13	FM	Coarse	10.5’	No	No	No	Sealed cracks
14	FM	Both	12.0’	No	No	No	No
15	FM	Coarse	10.5’	sharp left	uphill	No	Flushing, cracks
16	FM	Both	11.0’	slight left	uphill	Yes	No
17	FM	Both	11.0’	No	No	Yes	No
18	FM	Fine	12.0’	sharp left	downhill	Yes	No
19	FM	Coarse	11.5’	No	No	No	Several cracks
20	FM	Coarse	11.5’	No	No	No	Several cracks
21	US	Coarse	11.0’	slight right	No	Yes	No
22	US	Fine	11.0’	slight left	No	Yes	No
23	FM	Coarse	10.5’	No	uphill	No	Sealed cracks
24	FM	Coarse	10.5’	No	downhill	No	Sealed cracks
25	FM	Coarse	11.0’	sharp right	uphill	No	Sealed cracks
26	FM	Coarse	11.0’	sharp left	downhill	No	Sealed cracks

Table 3.1: Summary of main characteristics of survey sections.

Table 3.1 shows the main experimental variables and their levels for the selected pavement sections. In addition to the characteristics presented in Table 3.1, other

variables, such as presence of inner and outer stipe, were also taken into account for the analysis of the measured data.

The lane width of the stations located every 25-ft of each section were determined during the transverse profiles manual measurement. The lane width values reported in Table 3.1 are the average of the twenty-three lane width measured at each section. As indicated in the description of each site, some of the sections presented a variable lane width along the 550-ft.

The type of surface texture, as well as the presence and grade of horizontal and vertical curves were visually determined at site, and not based on measurements.

MANUAL DATA COLLECTION OF RUTTING

The manual rutting data collection comprised the measurement of transverse profiles at stations every 25-ft and the MRD values for both wheel-paths at stations every 5-ft. The values manually measured were used as the reference values for the evaluation of the precision and bias of the automated measurements.

All the manual measurements were performed by the research team under the supervision of an experienced distress rater.

The surveyed lane was closed to the traffic during the manual measurements. For each section, both the 23 transverse profiles and the 222 MRD (111 values at each wheel-path) values were measured the same day and simultaneously to minimize the use of traffic control.

The time required to complete the manual data collection was approximately three to four hours per section involving between five and six people (three people involved in the MRD measurements and two or three people for the transverse profiles). Manual rut data collection was performed during daylight conditions, and the pavement surface was

dry. Of the twenty-four sections used for the comparison, the first manual rutting data collection was performed on February 22nd, 2011, and the last on June 27th, 2011. The following sections describe the methodology and criteria adopted during the manual rutting data collection.

6-ft Straight-edge Maximum Rut Depth Measurement

The MRD values for both the IWP and the OWP were measured using a 6-ft straight-edge and a gage. The procedure adopted for the measurement of the MRD is the one described in the ASTM standard *"E1703/E1703M – 10: Standard Test Method for Measuring Rut-Depth of Pavement Surfaces Using a Straightedge"*. The procedure consisted of placing the straight-edge on the pavement perpendicular to the direction of traffic, and measuring the maximum distance between the pavement surface and the bottom of the straight-edge, taken perpendicularly to the straight-edge. In order to find the MRD of the wheel-path, the straight-edge was moved laterally to both sides and the depth was measured at different locations between the two contact areas of the straight-edge and the pavement surface, until the maximum depth was found.

Four raters performed more than 95% of the manual MRD measurements; two additional raters collected the remaining 5%. Figure 3.31 shows one rater per wheel-path manually measuring the MRD values at Section 24. As shown in the picture, in the majority of cases, the raters did not take the MRD measurements at the same station in the same moment in order to have enough free space available at the sides to laterally move the straightedge when looking for the MRD value. A third person recorded the readings being collected by the raters in a spreadsheet prepared for the experiment.

Figure 3.31: Manual measurement of MRD.

There were particular cases encountered during the manual data collection for which guidance is not provided in the ASTM standard. For these cases, the research team discussed the best approach at the site and adopted the same approach subsequently for consistency.

An example of these particular situations is the presence of construction joints whose size and shape made them capable of ponding water. Since the potential of ponding water is a major problem associated with rutting, the researchers decided to consider the depression formed by the joint when measuring the MRD.

Another example, in which the e researchers developed criteria for a condition not addressed in the standard, involved cases in which one of the maximum points of the IWP MRD was located outside the limits of the lane being surveyed; i.e. the rut projected into the opposing lane. For these cases, the raters placed one end of the straight-edge a maximum of 12in outside of the center line inner stripe, in order to reach the maximum

point. Although for these cases one of the support points of the straight-edge was outside of the lane limits, the point at which the MRD was located was always encountered within the lane limits. This situation is illustrated in Figure 3.32. The left maximum point is located between the two centerline stripes and therefore outside the lane width. This condition was found to be more prevalent for deep ruts on narrow Farm to Market roads as in this section.

Figure 3.32: Example of MRD with left most max point outside the lane width.

The two measuring gages used in the study consisted of 6in long, 0.25in wide and 3in high aluminum wedges, graduated to 16^{th} of an inch. Figure 3.33 and Figure 3.34 show a picture of the length and the width of the rut wedges, respectively. The adopted standard specifies a minimum of 0.75in for the width of the rut wedge in order to span areas of aggregate loss and texture. Although the wedges used in the study are narrower than the minimum width specified, their length made them long enough to span the aggregates and therefore, considered acceptable by the research team.

When the reading from the rut wedge was in between two marks, the value was rounded up. Thus, if a reading was in between the 8/16in and 9/16in marks, the reported value was 9/16in.

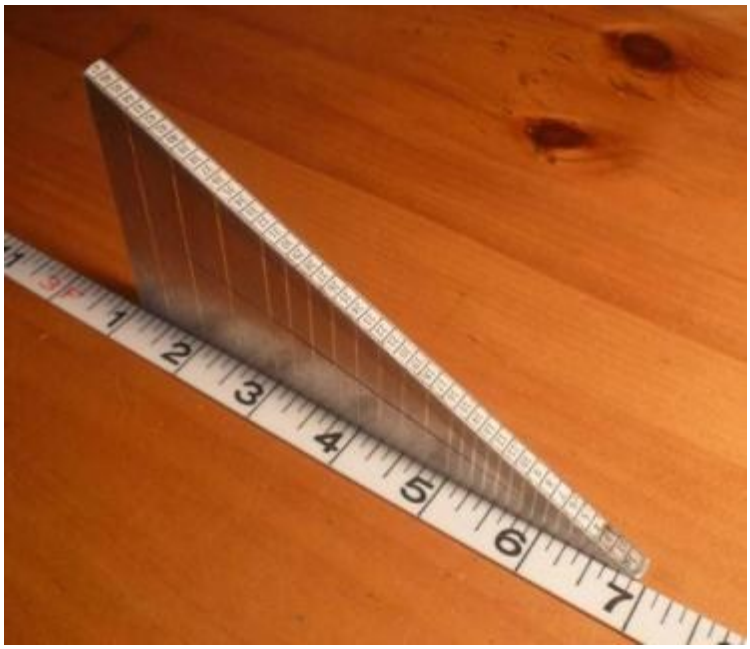

Figure 3.33: Rut wedge length.

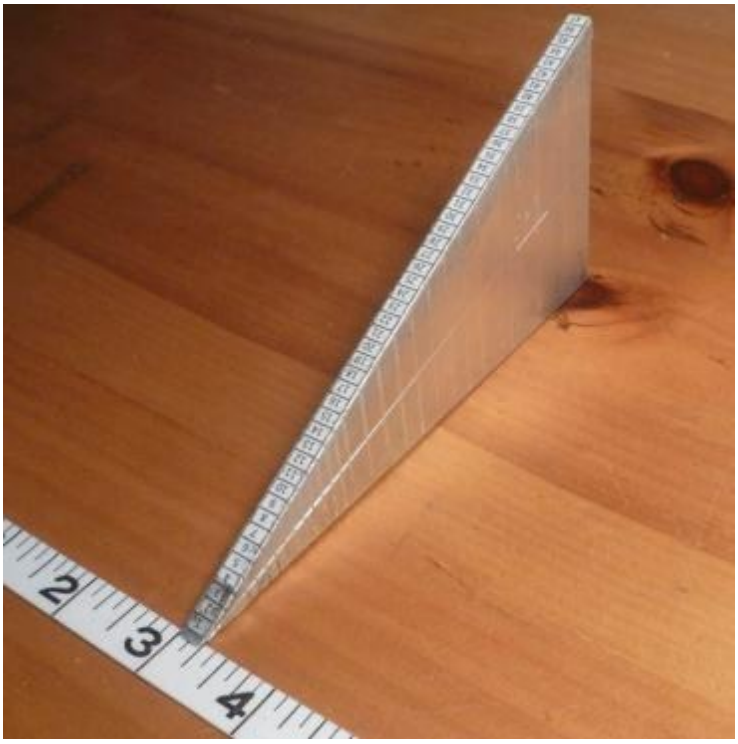

Figure 3.34: Rut wedge width.

Manual Measurement of Transverse Profiles

One transverse profile was collected every 25-ft, for a total of 23 profiles (stations) per pavement section. Figure 3.35 shows the set-up of the system used for measuring the coordinates of the transverse profiles and Figure 3.36 shows a close-up picture of the laser distance meter used. The system developed for this study (referred to by the researchers as the "Leica System") included:

- Laser distance meter Leica DISTO D8 with a reported accuracy of ±1.0mm [Leica Geosystems DISTO D8 Specifications];
- a 13.5ft long 6061-T6 aluminum structural channel beam C6"x1.92"x0.2";
- two tripods (one geared);
- a Mitutoyo 960-616 precision level with a 0.00024"/12" Sensitivity and ±0.00017" accuracy [Mitutoyo, Small Tool Instruments and Data Management Specifications];
- and the data acquisition system which consisted of a Panasonic Toughbook computer connected with the laser distance meter though a Bluetooth connection.

The beam was graduated in 6in increments along the top from 0 to 144in with two additional marks at -3in and 147in, comprising a total of 27 marks covering a maximum measuring width of 150in.

Figure 3.35: Leica Laser System for the measurement of transverse profiles.

Figure 3.36: Leica Laser distance meter.

The procedure for the collection of coordinates for each transverse profile consisted of placing 2in wide masking tape transversally along the lane width, then,

positioning and leveling the beam, and, finally, taking the readings. The masking tape was placed to bridge cracks and coarse aggregate macro-texture which might introduce error for the MRD calculation. The positioning of the beam consisted of moving the beam until the laser light projected vertically from the zero mark of the beam to the center of the center line paint stripe closest to the test section. Once the zero mark was aligned with this stripe, the laser light was projected at different points along the beam to check that the C beam was correctly placed over the surface of the tape. The position of the beam was corrected as necessary. The leveling of the beam was done to ensure the same reference plane for all the transverse profiles. The precision level was centered on the top of the beam and the height of the outer tripod was adjusted until the beam was leveled. Once set up was completed and checked, the Leica D8 was used to measure, the distance between the top of the beam and the pavement surface at each mark on the beam. The mark on the beam was determined as the "x" coordinate and the reading from the laser distance meter was the "z" coordinate for each profile point. As shown in Figure 3.35 and 3.36, the operator placed the laser distance meter in the "x" coordinate being measured and the laser was set to take automatic readings every 4 seconds. If the beam projected beyond the end of the pavement and a reading was therefore outside the lane width, it was not collected. As an example, Figure 3.37 shows the collected coordinates (red points) in inches of the transverse profile of a particular station on FM1063. The origin of the coordinates (x = 0, z = 0) was placed at the center of the inner stripe. Therefore, the "z" coordinates of all the points are relative to the "z" reading at x=0 (second point).

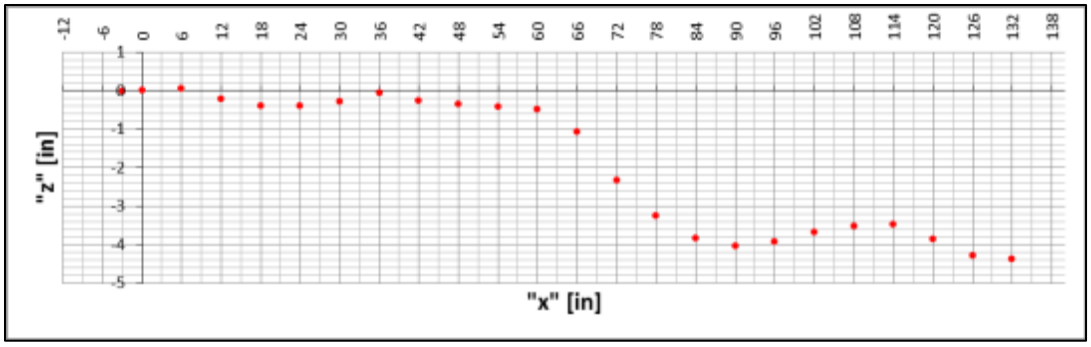

Figure 3.37: Transverse profile readings; “x”: transverse direction, “z”: depth.

From the twenty-four measured coordinates plotted in Figure 3.37 it is possible to clearly observe the shape of the pavement surface at that station. The IWP rut depression spans x=6in to x=36in whereas the OWP rut depression spans from x=60in to x=114in. The lane width of each measured station was determined as the last valid measured point of the transverse profile. For this particular case, the last valid point was measured at x=132in, therefore, the lane width of the station was determined as 11ft.

AUTOMATED DATA COLLECTION OF RUTTING

The transverse profiles and the MRD values for both wheel-paths were automatically measured at the same stations where the manual measurements were taken, by five different automated systems: TxDOT’s 3-D VRUT system, Pathway’s PathRunner XP system, Dynatest’s 5051 Mark III system, Roadware’s ARAN 9000 system and Applus’ RCMS system. Each participant operated an optical system capable of measuring the continuous transverse profile at highway speeds.

Figures 3.38 to 3.42 show the equipment used by each participant for the rutting data collection. The red and yellow regions in the pictures were drawn to indicate the laser and camera planes, respectively, and the dashed blue lines indicate the location of the pavement surface points being measured.

While the sensors used by each of the participants consisted of a laser and a camera, the configuration of the system as well as the number of sensors varied. Both TxDOT and Applus' systems project the laser plane perpendicularly to the pavement surface whereas the remaining systems project the laser plane at an angle. Pathway's system projects the laser at an angle closer to perpendicular plane than both Dynatest and Roadware's systems.

Regarding the number of laser sensors used by each participant, TxDOT's system uses one laser sensor and one camera contained in a single housing (Figure 3.38). Pathway's system uses one camera and two lasers (one per wheel-path) housed separately (Figure 3.39) and the remaining systems use two lasers and cameras (one per wheel-path) (Figure 3.40 to 3.42).

Figure 3.38: TxDOT' system for the automated measurement of rutting.

Figure 3.39: Pathway' system for the automated measurement of rutting.

Figure 3.40: Dynatest' system for the automated measurement of rutting.

Figure 3.41: Roadware' system for the automated measurement of rutting.

Figure 3.42: Applus' system for the automated measurement of rutting.

The hardware of both TxDOT's and Pathway's systems were developed in-house whereas the remaining participants used the hardware developed by INO. Both Dynatest and Roadware used INO Laser Rut Measurement System (LRMS) sensors and Applus used INO Laser Crack Measurement System (LCMS) sensors. The filters and algorithms (coded in the data processing software) for the calculation of the rut indexes is also proprietary and not made available to the research team. It is also interesting to consider that Applus' sensors were mounted on a trailer, whereas the other systems' sensors were directly mounted on the rear of a van.

Since all the participants used different algorithms to process their measured transverse profiles, the results could potentially be different even for the case of participants that used the same type of sensors.

Figure 3.43: TxDOT system's control unit.

All of the systems were equipped with a control unit installed in the cargo compartment of the survey vehicle, except for the system used by Applus. Each system required two people to perform the rutting data collection: one to drive and one to operate the host computer. Figure 3.43 shows the control unit of TxDOT's system and the space designated for the operator of the host computer.

Each participant measured each of the twenty-four sections three times and reported their best estimate of the transverse profile coordinates and MRD values of each wheel-path for all the indicated stations of the experiment. The author accompanied each participant during their data collection to guide them along the route, to document their system, and to record the speed and number of times each section was measured. The participants were requested to run each section a maximum of three times and at a speed between 45 and 50 mph, except for the sections 14, 25 and 26 whose posted speed limit were 30, 35 and 40 mph, respectively.

All the participants were able to complete the twenty-four sections in approximately six to eight hours without major difficulties, except for one vendor that had to cancel the data collection in two opportunities due to technical problems with their system.

Chapter 4: Analysis of Rutting Measurements

This chapter presents the analyses performed on the manual rutting data measured to establish the reference values, and the rutting and transverse profile data reported by the five automated rut measurement systems. The chapter is divided into three major sections: Analysis of Manual Measurements; Analysis of Automated Measurements; and Analysis of the Effect of the Experiment Factors on the Automated Measurement Errors.

The first section presents the results of the experiments conducted to estimate the precision of the manual measurements of the transverse profile coordinates and the Maximum Rut Depth (MRD) reference values.

The second section presents the processing and analysis performed on the rutting data reported by the participants. The analysis of each participant's measurements for both the transverse profiles and the MRD values consisted of the comparison between the reported values and the reference values. Different statistics, such as bias and precision, were computed for each participant's measurement errors to evaluate their individual performance and to establish a ranking.

The third section of this chapter contains the analysis performed to determine the effect that different characteristics of the roadway, such as the lane width, had on each participant's measurement errors.

ANALYSIS OF MANUAL MEASUREMENTS

The manual measurements of rutting consisted of the measurement of MRD values using a 6-ft straight-edge and the measurement of transverse profiles coordinates using a laser distance meter and a leveled beam. The manual measurements were used as the reference values for determining the bias and precision of the different automated rut measurement systems. An experiment was conducted to measure the variability of the

results produced by each manual method in order to estimate the precision of the reference values of the study. The precision of each method is a consequence of the combination of different sources of variation, which are defined as intermediate precisions. Examples of the sources of variability of the manual measurements performed in this study were: the participation of more than one rater; the variability of each rater, which depended on factors such as climatic conditions and fatigue; and the gage precision, among others.

As described in Chapter 3, the manual rutting data collection for each section was completed in three to four hours and involved two teams of multiple raters, which simultaneously measured the 222 MRD values and the 23 transverse profiles of the section. Field measurements were taken from February to June under a wide range of temperatures: from around 35°F to over 105°F with measured pavement temperatures up to 147°F. The tedious and repetitive processes involved in the manual data collection, the prolonged time under extreme temperatures and many other factors, such as coarse pavement surface texture, were expected to affect the operator and therefore the precision of the measurement.

Ideally, in order to determine each intermediate precision, an experiment combining all these factors should have been conducted. However, the large number of factors affecting the overall variability of the manual methods used in this study would make this ideal experiment impractical. Therefore, the precision of the manual measurements was estimated by measuring the spread of the results obtained in an experiment in which the different raters measured the same stations under conditions which were expected to cause an increase in the variability in the measurements. These unfavorable conditions were: very high temperatures; fatigue, since the experiment was

conducted after the raters performed several measurements in the section; and a pavement with coarse surface texture. Thus, the resulting variability would reflect a worst case condition and the estimated value for the precision of the manual measurement is therefore considered a conservative estimate.

One experiment was designed for estimating the overall precision of the manual measurements of transverse profiles and a second one for the MRD values. Both experiments were conducted at the same test site (Section 24). The results and conclusions of both experiments are presented in the following two sub-sections.

Precision of the Transverse Profiles Manual Measurements

The precision of the manually measured transverse profile coordinates was estimated by measuring the variability of different operators who collected data points for different transverse profiles under extreme conditions. Three operators were involved in the experiment. These three operators participated in the majority of the manual measurements of transverse profiles of the twenty-four sections of the study. Each operator measured the last five transverse profiles of Section 24: from Station 450 to Station 550. During the measurement of each transverse profile, the operator in charge performed all of the steps involved in the process of collecting data with the Leica Laser System, which were described in Chapter 3. Therefore, the operator placed the masking tape, positioned and leveled the beam, and took the readings. Once all the coordinates were measured, the operator removed the masking tape in order not to influence the next operator's process of measurement.

As an example, Figure 4.1 shows the transverse profile coordinates manually measured by the three operators at Section 24, Station 550. The blue points in the chart

are the coordinates measured by Operator 1, the red ones by Operator 2 and the green points by Operator 3. All the plotted coordinated are expressed in 16^{th} of an inch.

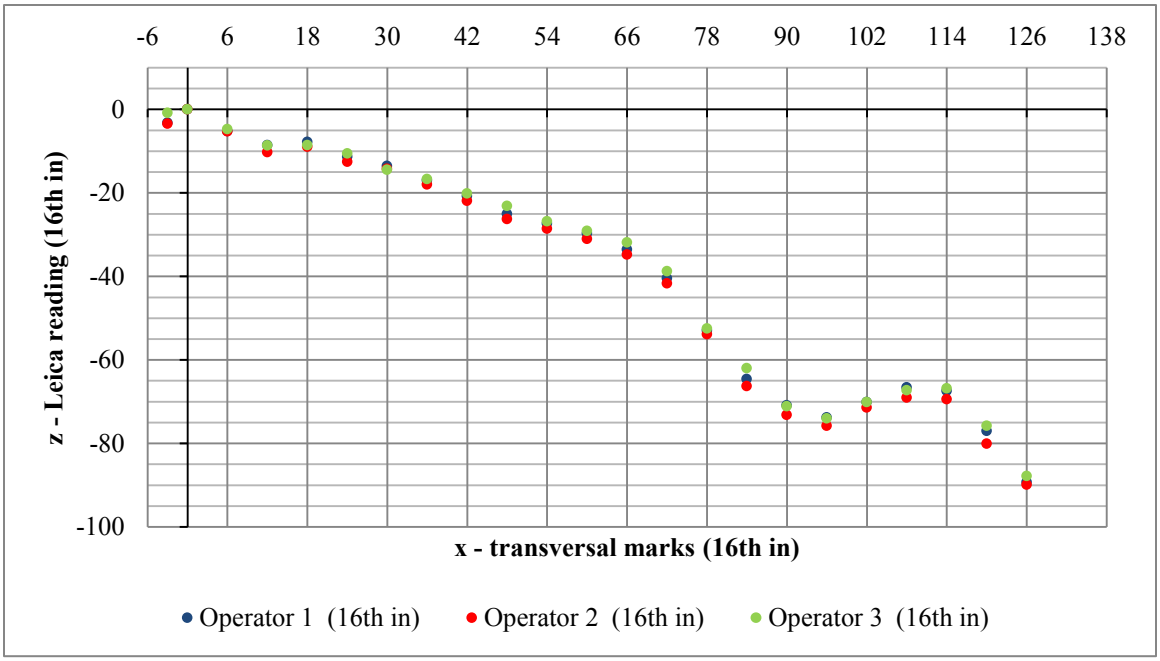

Figure 4.1: Transverse profile coordinates manually measured by 3 different operators.

As explained in Chapter 3, the readings were taken from the left to the right side (in the direction of traffic movement), starting at 3 inches to the left of the center of the inner stripe, and stopping if the next data collection point was located after the edge stripe or the pavement edge. The lane width of that station was defined as the difference between the first and last valid "x" coordinate measured. During the experiment it was observed that for two of the three measured profiles, the total number of measured valid points by one of the operators differed by one point, thus obtaining different lane width for the same profile. This particular section does not have a pavement edge stripe and the lane width is variable (see more information about the section in Chapter 3). These

factors introduced variability in determining the lane width value. The disagreement in the number of valid points for those profiles could also have occurred due to differences in the alignment of the beam. The lane widths of the stations were not used for the evaluation of the precision and bias of the automated rut measurement systems, but for studying the effect of the experimental variables on the error the automated measurements.

The transverse profiles were measured after the operators collected profiles for the previous 18 stations (from Station 000 to Station 425) in order to account for the expected higher variability of the results due to fatigue of the operators. This factor was exacerbated by the fact that the experiment was carried out under high temperature conditions.

Once the coordinates of the five transverse profiles were measured, the three operator's "z" (depth) values measured at each "x" (transverse location mark) coordinate for each of the five stations were analyzed. The error of each measurement was simply calculated as the difference between the measured depth value and the average of the three depth values measured for the same "x" coordinate. Therefore, three error values were computed for each transversal mark at each of the five measured stations.

The total number of measured coordinates considered in the experiment for estimating precision was 327. Figure 4.2 presents the histogram of the measurements errors of the experiment. Six error ranges were established to categorize the data. The horizontal axis contains the error range shown in 16^{ths} of an inch. The left vertical axis represents the number of observations for each error range which is illustrated by the vertical bars and cumulative percentages (right vertical axis) by the curve.

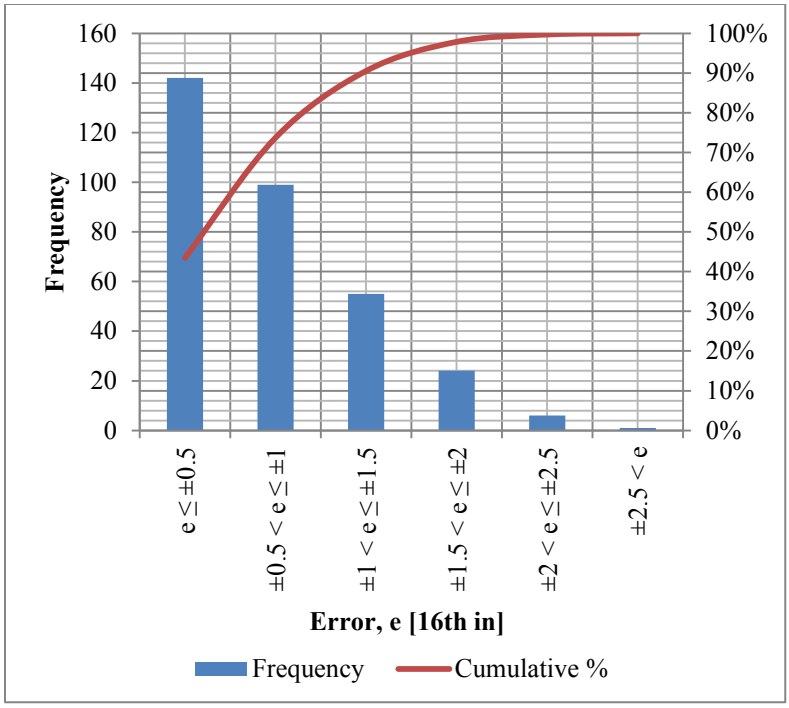

Figure 4.2: Histogram of errors of transverse profiles manual measurements.

Table 4.1 reports the measurement errors below which selected cumulative frequencies fall. Therefore, the difference between the coordinate 'z' depth value and the average of the three measured coordinate 'z' depth values (one per operator), was smaller than ±1.76 16th of an inch for 95% of the measurements. The standard deviation of the 327 measurements errors, which is also an estimator of the precision of the manual measurements, was equal to 0.89 16^{ths} of an inch.

Cumulative (%)	Error, e [16th in]
75%	e < ±1.04
90%	e < ±1.44
95%	e < ±1.76
99%	e < ±2.28

Table 4.1: Errors of transverse profiles manual measurements below which selected cumulative frequencies fall.

Precision of the Maximum Rut Depth Manual Measurements

The precision of the manual MRD measurements was also estimated by measuring the variability of different raters who measured the MRD values of both wheel-paths at the same stations under extreme conditions. For this experiment, four raters, who had measured more than 95% of the total MRD values of the study, performed measurements at sixty-two consecutive 5' stations (from Station 125 to Station 430) – Section 24. This exercise was carried out under high temperatures and the raters had performed actual test measurements for use in the study for a minimum of one hour prior to the experiment. Each of the four raters measured the MRD values for both wheel-paths at the sixty-two consecutive stations of Section 24. Therefore, a total of 248 (=62*4) values per wheel-path, or a total of 496 (=248*2) values for both wheel-paths, were obtained for determining the variability of the measurements.

Figures 4.3 and 4.4 illustrate the longitudinal distribution of the MRD values for the inner wheel-path (IWP) and the outer wheel-path (OWP), respectively. The horizontal axis represents the station number and the vertical axis represents the MRD values measured at each station in 16^{ths} of an inch. The blue, red, green and purple colors were used to distinguish the measurements taken by each of the four raters at each station.

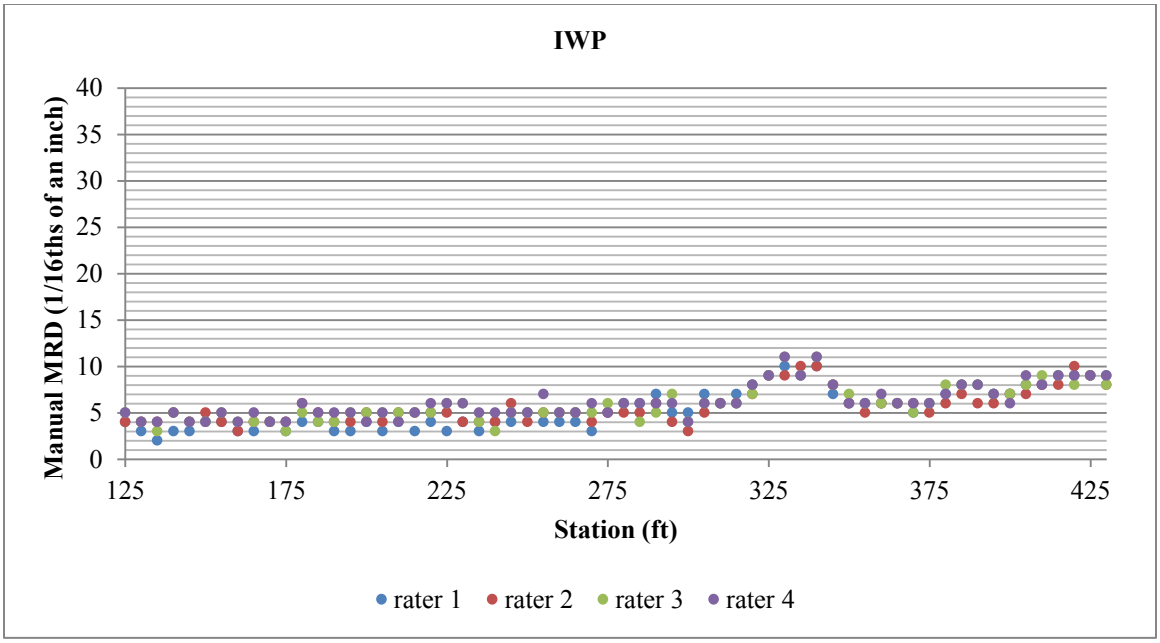

Figure 4.3: IWP MRD values manually measured by four different operators.

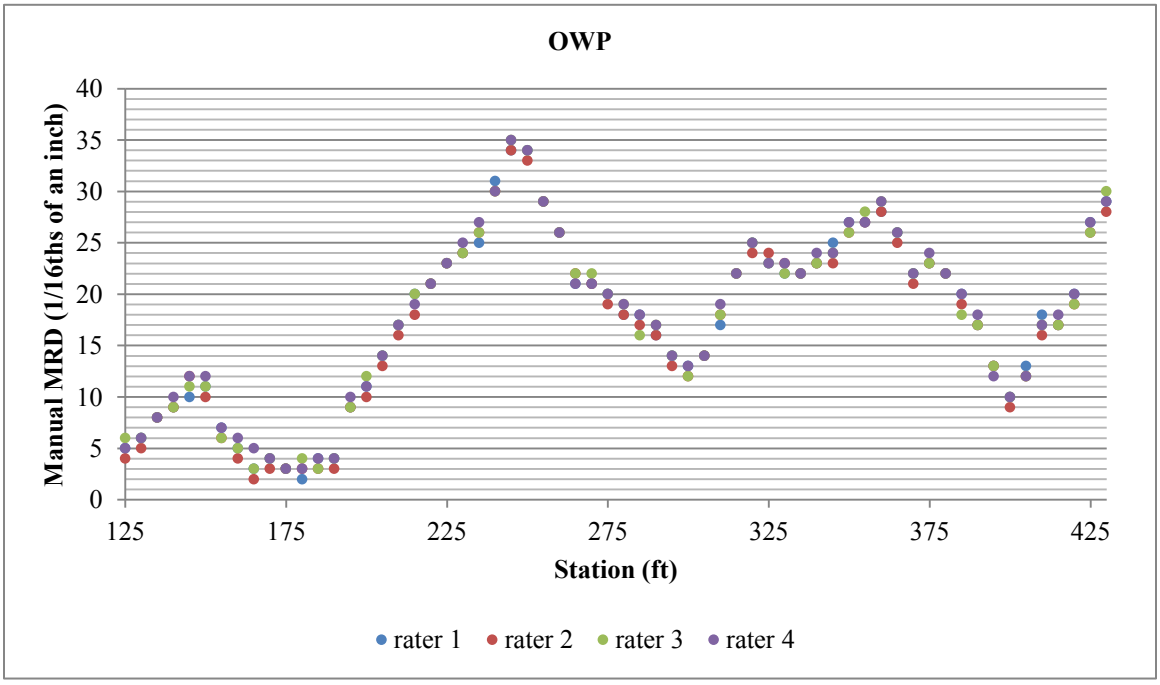

Figure 4.4: OWP MRD values manually measured by four different operators.

The error of each measurement was computed as the difference between the measured value and the average of the four measured MRD values for the same station. Therefore, four measurements errors were computed for each wheel-path at every station.

Figure 4.5 shows the histogram of the manual MRD measurement errors for each wheel-path. The horizontal axis contains the error range shown in 16ths of an inch. The left vertical axis represents the number of observations for each error range which is illustrated by the vertical bars and cumulative percentages (right vertical axis) by the curves.

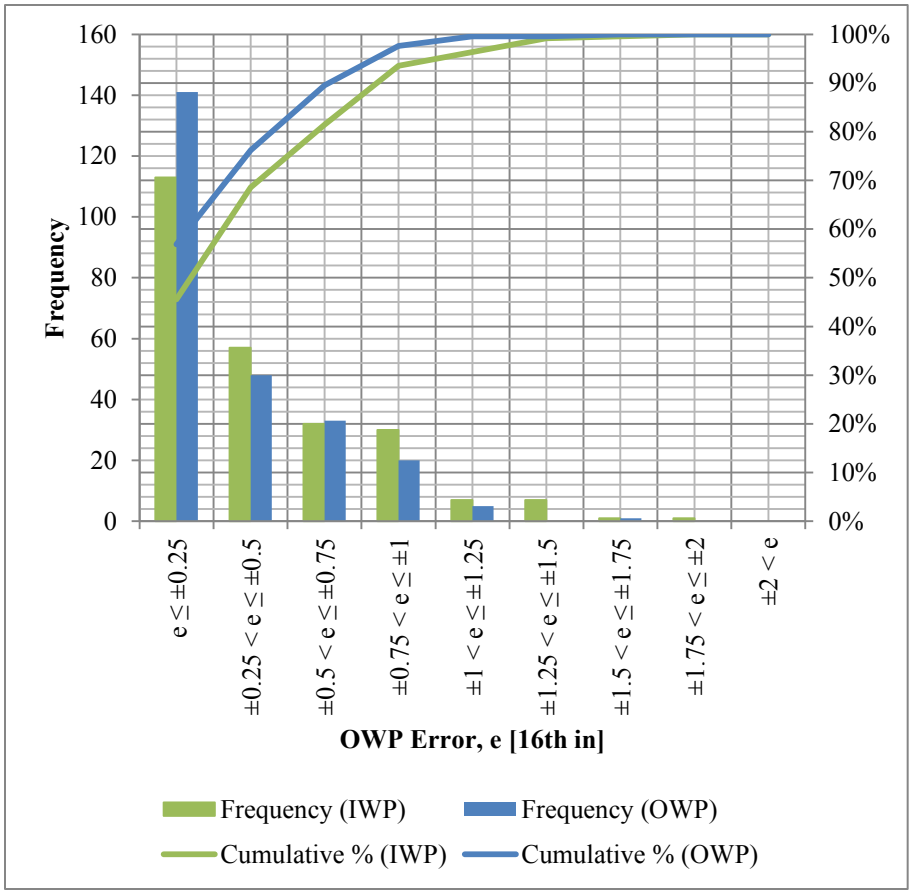

Figure 4.5: Histogram of errors of MRD manual measurements.

Table 4.2 reports the MRD measurement errors below which selected cumulative frequencies fall, for each wheel-path separately and combined. As reported, 96% of the MRD values manually measured differed from the average by less than ±1.00 16th of an inch for both wheel-paths and considering the overall results. Also, the standard deviation of the 496 measurement errors was equal to 0.58 16th of an inch.

Cumulative (%)	Error, e [16th in]		
	IWP	OWP	OVERALL
75%	e < ±0.50	e < ±0.50	e < ±0.50
90%	e < ±0.75	e < ±0.75	e < ±0.75
95%	e < ±1.00	e < ±1.00	e < ±1.00
98%	e < ±1.25	e < ±1.00	e < ±1.25

Table 4.2: Errors of MRD manual measurements below which selected cumulative frequencies fall.

ANALYSIS OF AUTOMATED MEASUREMENTS

The analysis of the measurements produced by the different automated rut measuring systems (ARMS) that participated in this study was performed in two parts: 1) the analysis of the reported transverse profiles and 2) the analysis of the reported MRD values. The five vendors were asked to report their best estimate of the transverse profiles coordinates and MRD values, measured at highway speeds, for the same locations at which the manual measurements were taken. The bias and the precision of the reported automated measurements were estimated using the manual measurements as the reference values.

This section is divided into three main subsections. The first subsection describes the processing applied to the automated measurements reported by the different ARMS. The second subsection presents the evaluation of the automated measurements and

includes the estimated bias and precision for each system. The third subsection contains the analysis performed to assess the effect that the different variables defined in the experiment design had on the error of the automated measurements.

Processing of Reported Automated Measurements

Every automated system reported their best estimate of the 23 transverse profiles per section and the 111 MRD values per wheel-path per section for the 24 sections. Therefore, 552 transverse profiles and 5,328 MRD values were reported by each of the five participants.

This subsection describes the processing applied to the reported rutting data measured by the automated systems and is divided into two parts: processing of the reported transverse profiles, and processing of the reported MRD values.

Processing of Reported Transverse Profiles

Each automated system that participated in the data collection reported data with different characteristics, such as different number of coordinates per transverse profile and different horizontal distances between coordinates. Table 4.3 contains the main characteristics of the transverse profiles reported by each participant. TxDOT was the first participant to measure the transverse profiles while the remaining participants collected data in the order listed in the table. The participants were requested to report the values in inches to three decimal places.

The second and third columns of Table 4.3 indicate how the participant reported the transverse profile data, including the number of decimal places and units of the coordinates. The fourth column presents the horizontal separation between coordinates, which was consistent for all stations and sections, except in a few cases in which

coordinates were not reported within the limits of a participant's profile. These cases apparently occurred due to out of-range readings or other anomalies.

Because the lane width of the sections varied and each participant used different methods to determine the starting and ending points of the reported transverse profiles, the width of measurement and the number of reported points per transverse profile were different for each participant at each station. The maximum width of a measured profile reported by each participant as well as the maximum number of coordinates, are presented in the fifth and sixth columns, respectively.

Participant	digits	unit	horizontal separation of coordinates		maximum width of measured profile		maximum number of coordinates
			in	mm	in	mm	
TxDOT	0.100	mm	0.109	2.8	168.0	4,267	1,536
Pathway	0.010	in	0.100	2.5	145.9	3,705	1,460
Dynatest	0.001	in	0.100	2.5	157.4	3,998	1,575
Roadware	0.001	in	0.800	20.3	118.4	3,007	149
Applus	0.001	in	0.079	2.0	152.6	3,876	1,939

Table 4.3: Format of the Reported Transverse Profiles.

The first point of each profile (extreme left-most point in the direction of traffic) was defined as the "zero coordinate", and the remaining profile points were recalculated by subtracting the coordinates of the first point. In addition, the values of all reported coordinates were converted to the same units for comparative purposes.

The manual transverse profiles were measured using a leveled beam, therefore, all coordinates are referenced to a horizontal plane. However, none of the automated systems used by the participants measured the transverse profile coordinates using a fixed reference plane so their reported profiles had to be rotated to match the orientation of the corresponding reference profile so that a comparison could be made.

In addition, when collecting the reference values, the zero coordinate of each profile was always measured at the center of the inner stripe. However, the profiles measured by the participants presented starting and ending points at different locations, and the participants were not able to indicate the position of the center of the inner stripe. Therefore, a horizontal and a vertical displacement were also applied to the reported profiles in order to perform the comparison.

The transverse profiles reported by the participants were rotated and displaced applying the Equation 4.1 and 4.2.

$$x_i' = h + x_i * \cos(\theta) - y_i * \sin(\theta) \qquad (4.1)$$

$$y_i' = v + x_i * \sin(\theta) + y_i * \cos(\theta) \qquad (4.2)$$

Where:

x_i' = Horizontal coordinates of the displaced profile;

y_i' = Vertical coordinates of the displaced profile;

x_i = Horizontal coordinates of the reported profile;

y_i = Horizontal coordinates of the reported profile;

h = Horizontal displacement;

v = Vertical displacement; and

θ = Angle of rotation.

Figure 4.6 shows a reported profile before and after the rotation and displacement were applied. The black dots in the figure represent reference coordinates; the green

points are the coordinates reported by a given participant and the blue line is the reported profile after applying the displacements and rotation.

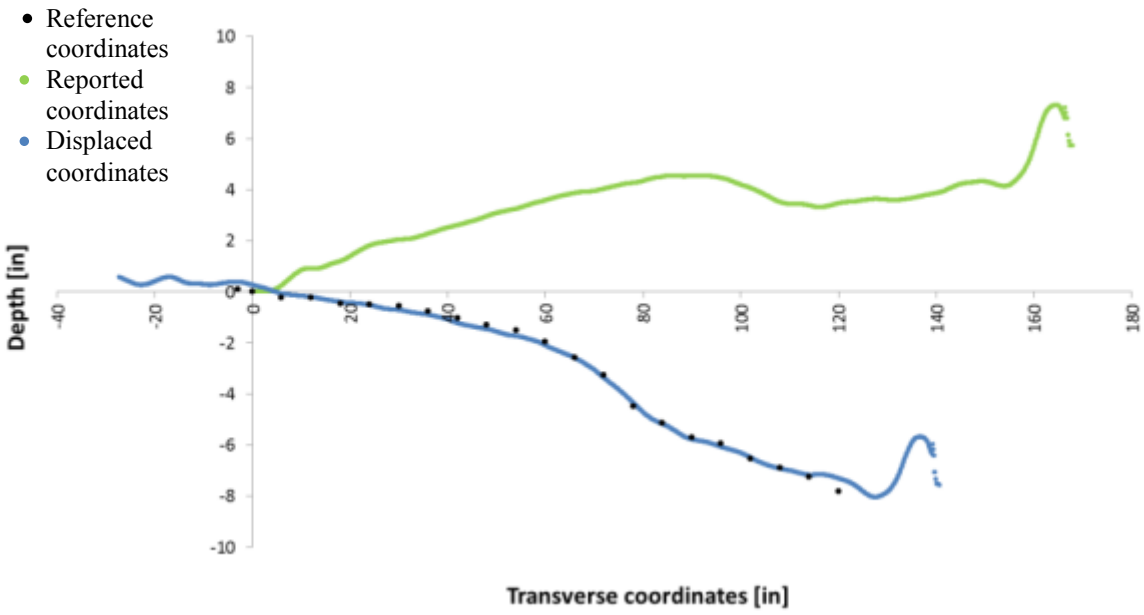

Figure 4.6: Reported (green points) and displaced (blue points) transverse profiles.

The profiles presented in Figure 4.6 consist of the reported coordinates, and they appear to be continuous lines in the plot due to the high density of measured points.

The values of h, v, and θ in Equations 4.1 and 4.2 were determined so as to minimize the sum of the squared residuals (SSE) between the manual transverse profile points and the participant's profile points.

The residuals of each profile were defined as the vertical difference between the coordinates of the reference profile and the participant's profile. The profiles reported by the participants did not consist of a continuous line, but rather of a number of coordinates. Therefore, most often there was not a specific point in the participant's transverse profile with the same horizontal coordinate as a given point of the reference

profile. Therefore, the value of the vertical coordinate used for calculating the residual was estimated by linearly interpolating between the two closest points of the participants profile relative to the reference point. Figure 4.7 illustrates the linear interpolation performed between the points of the displaced profile (x'_k, y'_k) and (x'_{k+1}, y'_{k+1}) used to calculate the residual, with the corresponding point of the reference profile $\left(x_i^{ref}, y_i^{ref}\right)$.

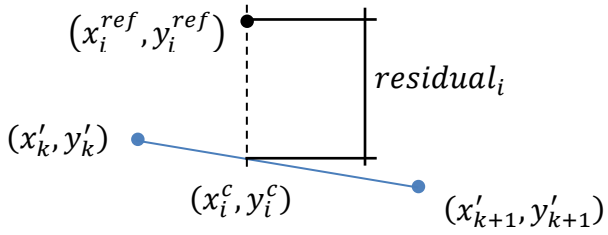

Figure 4.7: Linear interpolation used to calculate the residuals.

If a point of the reference profile was located on the left side of the first point of the participant profile, or on the right side of the last point of the participant profile (i.e., outside the range of the participants profile), it was not considered to calculate the residuals. For each of the remaining points of the reference profile, a new point was defined for the calculation of the residuals (as indicated in Figure 4.7, by the point with coordinates: x_i^c, y_i^c) and computed as a simple linear interpolation. Therefore, a new set of values was defined for each participant at every station with a number of coordinates equal to or less than the number of coordinates measured for the corresponding reference transverse profile.

The residuals and the SSE of each profile were calculated with Equations 4.3 and 4.4, respectively. As explained before, the value of *R* in Equation 4.4 is limited by the number of points of the reference profile.

$$\text{residual}_i = y_i^c - y_i^{ref}, \forall \text{ "i" such that } x_i^{ref} \in [x_1'; x_N'] \quad (4.3)$$

$$SSE = \sum_R \text{residual}_i^2 \quad (4.4)$$

Where:

residual_i = Residual of the point "i" of the displaced profile;

y_i^{ref} = Vertical coordinate of the point "i" of the reference profile;

x_i^{ref} = Horizontal coordinates of the point "i" of the reference profile;

x_1' = Horizontal coordinate of the first point of the displaced profile;

x_N' = Horizontal coordinate of the last point of the displaced profile;

SSE = Sum of the squared residuals; and

R = Number of residuals calculated in the profile.

As an example, Figures 4.8 to 4.12 show the displaced transverse profile measured by each participant along with the reference profile (black points) for Section 9, Station 375. It can be observed that the profiles presented by TxDOT and Pathway look like a continuous line, whereas the profiles presented by the remaining participants appear as a cloud of points. Each participant processed their measurements using proprietary algorithms not provided to the researchers.

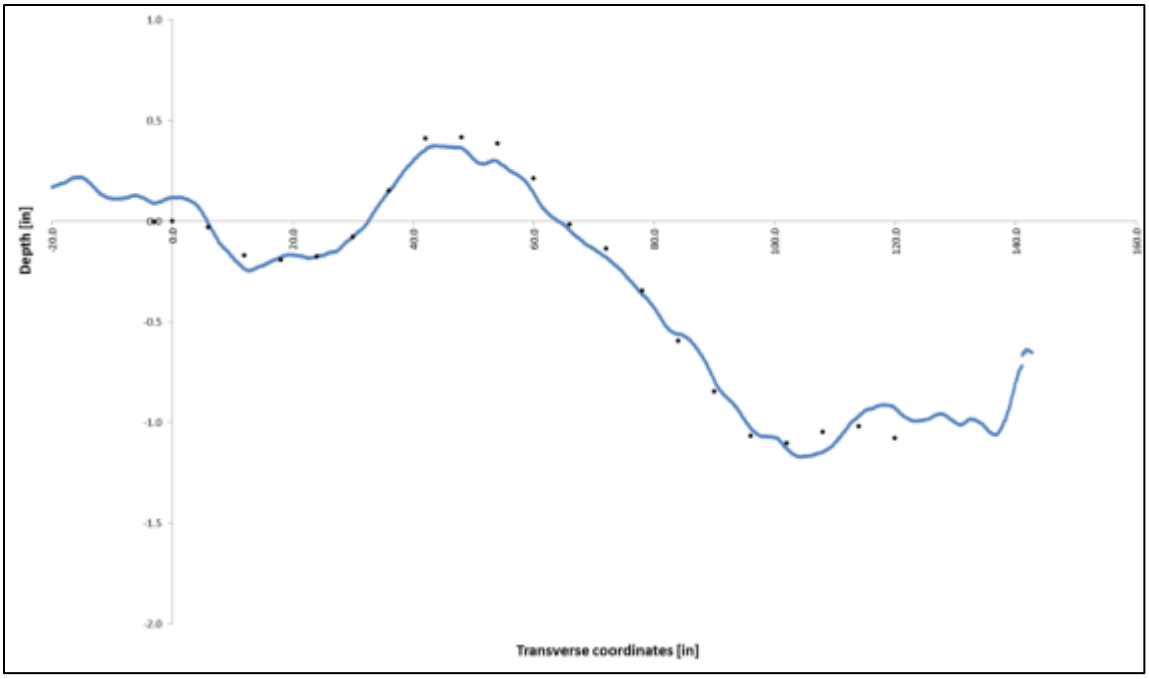

Figure 4.8: Reference (black points) and TxDOT (blue points) coordinates.

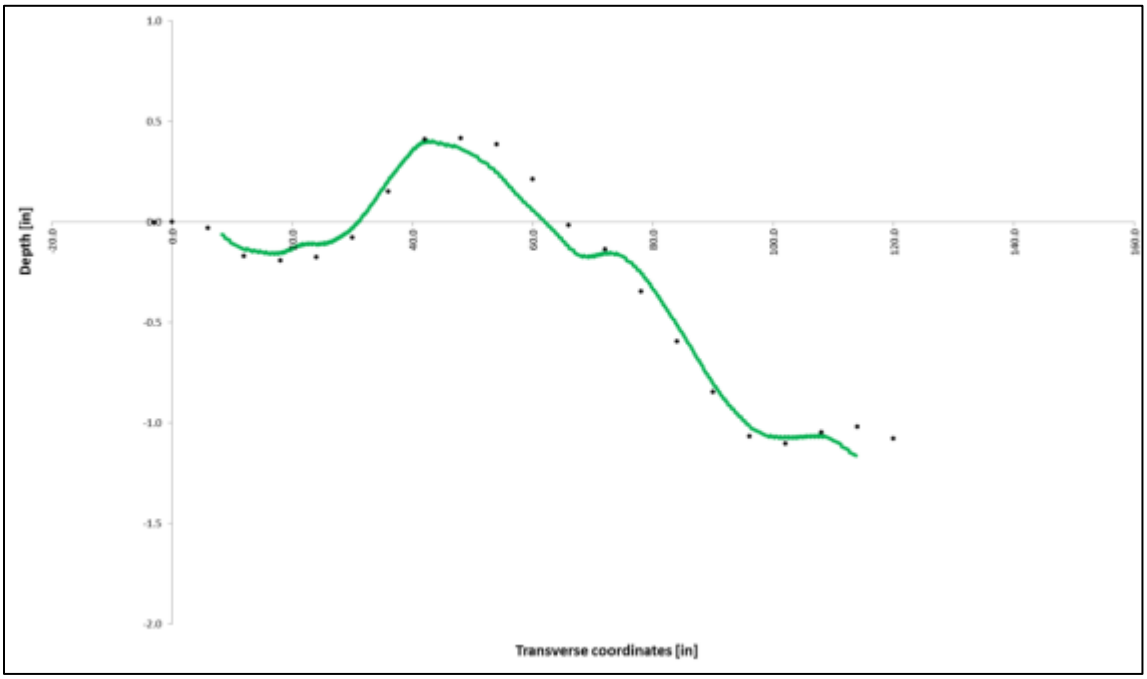

Figure 4.9: Reference (black points) and Pathway (green points) coordinates.

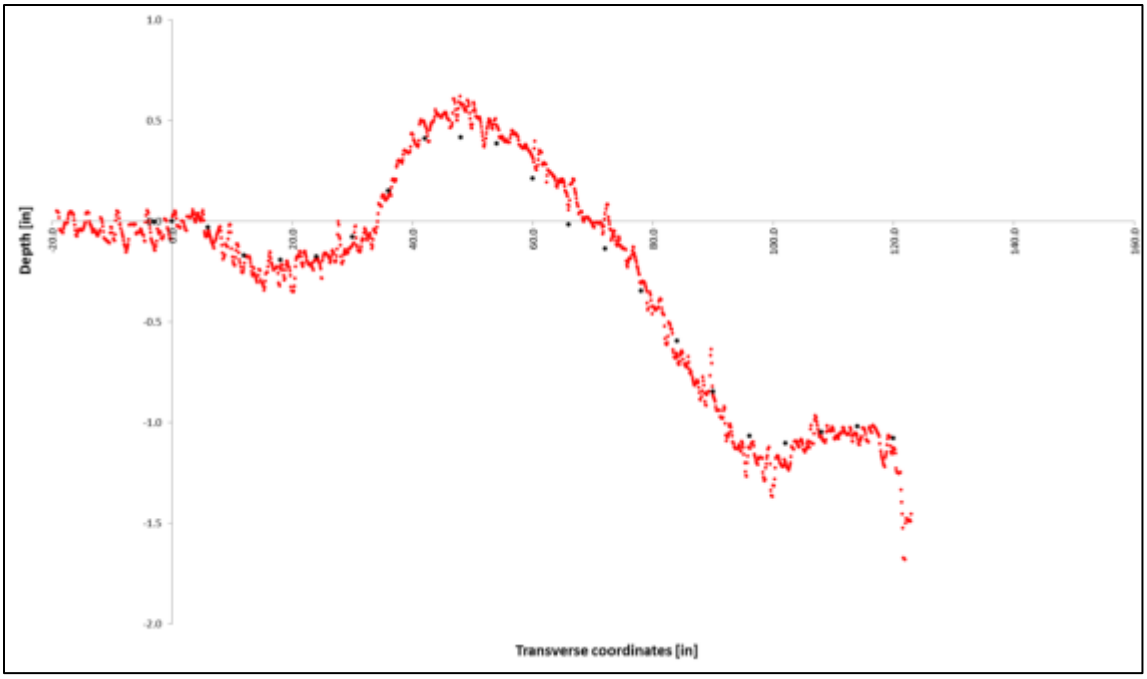

Figure 4.10: Reference (black points) and Dynatest (red points) coordinates.

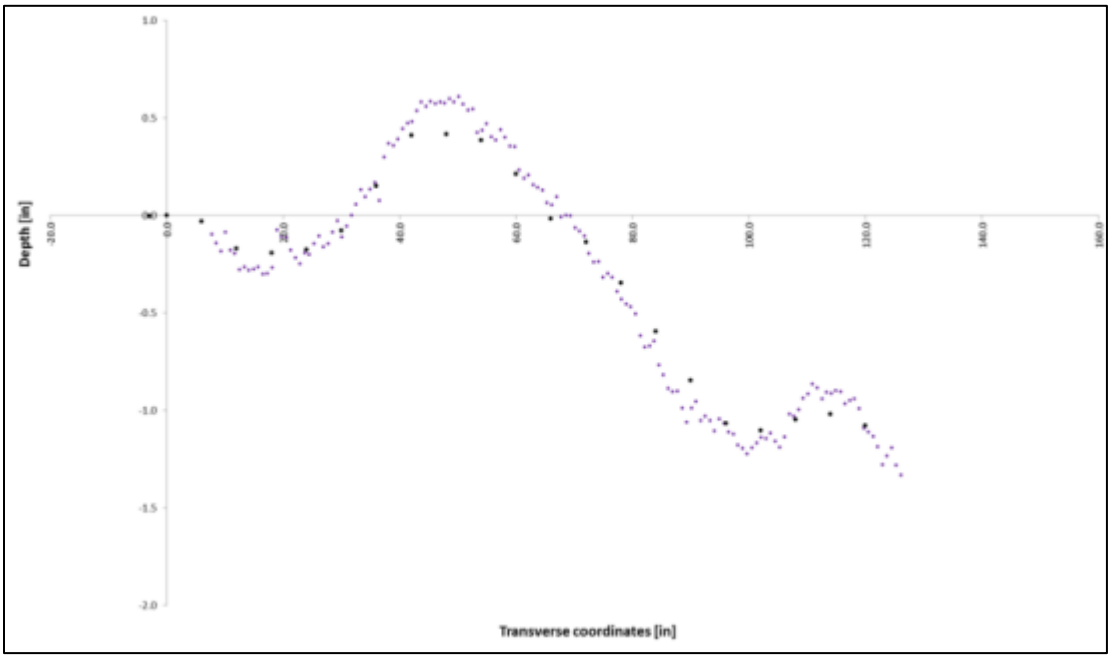

Figure 4.11: Reference (black points) and Roadware (purple points) coordinates.

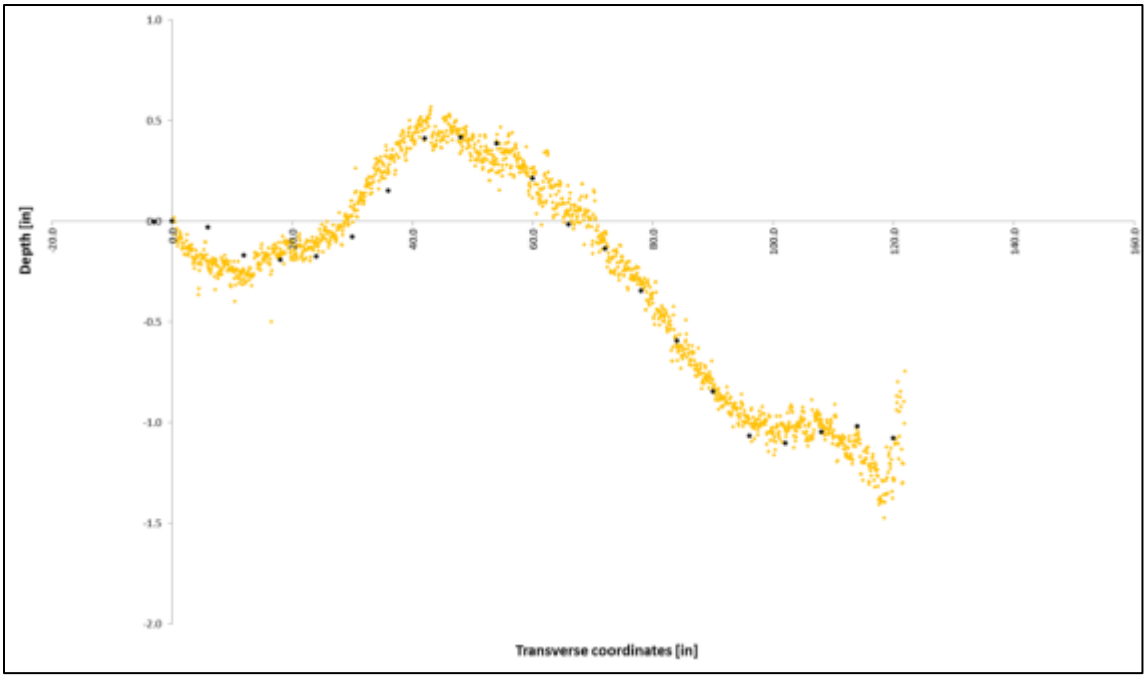

Figure 4.12: Reference (black points) and Applus (yellow points) coordinates.

As described in Chapter 3, the zero coordinate of the reference profiles in the plots was located at the center of the inner stripe and the last coordinate of the reference profile (from left to right) corresponds to the pavement edge stripe or outer limit of the paved travel lane. As illustrated in this example, for many of the test sections, at least some of the profiles reported by the ARMS were narrower than the reference profile: TxDOT and Dynatest reported points located on both the opposing lane and the shoulder; the width of the profile presented by Pathway was typically narrower than the width of the lane; and the width of the profiles presented by both Roadware and Applus was similar to the width of the lane. Since these profiles were also used to characterize rutting, the width of the measured profiles should ideally be equal to or greater than the width of the lane, and if the profile width is greater, the coordinates of the inner and outer limits of the lane should be properly located.

Processing of Reported Maximum Rut Depth Values

The participants reported their best estimate of the MRD values for each wheel-path in inches to two decimal places. Each of the participants calculated the MRD values applying proprietary algorithms to their measured transverse profiles. The methods and criteria adopted during the measurement of the ground truth MRD values were explained to the participants both before and on the day of testing prior to data collection.

The participants reported the MRD values for all the stations in the requested format and the only processing applied consisted of converting their values to 16^{ths} of an inch, which was the units used during the manual data collection. Once the conversion in units was applied to all the reported MRD values, the data was ready for the comparison to the reference values.

As an example, Figures 4.13 and 4.14 show the longitudinal distribution of the reported MRD values in 16th of an inch, along with the reference values, for both the IWP and the OWP of Section 9. The black line in each of the charts connects the 111 reference values measured along each wheel-path of the section. The blue line connects the values reported by TxDOT, the green line connects the ones reported by Pathway, the red line connects the ones reported by Dynatest, the purple one connects the values reported by Roadware, and lastly, the yellow line connects the points reported by Applus. Thus, when the two lines coincide, the participant's and the reference MRD values are equal. When the participant's line falls below the reference line, their measurements underestimated the reference values, and when the participant's line is above the line, their measurements overestimated the reference values.

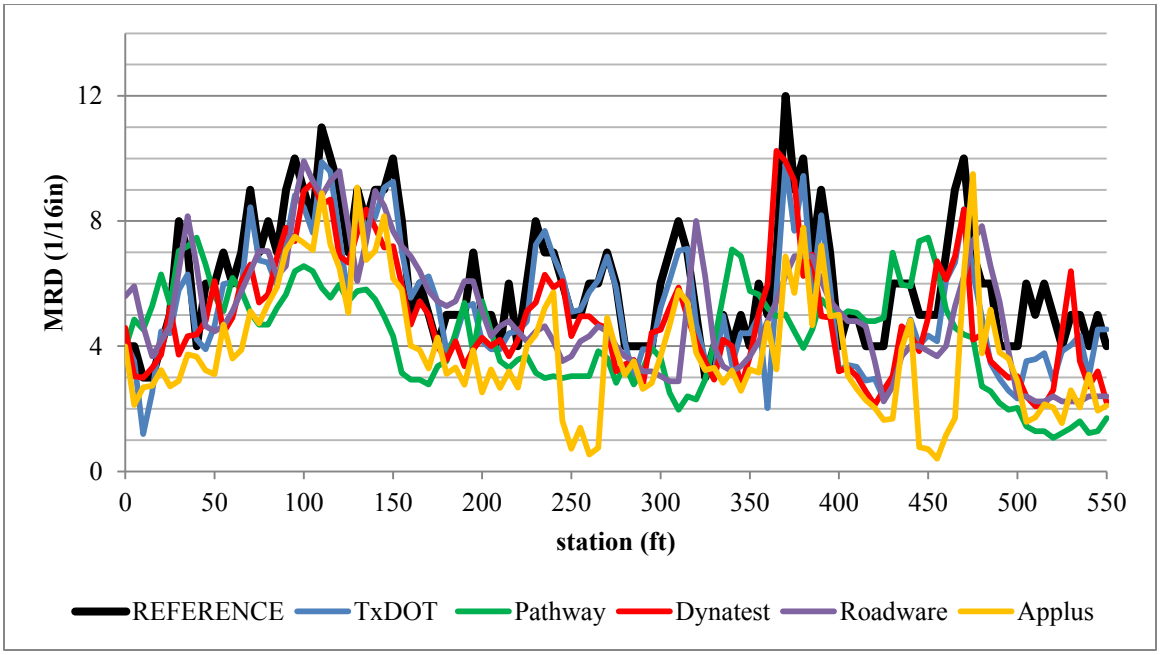

Figure 4.13: Longitudinal distribution of manual (black line) and automated measurements of the MRD for the IWP of Section 9.

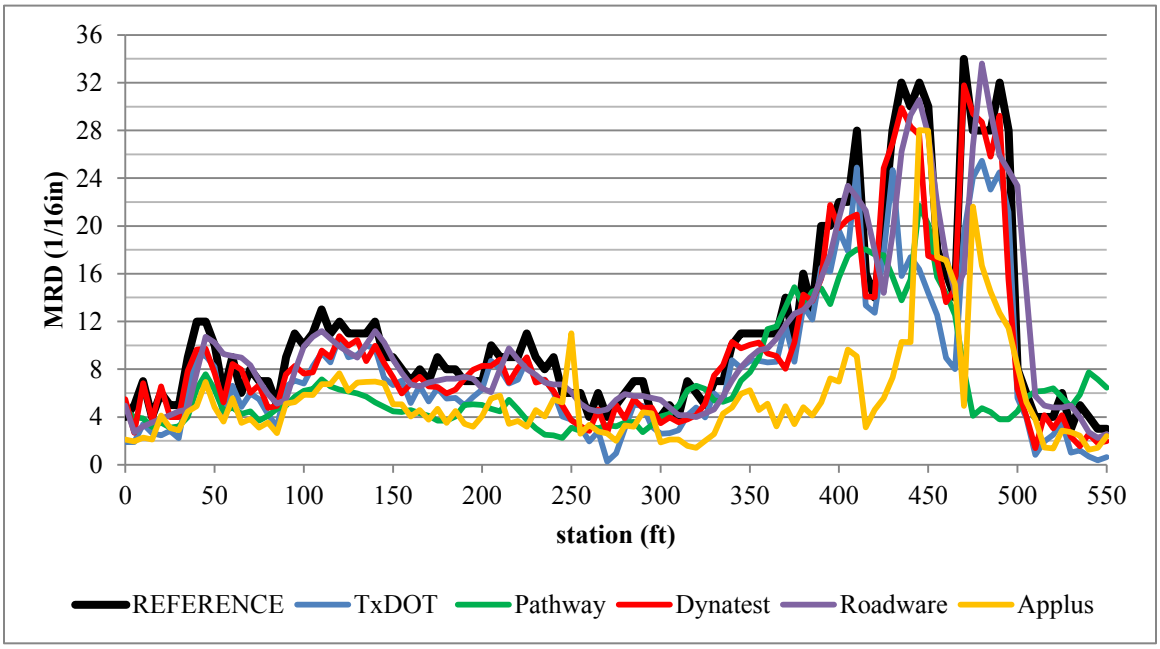

Figure 4.14: Longitudinal distribution of manual (black line) and automated measurements of the MRD for the OWP of Section 9.

Comparison of Reported Automated Measurements

Once all the reported rutting data measurements were processed, a comparison between the measurements made by the ARMS and the reference values was carried out. This section describes the calculations performed as well as the results for both the transverse profiles and MRD values comparison.

Comparison of Reported Transverse Profiles

This section presents the comparison between the transverse profiles reported by each of the five automated systems that participated in the study and the reference values.

Of the 552 stations selected for the study, six transverse profile locations were not manually measured. These stations were all from Section 3, and include Stations 275, 325, 375, 425, 475 and 525. Since no reference values were available for these six stations, they were not included in the comparison. Thus, the total number of transverse profiles used to evaluate the measurements of the automated systems was 546. Some of the participants' reported profiles were not included in the comparison, either because they did not report values for those stations or because they presented a large amount of outliers for the profile of those stations. The number of profiles not considered in the comparison for each of the participants is: TxDOT = 0, Pathway = 1, Dynatest = 15, Roadware = 6 and Applus = 14.

As explained in the section "Processing of the Reported Transverse Profiles" of this chapter, some of the reported profiles were narrower than the reference profile (as for the profile shown in Figures 4.9), thus missing the measurements for part of the profile. For those stations, the number of compared coordinates was less than the number of reference coordinates for the corresponding stations. Therefore, the number of total compared coordinates in the study was different for each participant.

The residual of each reported coordinate were computed as defined in the previous section (Equation 4.3) and the histogram of the errors for each automated system are presented in Figures 4.15 to 4.19. The horizontal axis displays the values of the residuals in intervals of 0.02 16^{ths} of an inch and the vertical axis displays the frequency of each interval expressed as a percentage of the total number of compared coordinates.

By observing the shape of the different histograms, it can be observed that the measurement errors of the three participants that operated INO systems (Dynatest, Roadware and Applus) are narrower (lower standard deviation) than the other two systems.

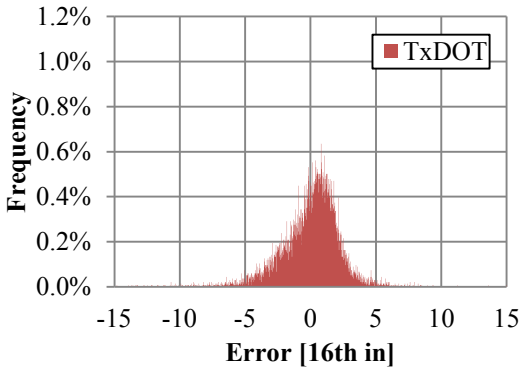

Figure 4.15: Histogram of profiles coordinates error of TxDOT.

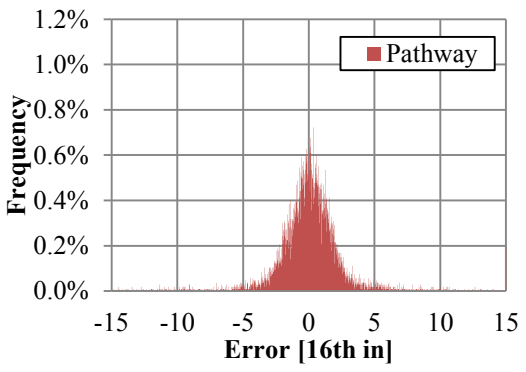

Figure 4.16: Histogram of profiles coordinates error of Pathway.

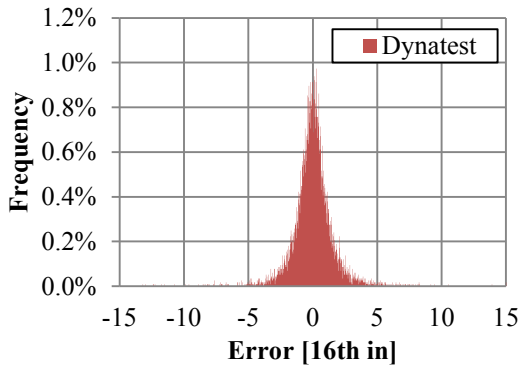

Figure 4.17: Histogram of profiles coordinates error of Dynatest.

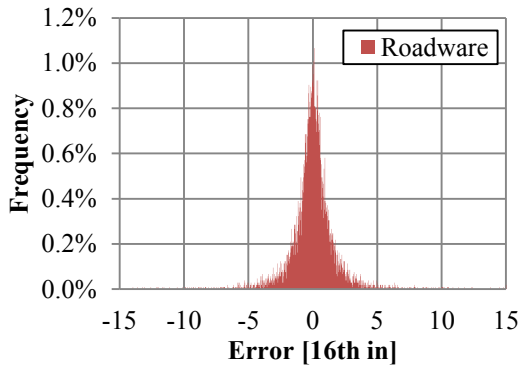

Figure 4.18: Histogram of profiles coordinates error of Roadware.

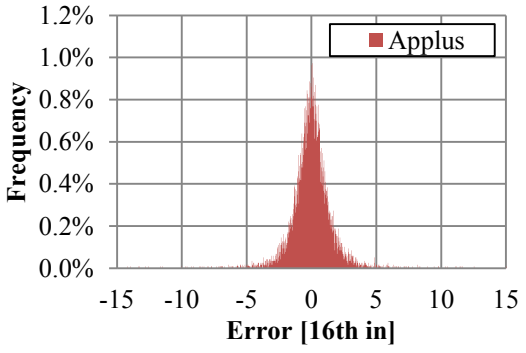

Figure 4.19: Histogram of profiles coordinates error of Applus.

From the plotted histograms it can also be noted than the residuals are centered around zero. This is a consequence of the adopted criteria of targeting the minimum SSE when applying the rotation and the horizontal and vertical displacements.

The statistics of the residuals calculated for all the transverse profiles coordinates reported in the study are presented in Table 4.4.

Participant	N	Nmax	N/Nmax	Mean	Std	Residual ≤ [16th in]				
	#	#	%	16^{th} inch	16^{th} inch	50%	75%	90%	95%	98%
TxDOT	13,381	13,639	98%	0.00	2.3	±1.3	±2.2	±3.4	±4.5	±5.9
Pathway	10,670	13,612	78%	0.00	2.8	±1.1	±1.9	±3.3	±5.0	±8.6
Dynatest	11,613	13,234	88%	0.00	1.5	±0.7	±1.3	±2.2	±3.0	±4.2
Roadware	10,506	13,502	78%	-0.06	2.3	±0.7	±1.4	±2.5	±3.5	±5.3
Applus	11,723	13,275	88%	0.00	1.5	±0.7	±1.3	±2.2	±2.9	±4.1

Table 4.4: Statistics of the residuals of all the reported transverse profile coordinates.

The second and third columns contain the total number of residuals computed for the comparison and the total number of coordinates manually collected in the study respectively. The values in the third column differ among the different participants because some of their reported profiles were not considered for the comparison for the reasons explained earlier. Since one residual value was computed per participant for each manually measured coordinate, and some reported profiles were narrower than the reference profiles; the values in the third column represent the maximum limit of compared residuals. The ratio between the total number of computed residuals for the comparison and the maximum limit for each participant indicates the percentage of coordinates that were not missed. Therefore, Pathway and Roadware missed 22% of the coordinates and were the participants that missed the greatest percentage. TxDOT' system, on the other hand, missed just 2% of the coordinates.

The fifth and sixth columns of Table 4.4 present the mean and standard deviation of all the calculated residuals of the study for each participant. The mean of residuals are essentially zero for all the participants as expected considering the processing applied to the reported profiles. Values greater than zero are mainly due to rounding errors and the presence of some outliers. The standard deviations are expressed in 16^{ths} of an inch and provide a measurement of the overall precision of each system. As can be observed, the overall variability of the automated systems is greater than the variability of the manual measurements. However, the standard deviations are small, especially considering that the automated measurements were taken at high speeds (at around 45mph or posted maximum speed limit) and many of the sections included in the study presented challenging conditions including very deep ruts and several distresses. Therefore, the overall precision of each automated rut measurement system is considered to be acceptable for pavement management applications in Texas.

It should be noted that although it was previously observed that the shapes of the plotted histograms of the participants that used INO systems were narrower than other systems, the calculated standard deviation of the residuals of Roadware's measurements is one of the highest. This is because the standard deviation is sensitive to the presence of outliers (i.e. longer tails in the distribution).

The last five columns of Table 4.4 report the residual values, in 16^{ths} of an inch, that are greater than, or equal to, the rest of the calculated residuals for each of the different selected percentages. Thus, for example, 90% of Applus residuals are less than, or equal to, ±2.2 16^{th} of an inch. By observing the values at the different percentages, it can be concluded that the three participants that used INO systems presented the least variability, and therefore the best overall precision.

Comparison of Reported Maximum Rut Depth Values

This section presents the comparison between the MRD values manually measured and the values reported by the five ARMS that participated in the study.

As described in Chapter 3, the manual measurements of the MRD values were performed using a 6-ft straight-edge in each wheel-path for the 2,664 stations included in the study, following the standard procedure described in ASTM 1703-10.

The different ARMS used the profiles analyzed in the previous section to calculate the MRD at each wheel-path using proprietary algorithms, which were not available to the researchers. Therefore, part of error of each reported MRD is due to the error of the transverse profile measurement.

Once the participants reported their best estimate of the MRD for all the stations, the error of each reported MRD values was computed as the difference between the reported and the corresponding reference value (Equations 4.5) within each wheel-path and at each station. Therefore, when the resulting error had a positive sign the measurement was underestimated, and when it had a negative sign the measurement was overestimated.

$$\text{error}_i = \text{MRD}_i^{\text{ref}} - \text{MRD}_i \tag{4.5}$$

Where:

error_i = Error of the MRD reported by the participant at station "i";

$\text{MRD}_i^{\text{ref}}$ = Reference value of the MRD at station "i"; and

MRD_i = MRD value reported by the participant at station "i";

As an example, the longitudinal distributions of each participant's MRD errors for both the IWP and the OWP of Section 9 are presented in Figures 4.20 and 4.21. The horizontal axis displays the station location, and the vertical axis displays each participant's MRD error for the corresponding station, in 16th of an inch.

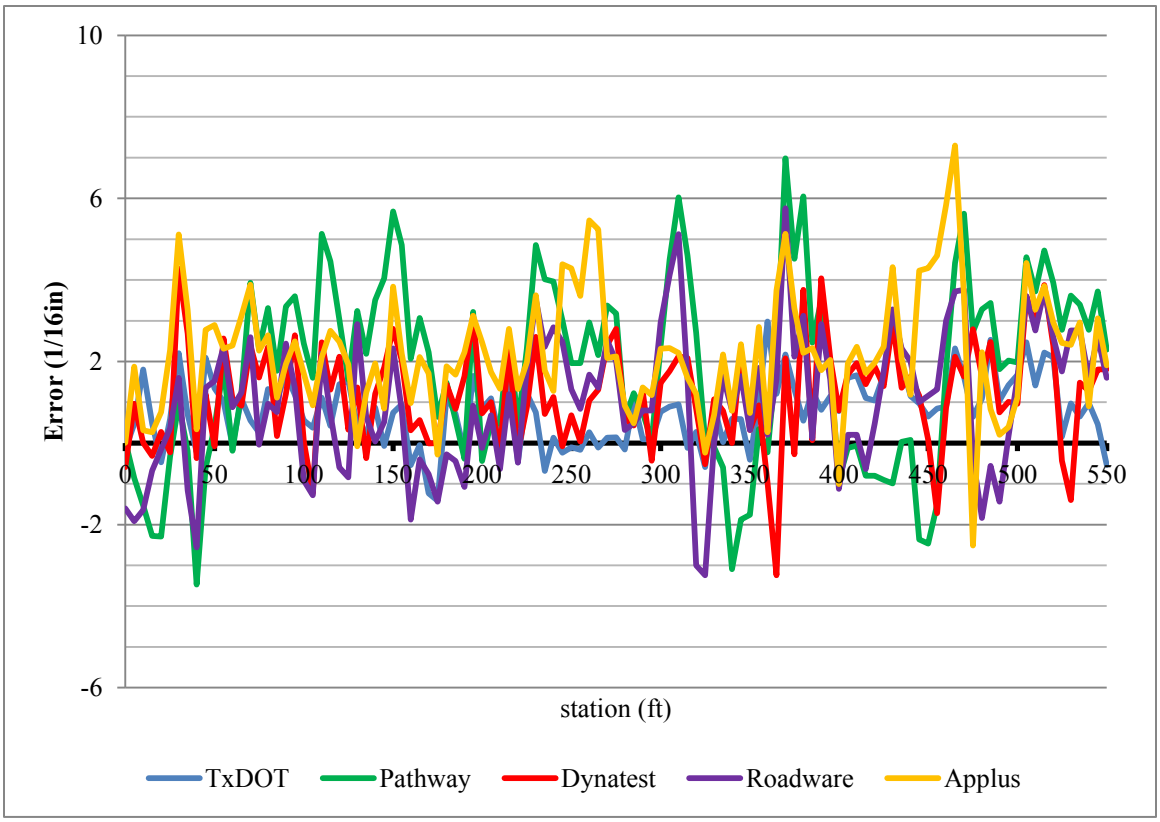

Figure 4.20: Longitudinal distribution of the MRD errors of the automated systems for the IWP of Section 9.

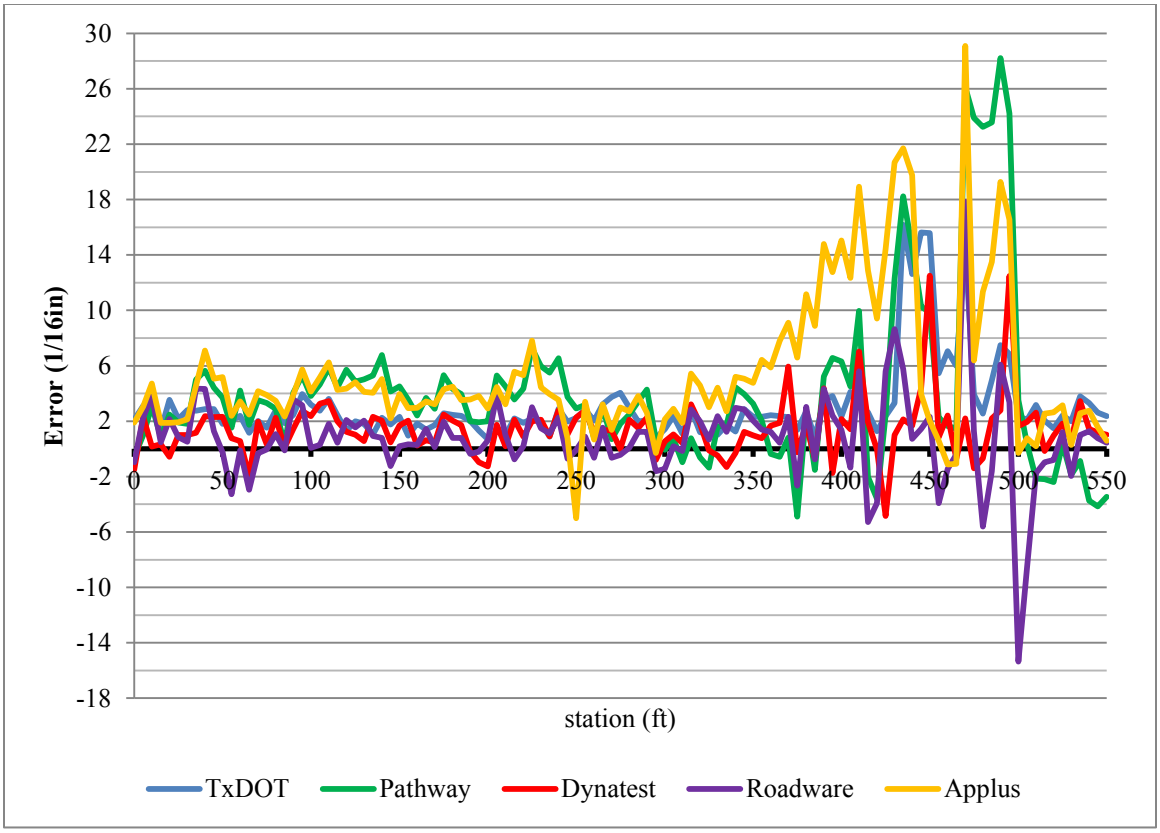

Figure 4.21: Longitudinal distribution of the MRD errors of the automated systems for the OWP of Section 9.

For Section 9 it can be observed that for both wheel-paths, the majority of MRD errors are positive for all the participants. Therefore, for this particular section, all the ARMS tended to underestimate the MRD values.

Interestingly, from Figure 4.21, it can also be observed that the errors of the MRD reported values for the OWP increased in magnitude for the second half of the section for all the participants. By observing the longitudinal distribution of the reported MRD values for the same section (Figure 4.14) it is noted that the stations at which the magnitude of the errors increased, correspond to the stations at which the MRD values also increased. This observation indicates that the error of the MRD values produced by

the automated systems may increase with the MRD value. The relationship between the MRD errors and the MRD values is analyzed in the next section of the chapter.

Figure 4.22 to 4.31 present the histograms of the errors of the reported MRD values for each participant and system. The horizontal axis of the histograms displays the MRD errors in intervals of 0.1 16^{ths} of an inch and the vertical axis displays the frequency of the intervals expressed as a percentage of the 2,664 values reported per wheel-path.

From the shape of the histograms presented in Figures 4.22 to 4.31, it can be observed that none of the participant's distributions is centered on zero, meaning that all of the systems present some bias. Furthermore, the bias appears to consistently be on the right side, indicating that all the participants tended to underestimate the reference values.

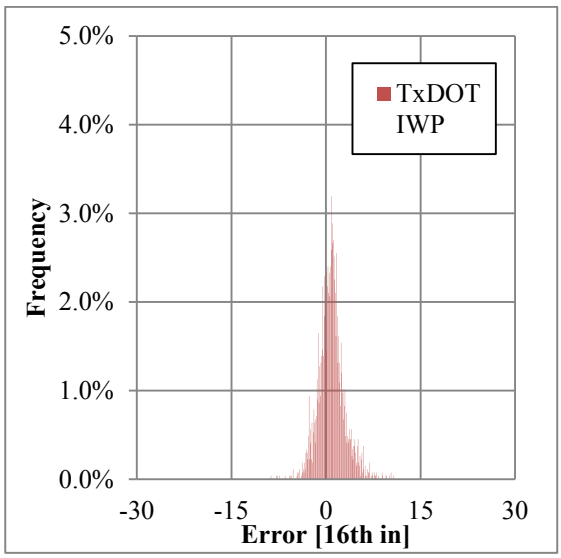

Figure 4.22: Histogram of IWP MRD error reported by TxDOT.

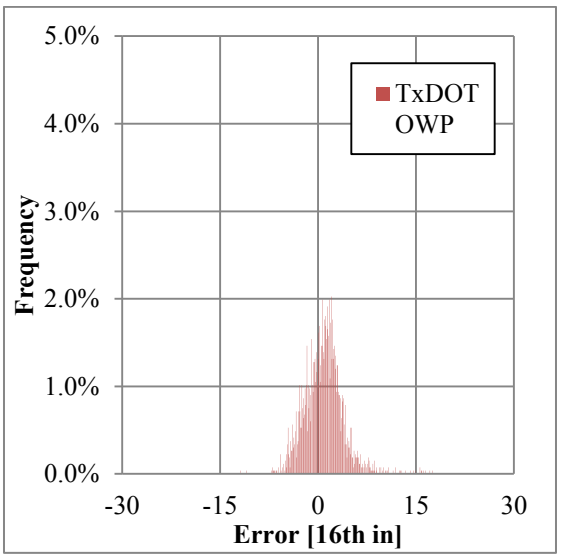

Figure 4.23: Histogram of OWP MRD error reported by TxDOT.

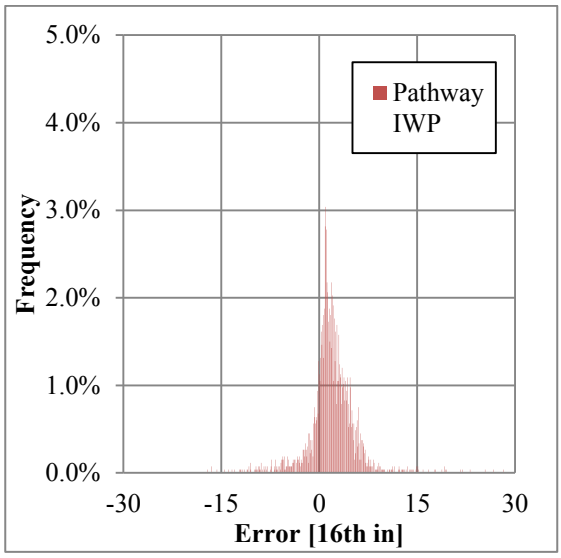

Figure 4.24: Histogram of IWP MRD error reported by Pathway.

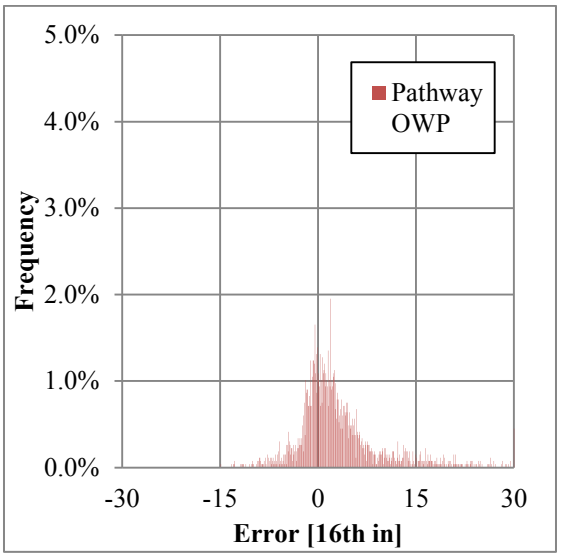

Figure 4.25: Histogram of OWP MRD error reported by Pathway.

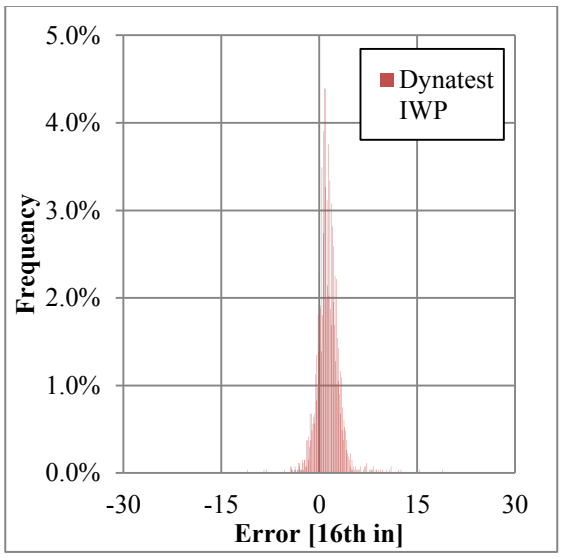

Figure 4.26: Histogram of IWP MRD error reported by Dynatest.

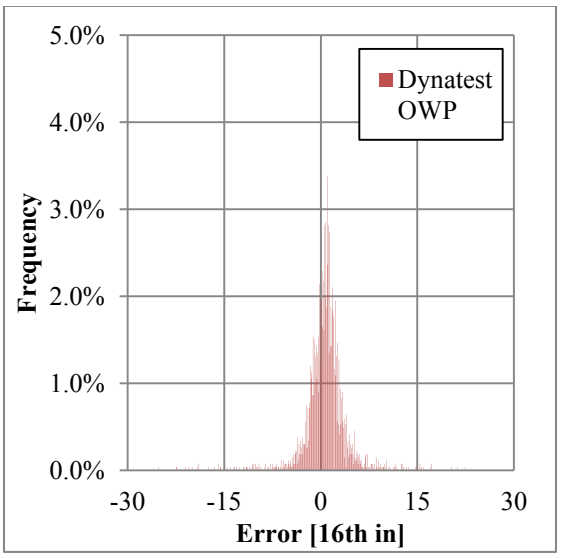

Figure 4.27: Histogram of OWP MRD error reported by Dynatest.

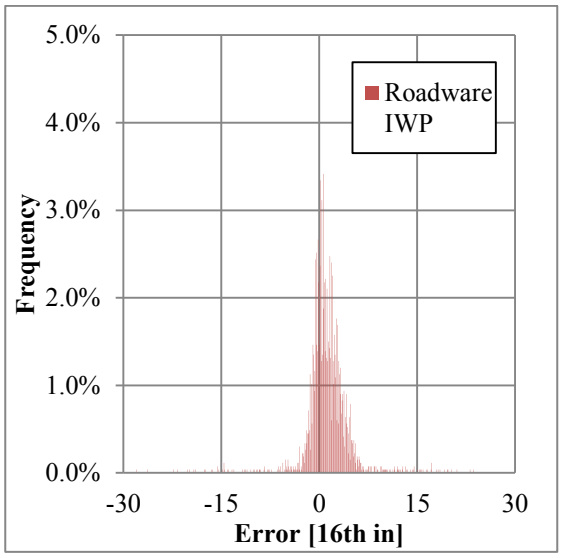

Figure 4.28: Histogram of IWP MRD error reported by Roadware.

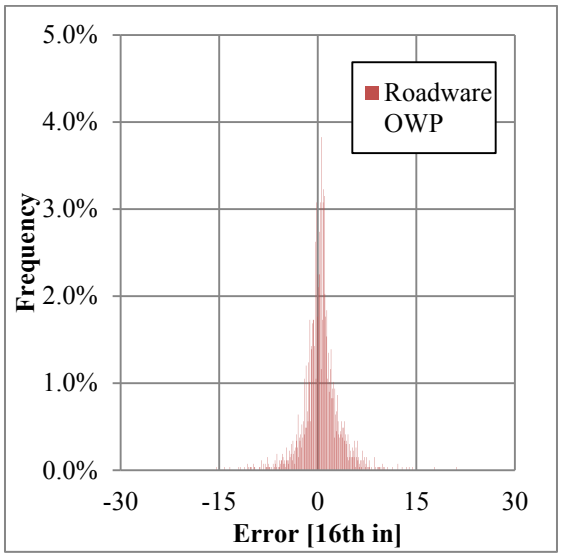

Figure 4.29: Histogram of OWP MRD error reported by Roadware.

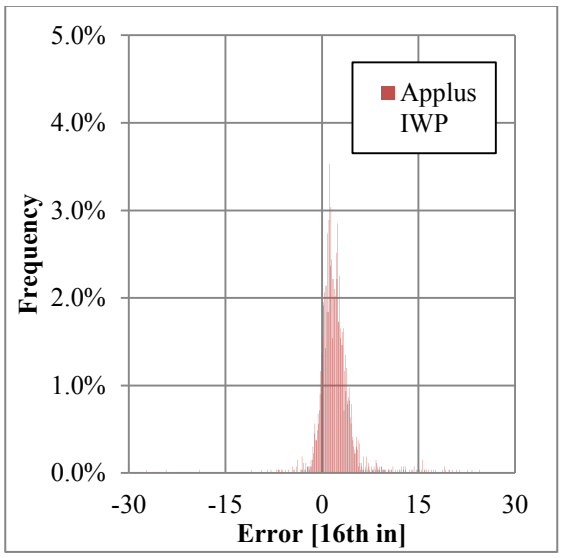

Figure 4.30: Histogram of IWP MRD error reported by Applus.

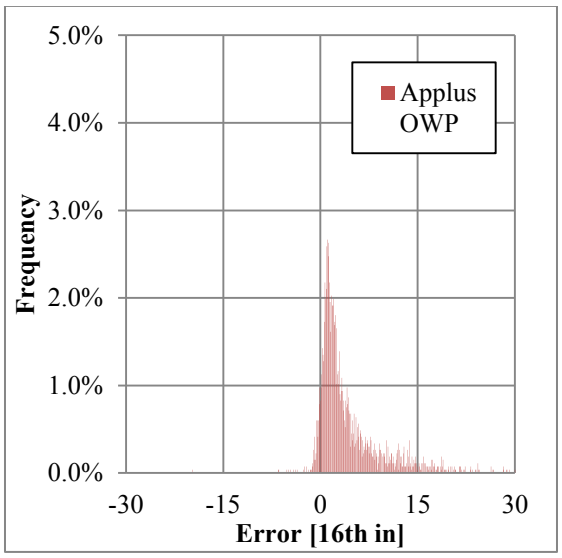

Figure 4.31: Histogram of OWP MRD error reported by Applus.

The histograms corresponding to the OWP MRD errors tends to be more spread out than the histogram corresponding to the IWP MRD errors, except for the case of

Roadware's MRD errors, which seem to have a similar variability. These observations are further analyzed by looking at the statistics of the histograms.

The Bias (mean of the residuals), Precision (standard deviation of the residuals) and Mean Squared Error (MSE) of the 2,664 MRD errors per wheel-paths were calculated using Equations 4.6, 4.7 and 4.8, respectively, for both the IWP and the OWP separately and considering both wheel-paths. The calculated statistics are reported in Table 4.5.

$$\text{Bias} = \sum_{i=1}^{111} \frac{\text{error}_i}{111} \tag{4.6}$$

$$Precision = \sqrt{\sum_{i=1}^{111} \frac{(error_i - Bias)^2}{111-1}} \tag{4.7}$$

$$MSE = \sqrt{Bias^2 + Precision^2} \tag{4.8}$$

Participant	Bias [16th inch]			Precision [16th inch]			MSE [16th in]		
	IWP	OWP	BOTH	IWP	OWP	BOTH	IWP	OWP	BOTH
TxDOT	0.87	0.88	0.87	2.05	2.92	2.52	2.23	3.05	2.67
Pathway	1.88	3.03	2.45	3.60	6.40	5.22	4.06	7.08	5.77
Dynatest	1.29	0.69	0.99	1.69	3.35	2.67	2.13	3.42	2.85
Roadware	1.18	0.47	0.83	3.46	2.73	3.14	3.66	2.77	3.24
Applus	2.04	4.16	3.10	3.42	4.92	4.37	3.98	6.45	5.35

Table 4.5: Statistics of the errors of the reported MRD of all the stations.

From Table 4.5 it is observed that the overall bias for both the IWP and the OWP is positive for all the participants, meaning that all the ARMS underestimated the manual measurements.

TxDOT's system was the only one that used one laser and one camera to measure the entire profile length while the other systems used one laser per wheel-path. The use of different pieces of hardware for the two wheel-paths might result in variations between the measurements in each wheel-path. However, considering the satisfactory overall performance of the systems for measuring the transverse profiles, the difference in bias between the two wheel-paths might be explained by algorithms used for the determination of the MRD values.

Based on the precision of each participant's system, as previously observed from the histograms presented in Figures 4.22 to 4.31, the variability of the MRD errors for the OWP are greater than the one for the IWP, except for the case of Roadware.

The MSE value accounts for both the bias and the precision, and it is used to measure the overall performance of the system. From Table 4.5 it is observed that Dynatest and Roadware presented the minimum MSE value for the IWP and the OWP respectively, and TxDOT presented the minimum MSE value when all the 5,328 MRD errors for both wheel-paths together are considered.

Table 4.6 presents the list of participants ranked from the smallest to the largest resulting value for each statistic. It can be observed that TxDOT, Roadware and Dynatest are ranked among the first three positions for the majority of the cases, indicating that the MRD measurement performance of these three participants is superior to the performance of the other two participants. Analyzing the rankings of each statistic and wheel-path separately, it is observed that Roadware was both the most accurate and precise system in the OWP, while it presented one of the highest variability of errors for the IWP. On the other hand, TxDOT was the most accurate system for the IWP whereas Dynatest was the most precise system for the IWP.

Bias of MRD errors			Precision of MRD errors			MSE of MRD errors		
IWP	OWP	BOTH	IWP	OWP	BOTH	IWP	OWP	BOTH
TxDOT	Roadware	Roadware	Dynatest	Roadware	TxDOT	Dynatest	Roadware	TxDOT
Roadware	Dynatest	TxDOT	TxDOT	TxDOT	Dynatest	TxDOT	TxDOT	Dynatest
Dynatest	TxDOT	Dynatest	Applus	Dynatest	Roadware	Roadware	Dynatest	Roadware
Pathway	Pathway	Pathway	Roadware	Applus	Applus	Applus	Applus	Applus
Applus	Applus	Applus	Pathway	Pathway	Pathway	Pathway	Pathway	Pathway

Table 4.6: Ranking of participants sorted from the smallest to the largest values of each statistic parameter and wheel-path.

As mentioned in the Background section of Chapter 1, transportation agencies define categories for the rutting severity levels to describe the condition of the pavement sections in their pavement management systems. TxDOT, for example, defines the following categories for their Pavement Management Information System (PMIS): No Rut, Shallow, Deep, Severe and Failure. One of these categories is assigned to each MRD measured at the surveyed pavement section. The ranges of MRD values defined for each PMIS category are presented in Chapter 1.

Since each rut category is defined by a range of MRD values, the reported MRD value may be biased and still fall into the same rut category as the reference value. In order to illustrate this situation, the scatter plot between all the reference (horizontal axis) and TxDOT (vertical axis) reported MRD values for the OWP is presented in Figure 4.32. If a point is located below the identity line (45° black line in the chart), TxDOT underestimated the MRD value for the corresponding station whereas if the point is above the identity line, the participant overestimated the MRD value.

The yellow lines in the chart indicate the boundaries of the rut categories as defined in TxDOT PMIS. The green boxes in the chart define the regions for which if a

point is located inside these boundaries, the participant's reported MRD value would still be placed in the same PMIS category as the reference MRD value. This would occur, even if the participant were underestimating or overestimating the reference value for the corresponding station. Therefore, the number of cases for which the participant reported values that fall within the correct and incorrect rut categories can be computed to evaluate the performance of each automated system on reporting rut categories to a PMS.

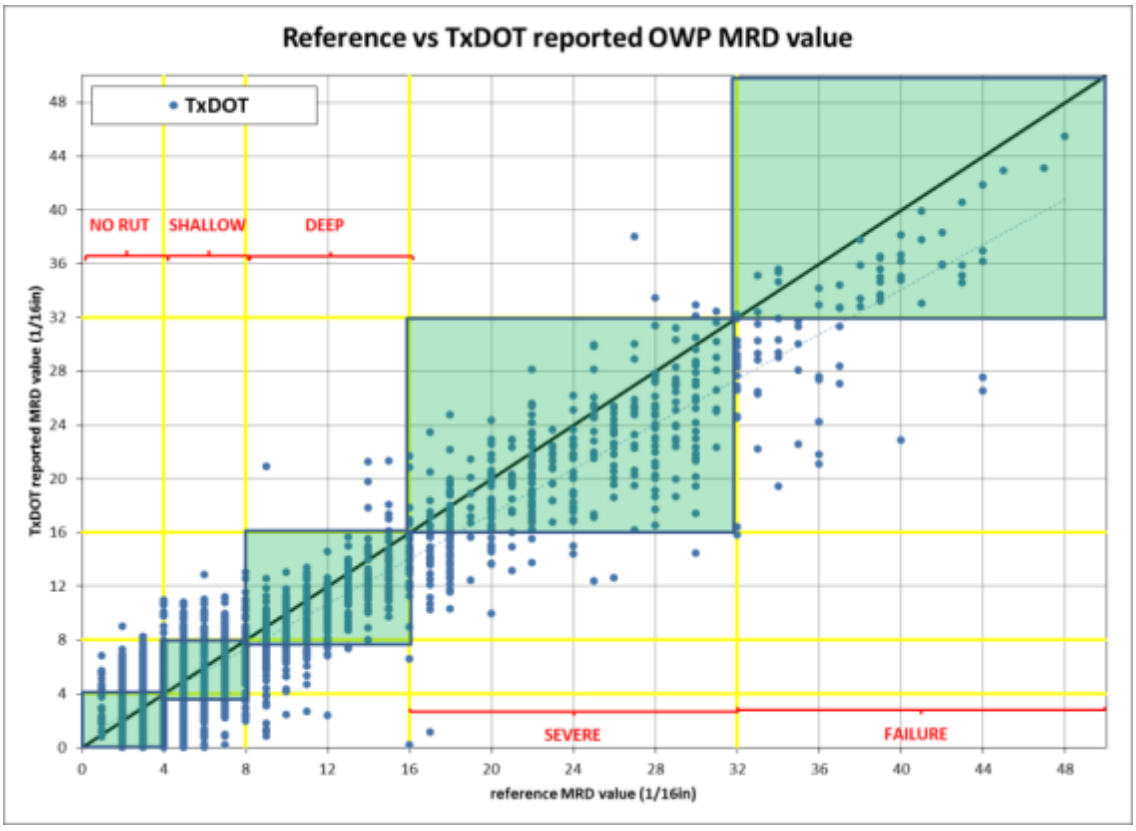

Figure 4.32: Reference vs. TxDOT reported OWP MRD values for all the stations.

As shown in Figure 4.32, for each station there is a rut category assigned to the reference MRD value and another category assigned to the reported value, which may be the same or not. Considering the five TxDOT PMIS rut categories, there are 25 possible

outcomes for the pair of categories assigned to the reference and reported values at each station and each participant.

The corresponding PMIS rut categories were assigned to all of the reference MRD values and all reported MRD values by each participant; the numbers of cases for the 25 possible outcomes were then computed. Table 4.7 presents the results of this analysis.

The number of cases falling into each of the 25 possible outcomes for each participant are reported in the white cells of the table, and expressed as a percentage of the total 2,664 MRD values per wheel-path of the study. The green cells indicate the percentage of stations for which the reference and reported MRD values fall into the same rut category. As observed in the previous analysis, all of the systems tended to underestimate the manual measurements.

From Table 4.7 it is also observed that the percentage of stations correctly categorized was greatest for the No Rut category, for all the participants. This observation is explained by the fact that all the systems tended to underestimate the measurement and the MRD values cannot be negative.

Except for the No Rut category, the observed percentages for the reported MRD values falling within the correct category (green cells) are relatively low for all participants.

		Reference (Manual Measurements)									
		IWP					OWP				
		NO RUT	SHALLOW	DEEP	SEVERE	FAILURE	NO RUT	SHALLOW	DEEP	SEVERE	FAILURE
TxDOT	FAILURE	0%	0%	0%	3%	89%	0%	0%	0%	1%	49%
	SEVERE	0%	0%	1%	61%	11%	0%	0%	2%	74%	49%
	DEEP	0%	1%	40%	29%	0%	0%	9%	64%	24%	1%
	SHALLOW	21%	57%	52%	7%	0%	40%	45%	30%	0%	0%
	NO RUT	79%	41%	7%	0%	0%	60%	46%	4%	0%	0%
Pathway	FAILURE	0%	0%	0%	0%	0%	0%	0%	0%	0%	0%
	SEVERE	1%	1%	2%	24%	44%	0%	1%	5%	24%	36%
	DEEP	3%	8%	18%	45%	33%	3%	11%	25%	56%	53%
	SHALLOW	3%	22%	47%	23%	22%	21%	31%	44%	18%	10%
	NO RUT	93%	70%	34%	8%	0%	76%	57%	27%	2%	1%
Dynatest	FAILURE	0%	0%	0%	0%	11%	0%	0%	0%	2%	58%
	SEVERE	0%	0%	0%	64%	89%	1%	2%	5%	78%	40%
	DEEP	0%	0%	45%	33%	0%	1%	5%	52%	17%	2%
	SHALLOW	6%	39%	51%	3%	0%	16%	43%	40%	3%	0%
	NO RUT	94%	60%	3%	0%	0%	83%	50%	3%	0%	0%
Roadware	FAILURE	0%	0%	0%	0%	0%	0%	0%	0%	6%	74%
	SEVERE	2%	0%	2%	23%	56%	0%	0%	8%	77%	25%
	DEEP	1%	3%	29%	53%	44%	0%	7%	51%	16%	1%
	SHALLOW	8%	44%	52%	24%	0%	10%	57%	36%	0%	0%
	NO RUT	89%	53%	16%	0%	0%	90%	35%	4%	0%	0%
Applus	FAILURE	0%	0%	0%	0%	0%	0%	0%	0%	0%	10%
	SEVERE	0%	0%	0%	9%	11%	0%	0%	0%	25%	64%
	DEEP	1%	1%	27%	76%	89%	0%	0%	19%	44%	21%
	SHALLOW	2%	25%	56%	15%	0%	0%	19%	51%	21%	4%
	NO RUT	97%	74%	17%	0%	0%	100%	80%	30%	11%	1%

Table 4.7: Distribution of manual and automated measurements of MRD values according to PMIS rut categories for both wheel-paths.

EFFECT OF THE EXPERIMENT FACTORS ON THE AUTOMATED MEASUREMENT ERRORS

This section of the chapter contains the analysis performed to assess the effect that different experiment variables had on the errors of the rutting measurements reported by each participant.

The main objectives of this analysis were to: 1) detect characteristics of the roadway that significantly affect the errors of the measurement produced by the automated systems; and 2) describe the relationship, when a relationship exists. In order to achieve this, multiple linear regression models to explain each system's measurements errors were estimated from the set of observed values for the variables defined in the experiment, and the magnitude and sign of the estimates for the model coefficients were analyzed. It is relevant to note that since this assessment was not part of the objectives of the research project for which the rutting data was collected [Serigos et al, in press], the original experiment was not designed to avoid problems such as multicolinearity or endogeneity.

Experiment Factors

Some of the experiment variables (discussed in Chapter 3) were selected as the explanatory variables of the models for the errors of the automated measurements. The variables initially selected for specifying the models along with a brief description of them and the reason of why they were considered relevant is presented in the following sub-sections.

Reference Inner and Outer Wheel-Path MRD Values

These two variables are the MRD values manually measured for the IWP (*IWP_MRD_ref*) and the OWP (*OWP_MRD_ref*) respectively using a 6-ft straight-edge

and a gage graduated to 1/16 in. Figure 4.33 presents the distribution of the 2,664 reference MRD values for each wheel-path using the TxDOT PMIS rut categories.

The observed number of stations presenting reference MRD values categorized as No Rut, Shallow, and Deep rutting are greater than the ones categorized as Severe and Failure rutting for both wheel-paths. This is because TxDOT's maintenance planning assigns the highest priority on sections with severe and failure rutting. Another interesting observation from Figure 4.33 is that the rutting is more severe in the outer wheel-path. This may be explained by the fact that many of the selected sections did not a paved shoulder and therefore the outer wheel path had less lateral support than the inner wheel path.

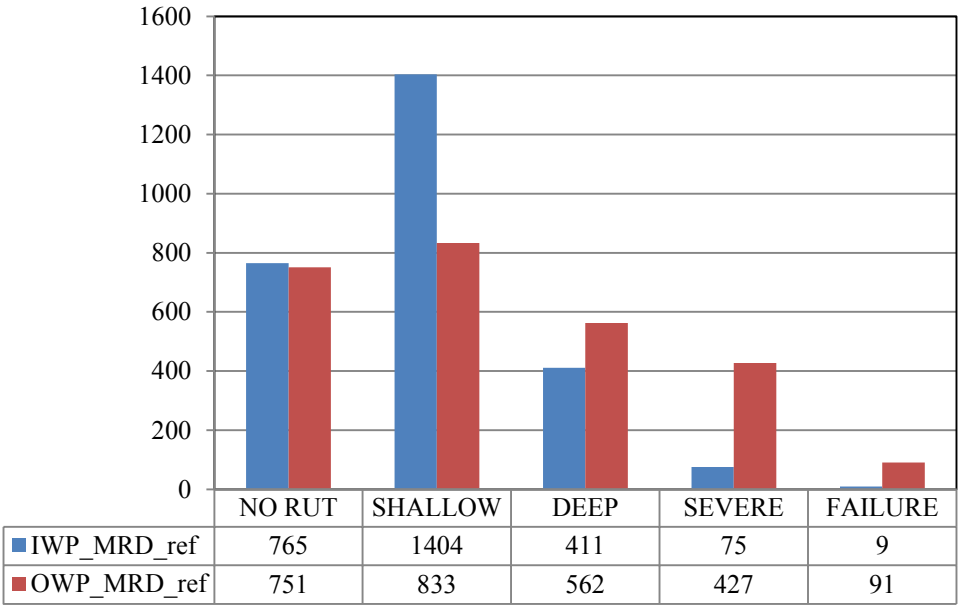

	NO RUT	SHALLOW	DEEP	SEVERE	FAILURE
IWP_MRD_ref	765	1404	411	75	9
OWP_MRD_ref	751	833	562	427	91

Figure 4.33: Reference vs. TxDOT reported OWP MRD values for all the stations.

By observing the charts prepared for the analysis of the automated rutting measurement, it was noted that the magnitude of the errors increased at stations where the

reference MRD values increased, as pointed out when presenting Figure 4.21 (see also Figure 4.14 to compare). The reference MRD values were considered in this analysis to evaluate that observation.

Lane Width

The lane width (LW) of the measured stations was defined as the distance between the inner and the outer stripes (or end of paved surface for pavements without an edge stripe) of the measured lane, and it is expressed in feet. Many of the sections presented variable paved widths. The paved width was obtained from the manually measured transverse profiles, as described in Chapter 3. For stations at which the profile was not measured, the assigned lane width value was the one corresponding to the closest station with a measured transverse profile.

The observed lane widths of the 2,664 stations of the study presented the following distribution: 16% presented a $LW \leq 10$ft; 35% were 10ft $< LW <$ 12ft; and 49% presented a $LW \geq 12$ft. Therefore, approximately 50% of the lane widths are defined as 'wide'.

This factor was included among the explanatory variables of the models because it was hypothesized that wider lanes might be more challenging for the optical systems presented by the five participants. This was considered because the lenses in the system's sensors introduce geometrical distortions which are more evident for points located further away from the sensors. Therefore, if these distortions are not properly corrected by the system, the wider the lane the greater the error in the measurements. Also, the wider the lane, the higher the risk of missing parts of the profile due to the lateral wandering of the survey vehicle.

Surface Texture

A value of '1' was assigned to the variable when the pavement surface texture (*ST*) of the station was coarse and a value of '0' when the surface texture was fine. The type of surface texture was determined visually in the field as explained in Chapter 3.

From the total 2,664 stations of the study, 85% presented a coarse surface texture and 15% a fine surface texture. This large proportion of coarse textured pavements in the study is due to the high proportion of Farm-to-Market (FM) roads selected, which are typically surface treated (seal coats). The number of selected FM roads was large in order to include a representative number of stations with high severity of rutting in the experiment.

Since the automated systems processed the measured profiles in order to filter out the effect of the texture on the calculated rut depth, the effectiveness of the methodology used by each participant was expected to affect the results. A higher error is expected for the stations with coarse surface texture since the effects of the applied filters would be more evident.

Presence of Sealed Cracks

A value of '1' was assigned to the variable "presence of sealed cracks" (PSC) when at least one sealed crack passed through the station and a value of '0' otherwise. From the total 2,664 stations of the study, 33% presented sealed cracks and 67% did not.

This factor was considered in the analysis because the localized change in color caused by the presence of a sealed crack was expected to affect the measurements of the optical systems. Therefore, the presence of sealed cracks was expected to cause an increase in the error of the reported measurements.

Presence of Inner Stripe

A value of '1' was assigned to the variable "presence of inner stripe" (PIS) when the station presented a painted stripe in the pavement center line and a value of '0' otherwise. The stations for which a value of zero was assigned were cases where the inner stripe of the section consisted of a dashed line and the considered station was located inside the interval without paint. Therefore, the sections with a dashed inner stripe contained some stations with a *PIS*=0 and some stations with a *PIS*=1. From the total 2,664 stations of the study, 78% presented a painted inner stripe and 22% did not. The larger proportion of stations that presented a painted inner stripe is because many of the selected sections presented a continuous inner stripe for dividing the lanes and designated a no-passing zone.

The different systems used proprietary algorithms for the detection of the inner and pavement edge stripes to define the limits of the transverse profile used for the calculation of rutting. Since for some stations the shape of the rut is such that the regions near the stripes are important in the determination of rutting, the effectiveness of the algorithms used for determining the boundaries of the profile was expected to affect the quality of the produced results. If the profile is truncated excessively, a significant error might be introduced depending on the shape of the rut. The error of the reported measurements was expected to increase with the presence of a painted inner stripe since it is hypothesized that the effect of these applied algorithms is more evident under that situation.

Presence of Outer Stripe

A value of '1' was assigned to the variable "presence of outer stripe" (POS) when the station presented a painted stripe in the outer side and a value of '0' otherwise. Since

none of the outer stripes were dashed, all the stations of the same section had the same assigned *POS* value, and generally the presence of an outer stripe was observed at sections on major roadways.

From the total 2,664 stations of the study, 46% presented a painted outer stripe whereas 54% did not. Therefore, the proportions of the assigned values for this variable were similar.

The reasons for which this factor was considered relevant, as well as the expected effect on the errors of the automated measurements, are the same as the exposed for the *PIS* variable.

Development of the Models

Once the observed values for each of the seven selected experiment variables were defined, one multiple linear regression model per participant and wheel-path was formulated to explain the MRD errors of each automated system.

The initial specification for the models corresponding to the IWP and the OWP for each automated system had the form presented at Equations 4.9 and 4.10, respectively. The *POS* variable was not included in the specification for the IWP model since the presence of painted outer stripe was not expected to explain the reported MRD error for the inner wheel-path. For the same reason, the *PIS* variable was not included in the OWP model. On the other hand, the *IWP_MRD_ref* variable was included in the OWP model and the *OWP_MRD_ref* variable was included in the IWP model. This is because it was hypothesized that a severe rut in any of the two wheel-paths may cause higher vibrations to the survey vehicle, what is expected to increase the errors of the measurements at both wheel-paths.

The variables *IWP_MRD_ref*, *OWP_MRD_ref* and LW are quantitative whereas the remaining variables are qualitative.

$$MRDerror_{participant}^{IWP} = \beta_0^{IWP} + \beta_1^{IWP} * MRD_{ref}^{IWP} + \beta_2^{IWP} * MRD_{ref}^{IWP} + \beta_3^{IWP} * LW + \beta_4^{IWP} * ST + \beta_5^{IWP} * PSC + \beta_6^{IWP} * PIS \quad (4.9)$$

$$MRDerror_{participant}^{OWP} = \beta_0^{OWP} + \beta_1^{OWP} * MRD_{ref}^{OWP} + \beta_2^{OWP} * MRD_{ref}^{OWP} + \beta_3^{OWP} * LW + \beta_4^{OWP} * ST + \beta_5^{OWP} * PSC + \beta_7^{OWP} * POS \quad (4.10)$$

Where:

$MRDerror_{participant}^{IWP}$ = calculated IWP MRD error of the participant;

$MRDerror_{participant}^{OWP}$ = Calculated OWP MRD error of the participant;

β_i^{IWP} = Regression parameter for the IWP;

β_i^{OWP} = Regression parameter for the OWP;

MRD_{ref}^{IWP} = Reference IWP MRD value;

MRD_{ref}^{OWP} = Reference OWP MRD value;

LW = Lane width;

ST = Surface texture (Coarse = 1, Fine = 0);

PSC = Presence of sealed cracks (present = 1, not present = 0);

PIS = Presence of painted inner stripe (present = 1, not present = 0); and

POS = Presence of painted outer stripe (present = 1, not present = 0).

Once the coefficients of the 10 models (=5participants*2wheel-paths) initially specified were estimated, the stability of the model was tested by adding and removing different explanatory variables and evaluating the effect on the estimated parameters. From the test, significant changes in the magnitude and sign of the estimated coefficients were observed, which indicated the presence of multicollinearity. Therefore, the specification of the models had to be modified in order to be able to make conclusions about the effect of the different factors on the reported measurement errors.

In order to design the new specification for the models, the correlations between the different explanatory variables were analyzed.

The first relationship analyzed was the reference MRD values for each wheel-path. This relationship was expected to be strong since both wheel-paths were exposed to the same traffic history, built with the same materials and under the same weather conditions. Therefore, higher MRD values at one wheel-path are expected to correspond to higher MRD values at the other wheel-path. From the chart in Figure 4.33 it can be observed that the distribution of the reference MRD values for each wheel-path are very similar to each other for some rut categories, which indicates a strong correlation between these two variables. The correlation coefficient between the two variables is equal to 0.60, which was considered high for the purpose of this analysis. Therefore, since the two variables *IWP_MRD_ref* and *OWP_MRD_ref* cannot be used at the same model, the variable *IWP_MRD_ref* was removed from the OWP model and the variable *OWP_MRD_ref* was removed from the IWP model.

From analyzing the relationship between the surface texture and the other variables, it was observed that all the stations with fine surface texture have a lane width equal to 12ft. Thus, the variables *ST* and *LW* are correlated. Since it was considered that

the observed values for the *LW* variable provided better information, the variable *ST* was removed from both the IWP and the OWP models.

The relationship between the reference OWP MRD values and the presence of outer stripe was analyzed by comparing the means of the *OWP_MRD_ref* variable grouped by the two possible values of the *POS* variable. The mean reference OWP MRD value was 12.0 16^{th} of an inch for the stations that did not exhibit an edge line stripe and 6.4 16^{th} of an inch for the stations that did exhibit an edge line stripe. This observation indicates that the stations that presented outer stripe also presented lower OWP MRD values. This may be explained by the fact that the stations with outer stripe corresponded to pavement sections at major highways, which were maintained in better condition that the sections at rural highways that did not present an outer stripe.

The calculated t-value for the difference of means was equal to 18, meaning that the mean reference OWP MRD values for both groups are significantly different from each other. Since the *POS* variable affects the distribution of the *OWP_MRD_ref* variable and the *OWP_MRD_ref* was preferred for explaining the reported measurements errors, the *POS* variable was removed from the OWP model.

The means of the *IWP_MRD_ref* variable were grouped by the two possible values of the PIS variable were also compared in order to analyze the association between the observed values for these two factors. The mean reference IWP MRD value was calculated as 6.3 16^{th} of an inch for the stations that presented inner stripe and 3.9 16^{th} of an inch for the stations that did not present inner stripe. The calculated t-value for the difference of means was equal to -15.2, meaning that the mean *IWP_MRD_ref* for both groups are significantly different between each other. Since the *PIS* variable affects the

distribution of the *IWP_MRD_ref* variable and the *IWP_MRD_ref* variable was preferred for specifying the model, the *PIS* variable was removed from the IWP model.

The analysis of the correlation between the presence of sealed cracks variable and the reference MRD values for both wheel-paths was also performed by comparing the means of the IWP and the OWP reference MRD values. From the obtained means, it was observed that the MRD values were higher for the stations that exhibited sealed cracks. The calculated t-values were -12 and -18 for the IWP and the OWP respectively, indicating that the means of the grouped reference MRD values are significantly different for both wheel-paths. Therefore, the *PSC* variable was also removed from both the IWP and the OWP models.

After having removed the variables *ST*, *PIS*, *POS*, and *PSC* from the initial specification of the models, the association between the lane width and the reference MRD values for both wheel-paths was analyzed. The calculated correlation coefficients between the *LW* and the *IWP_MRD_ref* and between the *LW* and the *OWP_MRD_ref* were equal to -0.27 and -0.28, respectively. Since the obtained correlation coefficients were considered low, it was decided to retain the lane width variable in the model specification. Thus, the new proposed specification for the IWP and the OWP are presented in Equations 4.11 and 4.12, respectively.

$$MRDerror_{participant}^{IWP} = \beta_0^{IWP} + \beta_1^{IWP} * MRD_{ref}^{IWP} + \beta_3^{IWP} * LW \qquad (4.11)$$

$$MRDerror_{participant}^{OWP} = \beta_0^{OWP} + \beta_1^{OWP} * MRD_{ref}^{OWP} + \beta_3^{OWP} * LW \qquad (4.12)$$

The coefficients for the new proposed specification were estimated, and the stability of the models were tested by removing one of the two variables at a time and evaluating the change produced in the re-estimated parameters. As observed for the initial specification, large changes in the estimated parameters occurred during this exercise, indicating that there was still collinearity in the models. As an example, considering the model for the OWP MRD error of Pathway, the estimated values for β_3^{OWP} when using both explanatory variables first and just the *LW* second, are equal to 0.68 and -1.02, respectively. The t-values of the coefficient calculated for each case were 9.2 and -7.7, respectively, and therefore the estimate was significant in both models.

The calculated correlation coefficient between the *LW* and the MRD error of Pathway for both wheel-paths were equal to -0.15 and -0.14, respectively, which are lower than those calculated between *LW* and *IWP_MRD_ref* and between *LW* and *OWP_MRD_ref*. The fact that *LW* is more related to the other explanatory variable than to the explained variable justifies the observed multicollinearity in the second specification of the model.

After analyzing the association between the different selected variables, and testing the stability of the models for different specifications it is concluded that the model has to be specified using one factor in order to be able to analyze the magnitude and sign of the estimated coefficients. Therefore, the final specifications of the models for the errors of the MRD reported by the different participants for both wheel-paths are presented in the Equations 4.13 and 4.14.

$$MRDerror_{participant}^{IWP} = \beta_0^{IWP} + \beta_1^{IWP} * MRD_{ref}^{IWP} \quad (4.13)$$

$$MRDerror_{participant}^{OWP} = \beta_0^{OWP} + \beta_1^{OWP} * MRD_{ref}^{OWP} \quad (4.14)$$

The results of the estimation of the model coefficients for each participant and wheel-path are presented in Table 4.8.

From observing the t-values of the coefficients on the reference MRD values presented at Table 4.8 it can be concluded that the rut depth significantly affected the error of the MRD reported by all the participants. Furthermore, the coefficients on the reference MRD values are positive in all the models, meaning that the error of the MRD reported by all the participants increased as the rut depth increased for both wheel-paths.

		β_0	β_1	
			coefficient	t-value
TxDOT	IWP	-0.04	0.16	17.9
	OWP	-0.67	0.17	29.3
Pathway	IWP	-1.21	0.54	42.0
	OWP	-2.75	0.61	79.9
Dynatest	IWP	0.21	0.19	27.6
	OWP	-0.19	0.09	13.0
Roadware	IWP	-1.78	0.52	41.9
	OWP	0.22	0.03	4.6
Applus	IWP	-0.82	0.50	40.3
	OWP	-0.01	0.44	66.6

Table 4.8: Estimated model coefficients for each participant and wheel-path.

By comparing the magnitude of the estimated coefficients, it is concluded that the measurements reported by some of the participants were more affected by the rut depth than for others. The participants for whose reported measurements were most affected by the rut depth were Pathway and Applus for both wheel-paths and Roadware for the IWP.

Chapter 5: Summary, Conclusions and Recommendations

This study evaluated the performance of state-of-the-practice automated rut measurement systems for measuring surface rutting in the field at highway speeds under Texas conditions. The analyzed rutting data consisted of the transverse profile coordinates and the calculated Maximum Rut Depth (MRD) index. The first analysis aimed to evaluate the ability of the various pieces of equipment to obtain an accurate representation of the pavement surface, thus assessing the hardware systems. The second analysis evaluated the characterization of rutting in terms of MRD which takes into account both the hardware and software systems. An additional analysis was carried out to assess the effect of different pavement characteristics on each automated system's measurement errors.

This chapter is divided into three sections: Summary; Important Findings and Conclusions; and Recommended Future Work.

SUMMARY

In the last few years, a variety of new technologies for the automated data collection of pavement distresses has become available and new technologies appear in the market continuously. Rutting is a major distress in flexible pavements, which constitute approximately 94% of the Texas roadway network. Rutting data have been traditionally collected manually, which is a time-consuming and labor-demanding process which is not feasible at the network level for Texas conditions. To date, however, manual methods are still preferred for research level investigations. Throughout the years, new technologies were developed that allowed for the automated measurements of rutting at high-speeds. These speeds are consistent with highway traffic speeds, thus,

improving efficiency and minimizing the potential for accidents. A more effective and reliable rutting data collection optimizes the management of the highway network.

Currently, the most advanced automated rut measurement systems measure the continuous transverse profile on short interval spacing at highway speeds with a high-resolution. The need for an independent assessment of these systems in the field under real conditions motivated the study described in this thesis.

The rutting measurements analyzed in this study were obtained from the Texas Department of Transportation (TxDOT) Research Project: *"0-6663 Evaluation of Pavement Rutting and Distress Measurements"* [Serigos et al, in press]. Five systems participated in the data collection: TxDOT's 3-D VRUT system (in-house developed 3-D system); Pathway's PathRunner XP system (in-house developed 3-D system); Dynatest's 5051 Mark III system (with an INO LRMS); Roadware's ARAN 9000 system (with an INO LRMS); and Applus' RCMS system (with and INO LCMS).

The data were collected on twenty-four 550' long test sections on highways in the TxDOT Austin District. These sections comprised different pavement characteristics, such as surface texture, distresses and lane width. The sections were selected in order to evaluate these systems on the pavement characteristics most frequently encountered in Texas and under situations that may be challenging for the automated systems.

The five participants surveyed the twenty-four sections at highways speeds and reported their best estimates of the transverse profiles coordinates at 552 stations and the MRD for each wheel-path at 2,664 stations. These measurements were compared with the manual measurements taken statically at the same locations. The reference transverse profiles were manually measured using a laser distance meter and a leveled beam and the reference MRD values were manually measured using a 6ft straight-edge and a gage

graduated to 16^{th} of an inch. Additional experiments were conducted in order to estimate the precision of each manual method used for determining the reference values of the comparison.

The bias, precision and mean squared error were calculated for each participant's set of measurement errors in order to evaluate the quality of their measurements and to rank the participants. In addition, the reported measurements were categorized into the TxDOT Pavement Management Information System (PMIS) rut severity levels and compared to the categorized reference values in order to evaluate their performance in reporting rutting as an input into TxDOT PMIS.

Finally, the effect of different experimental variables on each participant's measurement errors was analyzed aiming to detect which pavement characteristics are more challenging for the automated rut measurement systems.

IMPORTANT FINDINGS AND CONCLUSIONS

The following major findings and conclusions are based on the five automated rut measuring systems that participated in the study under the pavement conditions covered in the sections selected for the experiment:

- The analysis of the experiments conducted in order to estimate the precision of each manual method showed that the manual measurement bias was lower and the precision higher than the similar values obtained from the five automated systems involved in the study.
- Some of the participants either did not report values or they reported a large amount of outliers for some of the transverse profiles of the experiment. TxDOT and Pathway, which are the two systems that did not use INO sensors, missed the

least number of stations. However, the number of missed stations was low for all the participants (less than 3%).

- Some of the transverse profiles reported by the participants were narrower than the reference profiles, which were measured along the entire width of the lane, thus missing coordinates of the measured profile. TxDOT missed the least number of coordinates whereas Roadware and Pathway missed the largest number of coordinates.
- The three participants that used INO sensors presented the least variability for the measurement of transverse profile coordinates, therefore, they presented the best overall precision. However, the overall precision of all the participants was considered to be acceptable for pavement management applications in Texas.
- It is interesting to note that Dynatest and Roadware produced similar to, or in some cases superior measurement of transverse profile coordinates than the remaining participants, since they used INO LRMS, which are less complex and expensive than the rest of the systems.
- All the automated systems tended to underestimate the manual measurements of the maximum rut depth for both wheel-paths.
- TxDOT, Roadware and Dynatest ranked among the best when comparing the bias, precision and MSE of each participant's reported maximum rut depth values. Therefore, these three participants outperformed Pathways and Applus in their characterization of rutting.
- Roadware was both the most accurate and precise system in the OWP, while it presented one of the highest variability of errors for the IWP. On the other hand,

TxDOT's 3D system was the most accurate system for the IWP whereas Dynatest's was the most precise system for the IWP.

- Concluding from the findings listed above, the hardware systems used by all the participants performed satisfactorily whereas the combined performance of the hardware and the software systems of Dynatest, Roadware, and TxDOT was superior to Pathways and Applus. It should be noted that the reference MRD values used for the assessment of the combined effect of the hardware and the software systems were established based on particular criteria. The algorithms and filters that comprise the software system can be modified in order to meet these criteria more easily than the equipment that comprise the hardware system.
- For all the systems and wheel-paths, the greater the rut depth, the greater the error of the reported MRD values.
- Some of the participants' MRD errors were more affected by the rut depth than others, Pathway and Applus being the most affected for both wheel-paths and Roadware for the inner wheel-path.

RECOMMENDED FUTURE WORK

One objective of this thesis was to assess the effect that different pavement characteristics had on rutting measurement errors. The methodology consisted of estimating and interpreting the coefficients of regression models for which different experiment factors were selected to explain each participant's MRD errors. This approach was not successful due to the multicollinearity detected in the data set used in this thesis. Since this assessment was not part of the objectives of the research project for which the rutting data was collected, the original experiment was not designed to avoid the multicollinearity encountered.

A condition which leads to a robust model is that the explanatory variables are highly correlated with the explained variable but weakly correlated with each other. In order to complete the proposed assessment, a future experiment should be designed with this condition in mind.

All the pavements characteristics considered in this study carried out in this thesis to asses for their effect on each participant's performance should be considered in the proposed, future experiment design. Some of the variables used in the estimated models were binary, accounting for the presence or absence of the analyzed pavement characteristic in the station. These factors should be instead accurately quantified when possible, thus providing more information for estimating the models.

Regarding the manual rutting data collection, the researchers used ASTM 1703M standard to guide manual measurements of MRD using a 6' straightedge and gage. Although this standard is helpful, it did not provide guidance regarding how to consider or measure certain pavement features encountered in this study. It is recommended that further work is needed to expand and update standards used for manual rut depth measurements. Also, the researchers were unable to locate a national or international standard for manual transverse profile measurement equipment or data collection processes. It is recommended that new standards are developed to provide guidance for these two subjects.

References

AASHTO R48-10 (2005). Determining Rut Depth in Pavements. AASHTO Standards.

ARAN Rutbar Data Sheet. ARAN Smart Rutbar. Data Sheet. (http://www.fugroroadware.com/related/down-loads/Smart-Rutbar-Brochure).

ASTM E867-06. Standard Terminology Relating to Vehicle-Pavement Systems. ASTM Standards.

ASTM E1703/E1703M-10. Standard Test Method for Measuring Rut-Depth of Pavement Surfaces Using a Straightedge. ASTM Standards.

Bennett, C. R. and Wang, H. (2002). Harmonizing Automated Rut Depth Measurements. Transfund New Zealand Research Report.

Herr, B. (2001). Calibration and Operation of Pavement Profile Scanners. RPUG 2001 Lake Tahoe. Phoenix Scientific Inc. (http://www.phnx-sci.com/PPS/Downloads.html).

Huang, Y., Hempel, P. and Copenhaver, T. (2009). A Rut Measurement System Based on Continuous Transverse Profiles from a 3-D. Research and Development Project Report. Texas Department of Transportation.

Leica Geosystems, DISTO D8 Specifications. http://ptd.leica21geosystems.com/downloads123/cp/disto/general/brochures/Disto_family_en.pdf

Li Q., Yao M., Yao X. and Xu B. (2009). A real-time 3D scanning system for pavement distortion inspection. Center for Transportation Research. Texas, Austin.

Mitutoyo, Small Tool Instruments and Data Management Specifications. http://www.mitutoyo.ca/files/2009%20-%20e%20section_0.pdf

Pavemetrics INO LRMS Spec. Pavemetrics's laser rut measurement system. Specifications (http://www.pavemetrics.com/pdf/laser_rut.pdf).

Pavemetrics INO LCMS Spec. Pavemetrics's laser crack measurement system. Specifications (http://www.pavemetrics.com/pdf/laser_crack.pdf).

PSI PPS-2005 Spec. PPS-2005 Pavement Profile Scanner. Phoenix Scientific Inc. (http://www.phnx-sci.com/PPS/Downloads.html).

PSI PPS White Paper (2004). Pavement Profile Scanner White Paper. Phoenix Scientific Inc. (http://www.phnx-sci.com/PPS/Downloads.html).

Roberts, F. L., Kandhal, P. S., Brown, E. R., Lee, D. Y. and Kennedy, T. W. (1996). Hot Mix Asphalt Materials, Mixture Design and Construction. Second Edition. National Asphalt Pavement Association Research and Education Foundation, Lanham, Maryland.

ROMDAS TPB-Reference Profiler Spec. The ROMDAS Transverse Profile Beam (TPB) Reference Profiler. Specifications (http://www.romdas.com/hard/specs/sp-tpb.pdf).

ROMDAS TPL-URB Spec. Transverse Profile Logger - Ultrasonic Rut Bar (TPL-URB). Specifications (http://www.romdas.com/hard/specs/sp-tpl.pdf).

Serigos, P.A., Prozzi, J.A., Nam, B. H., and Murphy, M. R., (in press). Field Evaluation of Automated Rutting Measuring Equipment. Report No. FHWA/TX-12/0-6663-1. Center for Transportation Research. Austin, Texas.

Simpson, A. L. (2001a). Characterization of Transverse Profiles. Publication FHWARD-01-024. Federal Highways Administration, McLean, VA.

Simpson, A. L. (2001b). Measuring of Rutting in Asphalt Pavements. Ph.D. Thesis. Department of Civil, Architectural, and Environmental Engineering. The University of Texas at Austin.

TxDOT (2009). Pavement Management Information System Rater's Manual Fiscal Year 2010. Texas Department of Transportation.

Vedula, K., Reigle, J. and Miller, R. (2002). Comparison of 3-point and 5-point Rut Depth Data Analysis. Presentation in Pavement Evaluation 2002 Conference, Roanoke, Virginia, October 21-25, 2002.

Wang, H. (2005). Development of Laser System to Measure Pavement. M.S. Thesis. Department of Civil and Environmental Engineering College of Engineering. University of South Florida.